Aus dem Institut für Translationale Immunologie (TIM)
der Universitätsmedizin der Johannes-Gutenberg-Universität Mainz

In Vitro Testing of Novel siRNAs for Macrophage Reprogramming

In-vitro Testung neuer siRNAs zur Umprogrammierung von Makrophagen

Inauguraldissertation
zur Erlangung des Doktorgrades der
Medizin
der Universitätsmedizin
der Johannes-Gutenberg-Universität Mainz

Vorgelegt von

Klajdi Begaj
aus Tirana

Mainz, 2024

Wissenschaftlicher Vorstand: Univ.-Prof. Dr. H. Schild

1.Gutachter: [redacted]

2. Gutachter: [redacted]

Tag der Promotion: 16. Dezember 2024

To my family and friends.

Table of Contents

Abbreviations

AHR	Aryl Hydrocarbon Receptor
AIRE	Autoimmune Regulator
Arg1	Arginase 1
BMDM	Bone Marrow-Derived Macrophages
bp	Base Pairs
CAR-M	Chimeric Antigen Receptor-Macrophages
CCL4	Tetrachloromethane
CCR2	C-C Chemokine Receptor Type 2
C_t	Threshold Cycle
CXCL2	C-X-C Motif Chemokine Ligand 2
DMSO	Dimethyl sulfoxide
ECM	Extracellular Matrix
EMT	Epithelial to Mesenchymal Transition
FCS	Fetal Calf Serum
FDA	Food And Drug Administration
Fra2	Fos-Related Antigen 2
GOI	Gene of Interest
GPR65	G Protein-Coupled Receptor 65
Havcr2	Hepatitis A Virus Cellular Receptor 2
HCC	Hepatocellular Carcinoma
ICOS-L	Inducible T-Cell CO-Stimulator Ligand
IFN	Interferon
IL	Interleukin
iNOS	Inducible Nitric Oxide Synthase
LAG3	Lymphocyte-Activation Gene 3
LGALS9	Galectin-9
LPS	Lipopolysaccharide
LRRC32	Leucine-Rich Repeat-Containing Protein 32
LUC	Luciferase
M-CSF	Macrophage Colony-Stimulating Factor

M-CSF	Macrophage Colony Stimulating Factor
MoM	Monocyte-Derived Macrophages
mRNA	Messenger RNA
NASH	Non-Alcoholic Steatohepatitis
Nectin2	Nectin Cell Adhesion Molecule 2
NF-κB	Nuclear Factor Kappa-Light-Chain-Enhancer of Activated B Cells
Olfr2	Olfactory Receptor 2
PDGF	Platelet-Derived Growth Factor
Pen-Strep	Penicillin-Streptomycin
PIK3CG	Phosphatidylinositol-4,5-Bisphosphate 3-Kinase Catalytic Subunit Gamma
PPARγ	Peroxisome Proliferator-Activated Receptor Gamma
PVR	Poliovirus Receptor
R848	Resiquimod
RBC	Red Blood Cell
REF	Reference Gene
RISC	RNA-Induced Silencing Complex
RNAi	RNA Interference
RT-qPCR	Reverse Transcription-Quantitative Polymerase Chain Reaction
SAMs	Scar-Associated Macrophages
SD	Standard Deviation
siGENE	siRNA-targeting GENE
siNTC	Non-Targeting Control siRNA
siRNA	Small Interfering RNA
SIRPA	Signal Regulatory Protein alpha
STAT6	Signal Transducer and Activator of Transcription 6
TAMs	Tumor Associated Macrophages
TGF-β	Transforming Growth Factor Beta
Th	T Helper Cell
TIGIT	T Cell Immunoreceptor with Ig and ITIM Domains
Timp1	Tissue Inhibitor of Metalloproteinases 1
TLR	Toll-Like Receptor
TME	Tumor Microenvironment

TMEM173	Transmembrane Protein 173
TNFα	Tumor Necrosis factor alpha
Treg	Regulatory T Cell
Twist1	Twist Family bHLH Transcription Factor 1
Twist2	Twist Family bHLH Transcription Factor 2
VEGF	Vascular Endothelial Growth Factor

Figures

Abstract

This study focuses on macrophages, crucial cellular components of the immune system and attractive targets for developing novel immunotherapies. They are derived from embryonic precursors within the tissue of origin or recruited from bone marrow monocytes, and exhibit remarkable plasticity, allowing them to partake in various biological processes and adopt different functional phenotypes—primarily pro-inflammatory M1-type and anti-inflammatory M2-type macrophages. These cells play critical roles in conditions such as cancer and fibrotic diseases, often being manipulated by the surrounding microenvironment to promote disease initiation and progression. However this binary classification is an over-simplification, and the characterization of macrophage phenotypes and their role in homeostasis and disease remains a focal point of current research.

The purpose of this thesis was to explore the potential of novel small interfering RNAs targeting specific genes to reprogram macrophages from the M2 to the M1 phenotype, which may promote their anti-cancer as well as antifibrotic activities.

The experimental approach involved an extensive optimization process, refining incubation periods for cell polarization, siRNA transfection, and RNA extraction to ensure the accuracy and reliability of results. Murine bone marrow-derived macrophages polarized towards the M2 phenotype were transfected with various siRNAs and their effects were assessed using RT-qPCR to measure the expression of M1 and M2 marker genes, such as CD206, Arg1, Timp1, YM1 (for M2), and CCL2, iNOS, IL12 (for M1). Target genes included AHR, AIRE, CCR2, CXCL2, Fra2, GPR65, Havcr2, ICOS-L, LAG3, LGALS9, LRRC32, Nectin2, Olfr2, PIK3CG, PPARG, PVR, SIRPA, STAT6, TIGIT, TMEM173, Twist1, and Twist2.

The results presented in this thesis highlight the complexity of macrophage polarization and its regulatory pathways. The study demonstrates the potential of siRNA-mediated macrophage reprogramming as a promising approach for treating diseases. By targeting genes potentially involved in macrophage polarization, such as Twist1 and STAT6, siRNAs can shift macrophages from an immunosuppressive M2 phenotype to a pro-inflammatory M1 phenotype.

The study's findings pave the way for further exploration and development of siRNA-based immunotherapies. Additionally, the research supports the development of personalized treatment strategies tailored to individual patients, improving treatment outcomes and reducing side effects. Future research should focus on optimizing siRNA delivery systems and validating the therapeutic efficacy of these approaches in animal models and clinical settings.

Zusammenfassung

Diese Studie konzentriert sich auf Makrophagen, die wesentliche zelluläre Bestandteile des Immunsystems sind und attraktive Ziele für die Entwicklung neuer Immuntherapien darstellen. Sie stammen entweder von embryonalen Vorläufern im Urpsrungsgewebe ab oder werden aus Knochenmarkmonozyten rekrutiert und zeigen eine bemerkenswerte Plastizität, die es ihnen ermöglicht, an verschiedenen biologischen Prozessen teilzunehmen und unterschiedliche funktionelle Phänotypen anzunehmen—vorwiegend den pro-entzündlichen M1 und den anti-entzündlichen M2. Diese Zellen spielen eine entscheidende Rolle bei Krankheiten wie Krebs (TAMs) und fibrotischen Erkrankungen (SAMs), wobei sie oft durch das umgebende Mikromilieu beeinflusst werden, um die Krankheitsinitiierung und -progression zu fördern. Diese binäre Klassifizierung stellt jedoch eine Vereinfachung dar, und die Charakterisierung der Makrophagenphänotypen und ihre Rolle bei der Homöostase und Krankheit bleibt ein zentraler Punkt der aktuellen Forschung.

Das Ziel der vorgelegten Dissertation ist es, das Potenzial neuartiger siRNAs zu untersuchen, die gezielt spezifische Gene ansprechen, um Makrophagen vom M2- zum M1-Phänotyp umzuprogrammieren, was ihre antitumoralen sowie antifibrotischen Aktivitäten fördern könnte.

Der experimentelle Ansatz umfasste einen umfangreichen Optimierungsprozess zur Verfeinerung der Inkubationszeiten für die Zellpolarisierung, die siRNA-Transfektion und die RNA-Extraktion, um die Genauigkeit und Zuverlässigkeit der Ergebnisse sicherzustellen. Knochenmarkabgeleitete Makrophagen (BMDMs), die zum M2-Phänotyp polarisiert wurden, wurden mit verschiedenen siRNAs transfiziert. Die Auswirkungen dieser Transfektionen wurden mittels RT-qPCR bewertet, um die Expression von Markergenen für M1 und M2, wie CD206, Arg1, Timp1, YM1 (für M2) sowie CCL2, iNOS und IL12 (für M1) zu messen. Zielgene umfassten AHR, AIRE, CCR2, CXCL2, Fra2, GPR65, Havcr2, ICOS-L, LAG3, LGALS9, LRRC32, Nectin2, Olfr2, PIK3CG, PPARG, PVR, SIRPA, STAT6, TIGIT, TMEM173, Twist1 und Twist2.

Die Ergebnisse dieser Arbeit unterstreichen die Komplexität der Makrophagenpolarisierung und ihrer regulatorischen Mechanismen. Die Studie demonstriert das Potenzial der siRNA-vermittelten Makrophagenumprogrammierung als vielversprechenden Ansatz zur Behandlung von Krankheiten. Durch das Targeting von Genen, die potenziell an der Makrophagenpolarisierung beteiligt sind, wie Twist1 und STAT6, können siRNAs Makrophagen von einem immunsuppressiven M2-Phänotyp zu einem pro-entzündlichen M1-Phänotyp umschalten.

Die Erkenntnisse der Studie bahnen den Weg für weitere Untersuchungen und die Entwicklung von auf siRNA-basierenden Immuntherapien. Zusätzlich unterstützt die Forschung die

Entwicklung von personalisierten Behandlungsstrategien, die auf den einzelnen Patienten zugeschnitten sind, um die Behandlungsergebnisse zu verbessern und Nebenwirkungen zu reduzieren. Zukünftige Forschungen sollten sich auf die Optimierung von siRNA-Transportsystemen konzentrieren und die therapeutische Wirksamkeit dieser Ansätze in Tiermodellen und klinischen Studien validieren.

1 Introduction

The immune system is a complex network of cells, tissues, and organs that work in synergy to defend the body against pathogens and disease. Among the myriads of cell types involved in the immune response, macrophages play a pivotal role in both the maintenance of homeostasis and the pathogenesis of diseases.

This dissertation explores the potential of targeting macrophages through RNA interference immunotherapies, highlighting novel approaches in the treatment of cancer and other chronic inflammation-related conditions, such as fibrosis.

1.1 Macrophages and their role in Homeostasis and Diseases

Macrophages are integral components of the immune system, renowned for their versatility and key roles in both innate and adaptive immunity. Originating from precursor cells in the bone marrow, they differentiate from monocytes that circulate in the bloodstream. Upon entering tissues, these monocytes mature into macrophages, where they adapt to the local environment and assume diverse functional phenotypes. This adaptability allows them to partake in a wide array of biological processes, including pathogen clearance (phagocytosis), dead cell removal (efferocytosis), and regulation of inflammatory responses. However certain organ-specific tissue resident macrophages derive from embryonic precursors within the specific tissue itself (1, 2).

Functionally, macrophages are best known for their phagocytic activity, engulfing and digesting cellular debris, pathogens, and foreign substances. This capability is central to their role in innate immunity and the initiation of the adaptive immune response by presenting antigens to T cells. Additionally, macrophages secrete a wide range of cytokines and chemokines, which play critical roles in modulating inflammation and the recruitment of other immune cells to sites of infection or injury (3-5).

The interaction between macrophages and other cells is fundamental to the immune system's orchestration. Macrophages interact with T cells to facilitate the adaptive immune response, secreting cytokines that help determine T cell differentiation and function. Furthermore, their interaction with fibroblasts and endothelial cells is crucial for wound healing and tissue regeneration, illustrating their importance beyond mere immune surveillance (6-8).

At the molecular level, macrophage activity is governed by a complex network of signaling pathways triggered by interactions with various receptors, including Toll-like receptors (TLRs) and receptors for cytokines and growth factors. These interactions initiate signaling cascades that modulate macrophage behavior, influencing their phenotype and function in response to environmental cues. Key pathways include the nuclear factor kappa B (NF-κB) pathway, critical for pro-inflammatory responses, and PPAR and the STAT pathways, which influence cytokine signaling and macrophage activation (9-11).

1.1.1 Macrophage Phenotypes

Macrophages, as key players in the immune system, exhibit remarkable plasticity, enabling them to perform a spectrum of functions that range from initiating inflammatory responses to promoting tissue healing. Their functional diversity is often categorized into two primary

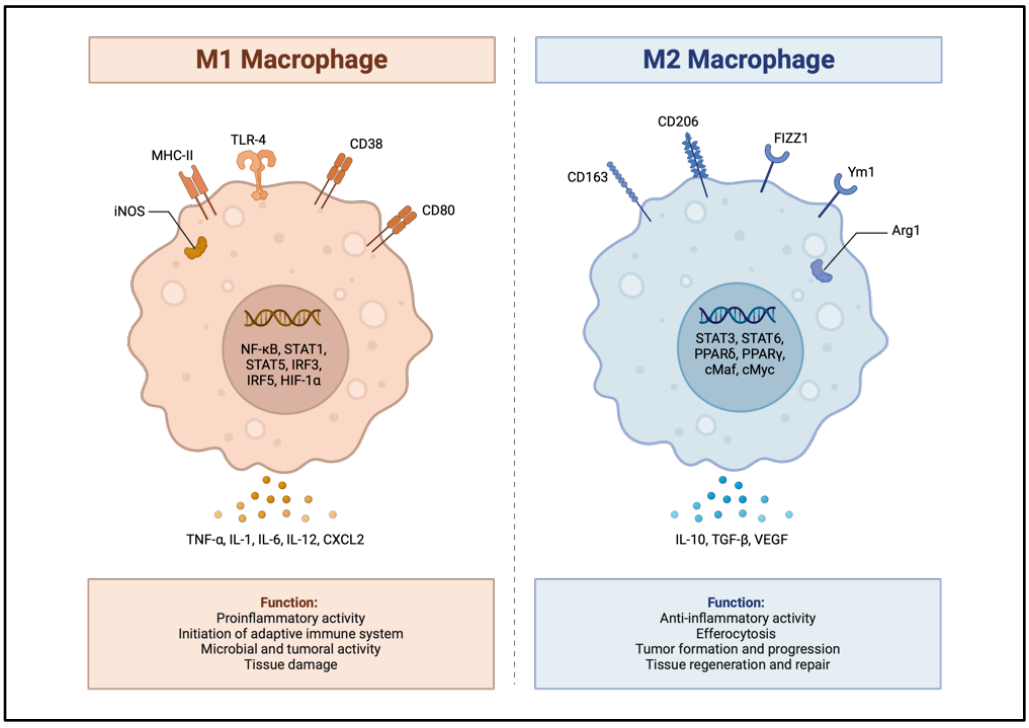

Figure 1: Key characteristics of M1-type and M2-type macrophages

The M1 and M2 states represent the two extremes of in vitro macrophage polarization model. M1 macrophages, characterized by transcription factors like NF-κB and STAT5, release cytokines such as TNF-α and IL-12, and express iNOS and receptors like TLR4 and MHCII, promoting inflammation and antimicrobial activity. Alternatively, the M2 phenotype, with transcription factors like STAT6 and PPARγ, secretes cytokines IL-10 and TGF-β, and expresses Arg1 and receptors such as CD206 and YM1, facilitating tissue repair and anti-inflammatory effects. It is important to note that there are many more "shades" in vivo. Figure created in BioRender.

phenotypes: the pro-inflammatory M1-type and the anti-inflammatory M2-type macrophages, homologous to the T helper response profile Th1 and Th2, which macrophages can initiate and direct (12-14).

Key characteristics of the two primary macrophage phenotypes are depicted in *Figure 1*.

In vitro, the M1 phenotype is typically induced by interferon-gamma (IFN-γ) and lipopolysaccharide (LPS), leading to the production of pro-inflammatory cytokines and reactive nitrogen and oxygen species that play crucial roles in host defense against pathogens and tumor cells. Conversely, the M2 phenotype, induced by interleukin-4 (IL-4) and interleukin-13 (IL-13), is associated with the resolution phase of inflammation, wound healing, tissue repair, and immunoregulation, producing anti-inflammatory cytokines and growth factors (10, 15, 16).

However, the dynamic and context-dependent nature of macrophage polarization highlights a more complex regulatory mechanism beyond the M1/M2 dichotomy, emphasizing the need for a deeper understanding of macrophage function in health and disease (17, 18).

1.1.2 Role of Macrophages in Cancer and Fibrotic Diseases

Macrophages do not only play a pivotal role in immune defense but also in the pathogenesis and progression of various pathological conditions, including cancer and fibrosis. Their role in these diseases is complex and multifaceted, as they can exhibit different phenotypic states, each with distinct molecular characteristics and functions (19-21).

In the context of cancer, macrophages are often referred to as tumor-associated macrophages (TAMs), which predominantly exhibit an M2-like phenotype and are linked to therapy resistance and overall poor survival rates (22, 23).

These macrophages are characterized by the expression of markers such as CD206, CD163, and Arginase-1. They produce anti-inflammatory cytokines like IL-10 and growth factors such as vascular endothelial growth factor (VEGF), contributing to tumor growth, angiogenesis, and suppression of the adaptive immune response. The recruitment of TAMs to the tumor microenvironment (TME) is mediated by chemokines like CCL2, and the complex interaction between TAMs and cancer cells supports the tumor-sustaining microenvironment by promoting immune evasion (24, 25).

TAMs, which are usually recruited and sustained by the cancer cells, play a crucial role especially in inflammation-related cancers such as hepatocellular carcinoma (HCC), fostering a pro-tumorigenic environment and leading to tumor progression (26, 27).

In fibrotic diseases, macrophages play a crucial role in the initiation, progression, and resolution of fibrosis. The transition from a fibrotic state to tissue repair is mediated by the dynamic change in macrophage phenotypes (19, 28, 29).

Previous studies conducted in our Institute by Weng and colleagues (30) highlight the dual nature of macrophages in liver fibrosis, via their contribution to both the initiation and progression of fibrosis.

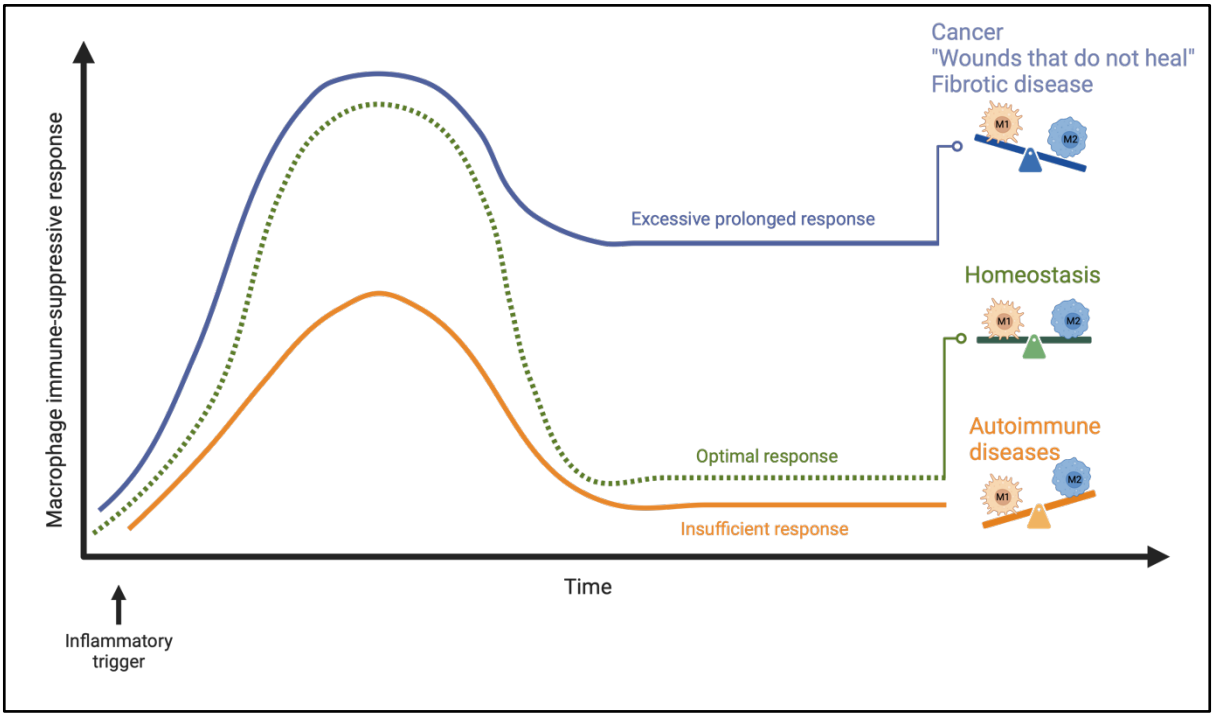

Figure 2: Dysregulation of macrophage immune-suppressive functions

After an inflammatory trigger, resolution ensures a return to homeostasis. In an optimal response (green line), there is an initial increase in pro-resolution functions, followed by a reduction in the macrophage's anti-inflammatory response. In cancer and "wounds that do not heal" (blue line), this response is characterized by excessive and prolonged resolution, shifting the balance towards the M2 phenotype spectrum. In fibrosis, however, this depiction is less straightforward, as the imbalance of fibrosis pro-resolution phenotypes, rather than an abundance of M2 macrophages, is the primary issue (Casari et. al., Frontiers in Immunology, 2023). In contrast, autoimmune diseases may arise due to insufficient resolution, characterized by an overabundance of M1 macrophages. Nonetheless, this is a simplified representation of the roles that M1 and M2 macrophages play in either restoring homeostasis or contributing to disease. The actual pathophysiological processes in vivo are far more complex. Figure modified from Rodríguez-Morales and Franklin, Trends in Immunology (2023) and made using BioRender.

Initially, during tissue injury, M1 macrophages dominate, characterized by the expression of tumor necrosis factor alpha (TNF-α), IL-1β, and IL-6, which promote inflammation and removal of damaged cells. However, as the healing process progresses, there is a shift towards an M2

phenotype, which is crucial for wound healing and tissue repair. M2 macrophages, expressing cytokines such as transforming growth factor beta 1 (TGF-β1), drive the production of extracellular matrix components, leading to restoration of the damaged extracellular matrix (ECM). In pathological conditions such as chronic inflammation, the balance between the pro- and anti-fibrotic mechanisms is distorted, leading to disproportionate ECM deposition (19, 30, 31).

In 2019, Ramachandran and colleagues (32) identified a $TREM2^{+}CD9^{+}$ macrophage subpopulation, which expands in cirrhotic livers and plays a significant role in the fibrotic niche. These so-called scar-associated macrophages (SAMs) are implicated in the progression of fibrosis, indicating their excessive pro-fibrotic nature, which aligns with the general characteristics of M2 macrophages.

SAMs produce a variety of growth factors and cytokines, such as TGF-β1, IL-10, and Platelet-Derived Growth Factor Beta (PDGF-B), which contribute to the synthesis of ECM components and suppression of inflammatory and anti-fibrotic responses. This profile supports fibrogenesis and the formation of scar tissue in chronic inflammatory diseases (32, 33).

The complexity of macrophage roles in different pathologies, including liver fibrosis and HCC, underscores the therapeutic potential of targeting macrophage phenotypes, offering promising avenues for the development of novel strategies to treat cancer and chronic inflammation-related diseases (24, 34).

1.2 RNA Interference

RNA interference (RNAi) represents a powerful and precise mechanism for silencing genes, where small interfering RNA (siRNA) molecules lead to the breakdown of specific messenger RNA (mRNA) targets. This pathway has been described as a naturally occurring autoregulatory mechanism to attenuate the effects of excessive transcription and translation of developmental and regulatory genes (35). The use of synthetic siRNA offers a promising approach for inhibiting the expression of various pathological proteins, including those that are traditionally challenging to target selectively via conventional pharmaceutical methods like small molecules or protein-based drugs. As a result, RNAi therapies are emerging as a versatile class of drugs with potential applications across a wide array of pharmacological areas (36, 37).

1.2.1 Mechanism of RNA Interference

The Mechanism of RNA Interference is depicted in **Figure *3*** and briefly described in the following paragraph.

The process begins with the cleavage of long double-stranded RNA molecules by an enzyme known as Dicer. This process produces siRNAs, which are introduced to a multiprotein complex with RNase activity called the RNA-Induced Silencing Complex (RISC). Within the RISC complex, the siRNA is unwound into single strands. The active single-stranded siRNA

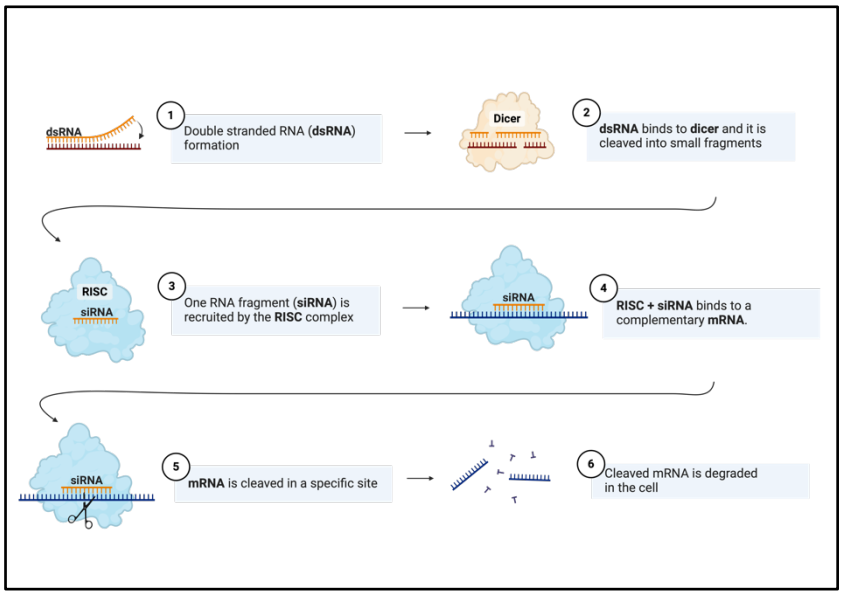

Figure 3: Mechanism of RNA interference

Simplified illustration of the mechanism of action of siRNA. Figure created in BioRender.

within the RISC then seeks out and binds to its complementary mRNA target, leading to the cleavage of the mRNA. This cleavage marks the mRNA for degradation, preventing it from being translated into proteins and effectively silencing the gene responsible for its creation (38, 39).

1.2.2 Synthetically engineered siRNA

Synthetic siRNAs are engineered to skip the Dicer step and directly integrate into the RISC. The principle of RNAi therapy lies in the use of small (around 20 base pairs) double-stranded siRNAs. The development of therapeutic siRNAs involves two essential steps; designing siRNAs that are highly specific to the intended mRNA target with minimal unintended effects, such as the inhibition of non-target mRNAs or the activation of innate immune responses through immunogenicity potential of the siRNA molecule and devising an effective delivery system that can transport the siRNAs into the cells of interest (40).

1.3 Aim of the Project

The aim of this dissertation was to explore the macrophage reprogramming potential of small interfering RNA (siRNA), targeting various selected genes. These new targets were to be tested *in vitro* in M2-polarized murine Bone Marrow Derived Macrophages (BMDM), as shown in *Figure 4*.

This dissertation is part of a larger research project for the development of new immunotherapies for liver diseases as shown in *Figure 5*.

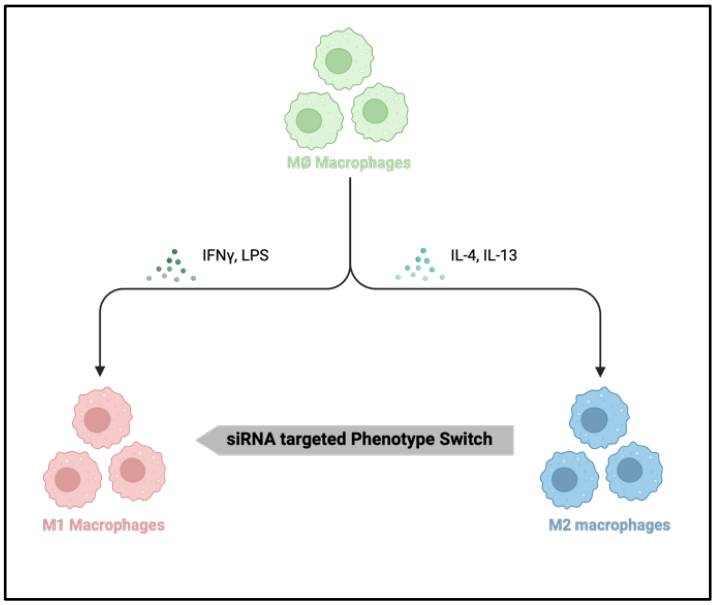

Figure 4: Aim of dissertation

After establishing the in vitro M1 and M2 polarization of naïve macrophages (MØ), derived from murine bone marrows, using either IFNγ and LPS for M1 or IL-4 and IL-13 for M2, the M2 macrophages will be transfected with different siRNA candidates targeting a phenotype switch towards the M1 phenotype. Figure created in BioRender.

After the screening process, the most effective targets will subsequently be developed for *in vivo* applications utilizing established syngeneic HCC and liver fibrosis mouse models, developed in the Institute for Translational Immunology at the University Medical Center Mainz. Further evaluation of preselected targets would cover aspects such as toxicity, biodistribution, target knockdown, and overall effectiveness in animal models.

The research project also leverages established lipoplexes and block copolymer-based cationic nanogels as effective in vivo delivery systems for siRNA.

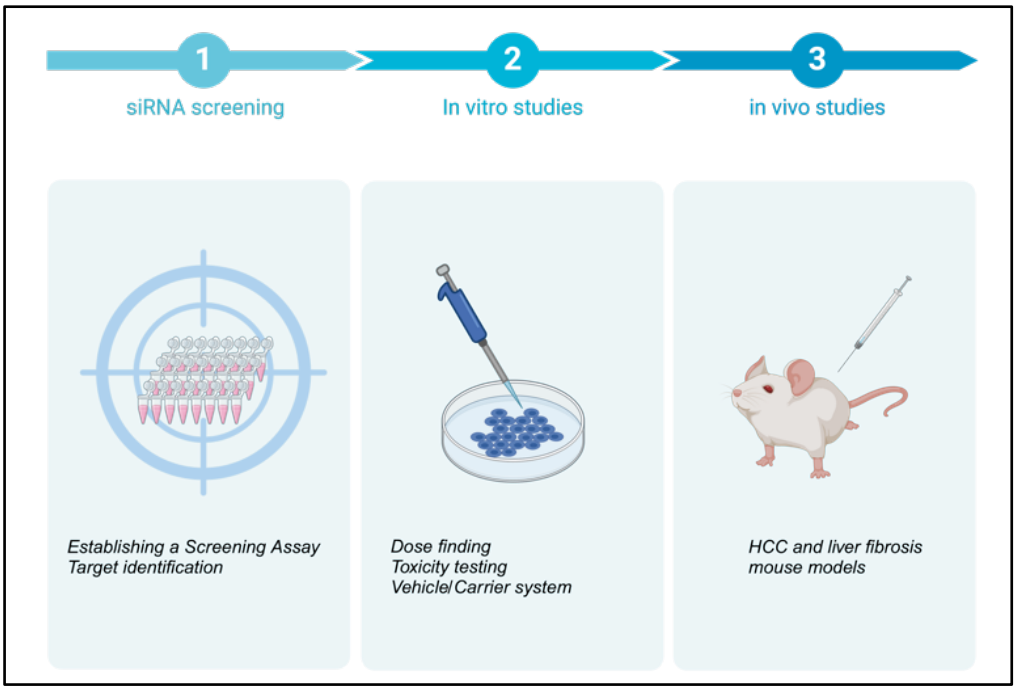

Figure 5: Project overview

The project consists of three stages. Firstly, to identify suitable targets, a screening assay will be established to test siRNA candidates. After identifying potential candidates, in vitro studies will be conducted to test for optimal dose, toxicity, and different carrier systems. This will prepare for the final step of the project – the in vivo studies, where siRNA candidates will be tested in mouse models of liver fibrosis and hepatocellular carcinoma as novel therapeutic strategies. Figure created in BioRender.

The implications of this research extend far beyond the treatment of liver fibrosis and HCC. M2 macrophages play a central role in the progression of many tumors and fibrotic diseases affecting various other organs, such as the pancreas, kidneys and lungs (41-44). Therefore, the ability to reprogram these cells offers a promising avenue for developing novel therapies. Through this dissertation, the potential for siRNA to serve as a powerful tool in reprogramming

macrophages towards a phenotype that supports disease resolution rather than progression is explored.

1.3.1 Targeted Genes

The targeted genes for siRNA inhibition were carefully selected in collaboration with the Director of the Institute for Translational Immunology, Prof. Dr. Dr. D. Schuppan, and are subject to potential intellectual property claims. The results of this thesis are to be considered confidential.

The following table provides a list of the target genes, and some information on their known function.

Gene	**Function and links to macrophage phenotypes.**
AHR	Aryl Hydrocarbon Receptor (AHR) is a transcription factor that plays a role in mediating responses to environmental toxins and regulating immune responses. Its activation is associated with the modulation of macrophage polarization. It can diminish M1 macrophage polarization and promote M2 macrophage polarization through specific pathways, suggesting its potential role in inflammatory diseases and cancer (45-47).
AIRE	Autoimmune Regulator (AIRE) is primarily known for its crucial role in the negative selection of autoreactive T cells in the thymus, thus preventing autoimmune diseases by promoting central tolerance. Its direct role in macrophage polarization might be more indirect or part of broader immunological processes rather than a direct influence on macrophage phenotype (48-50).
CCR2	C-C Chemokine Receptor Type 2 (CCR2) is a receptor involved in the recruitment of monocytes and other immune cells to sites of inflammation in response to chemokine signals. It plays a crucial role in macrophage polarization, especially in directing the migration of monocytes that can differentiate into macrophages at the site of inflammation. It is involved in various diseases through its influence on macrophage behavior (51, 52).

Gene	Function and links to macrophage phenotypes.
CXCL2	C-X-C Motif Chemokine Ligand 2 (CXCL2) is a chemokine that plays a role in inflammation and immune cell recruitment. It has been implicated in regulating TAMs and influencing their polarization. Its signaling is associated with promoting M2-like macrophage polarization, which can support tumor growth and metastasis (53-55).
Fra2	Fos-Related Antigen 2 (Fra2) is a component of the AP-1 transcription factor complex, involved in regulating gene expression in response to physiological and pathological stimuli. It influences macrophage polarization towards the pro-fibrotic M2 phenotype, playing a crucial role in inflammatory responses and fibrogenesis (56).
GPR65	G Protein-Coupled Receptor 65 (GPR65) is receptor with roles in immune regulation and cell signaling. It has been implicated in influencing macrophage polarization, particularly in contexts like hepatic inflammation and fibrosis, by modulating signaling pathways such as JNK and NF-κB (57, 58).
Havcr2	Hepatitis A Virus Cellular Receptor 2 (Havcr2), known as Tim-3, is involved in regulating immune responses, particularly in the context of T-cell exhaustion and immune checkpoint regulation. Its expression is associated with M2 polarization of macrophages in various contexts, including the TME, indicating its potential role in modulating immune responses and suggesting therapeutic targets for diseases where macrophage polarization is critical (59, 60).
ICOS-L	Inducible T-Cell CO-Stimulator Ligand (ICOS-L) is a co-stimulatory molecule that interacts with its receptor ICOS on T-cells, promoting T-cell activation and proliferation. ICOS-L signaling may influence macrophage-T cell interactions, potentially affecting macrophage polarization indirectly through T-cell mediated immune responses (61, 62).

Gene	Function and links to macrophage phenotypes.
LAG3	Lymphocyte-Activation Gene 3 (LAG3) is a protein that negatively regulates T-cell activation by binding to MHC class II molecules, contributing to immune tolerance and suppression of immune responses. Its involvement in immunosuppression and modulation of T-cell responses indirectly affects the tumor microenvironment and potentially influences macrophage polarization (63, 64).
LGALS9	Galectin-9 (LGALS9) is a galectin protein involved in immune regulation and inflammation. It can modulate immune responses, affect T-cell function, and promote regulatory T-cell development. It has been implicated in the modulation of macrophage polarization, influencing both the M1 and M2 phenotypes (65, 66).
LRRC32	Leucine-Rich Repeat-Containing Protein 32 (LRRC32), known as GARP, is associated with T-cell activation, and is involved in the regulation of immune responses, including the activation of TGF-beta. It has been implicated in the modulation of macrophage polarization, particularly in relation to the tumor microenvironment and inflammatory conditions (67-69).
Nectin2	Nectin Cell Adhesion Molecule 2 (Nectin2), as part of the nectin family, plays a significant role in cell adhesion, signaling, and in the modulation of the immune system, which could indirectly influence macrophage behavior and polarization within the context of immune responses and disease environments (70).
Olfr2	Olfactory Receptor 2 (Olfr2) is a type of G protein-coupled receptor involved in the sense of smell. The studies highlight Olfr2 signaling in macrophages, suggesting it likely follows a known signaling cascade described in the olfactory epithelium. This suggests that olfactory receptors, including Olfr2, may play a role in macrophage behavior and potentially in their polarization (71, 72).

Gene	Function and links to macrophage phenotypes.
PIK3CG	Phosphatidylinositol-4,5-Bisphosphate 3-Kinase Catalytic Subunit Gamma (PIK3CG) is an enzyme, which plays a crucial role in cell signaling, including immune responses. Studies indicate that PIK3CG is involved in various immune functions, including macrophage polarization (73, 74).
PPARγ	Peroxisome Proliferator-Activated Receptor Gamma (PPARγ) is a transcription factor involved in the regulation of various cellular processes, including immune regulation and adipocyte differentiation. It plays a crucial role in macrophage polarization, influencing the shift towards the M2 phenotype, which is associated with anti-inflammatory functions. Activation of PPARγ leads to anti-inflammatory effects and is considered a therapeutic target for inflammatory diseases (75, 76).
PVR	Poliovirus Receptor (PVR) is involved in cell adhesion and immune responses. It interacts with TIGIT and other receptors to regulate immune cell functions. Studies have shown that the interaction between PVR and checkpoint molecules like TIGIT can influence macrophage polarization. For example, TIGIT interaction with PVR has been found to induce M2-type macrophage polarization, which could play a role in tissue graft rejection and the regulation of immune responses in the tumor microenvironment (70, 77, 78).
SIRPA	Signal Regulatory Protein Alpha (SIRPA) is involved in the regulation of immune responses and cell signaling, including inhibitory signaling in immune cells. Its role in macrophage polarization is linked to its interaction with CD47, affecting macrophage phagocytosis and potentially influencing the polarization towards an M2 phenotype in tumor environments (79-82).
STAT6	Signal Transducer and Activator of Transcription 6 (STAT6) is a transcription factor that is important in mediating signaling pathways for cytokines like IL-4 and IL-13, involved in immune responses and inflammation. It plays a crucial role in the polarization of macrophages towards the M2 phenotype. Its activation is associated with anti-inflammatory responses and tissue repair processes. Pharmacological inhibition of STAT6 has been shown to affect macrophage polarization and has therapeutic potential in conditions such as renal fibrosis (75, 83, 84).

Gene	Function and links to macrophage phenotypes.
TIGIT	T Cell Immunoreceptor with Ig and ITIM Domains (TIGIT) is a protein that regulates T-cell activation and immune responses. It interacts with ligands such as PVR and Nectin2. TIGIT blockade has been shown to repolarize M2 macrophages to an M1 phenotype, highlighting its potential role in modulating macrophage polarization and suggesting therapeutic targets for diseases where macrophage polarization is critical (85, 86).
TMEM173	Transmembrane Protein 173 (TMEM173), also known as STING (Stimulator of Interferon Genes), plays a crucial role in the detection of intracellular DNA and initiation of innate immune responses. It has been implicated in the regulation of macrophage polarization, especially in the context of inflammatory responses and tumor immunity. Its activation can lead to the production of type I interferons and other cytokines, which influence macrophage behavior and polarization (87-90).
Twist1	Twist Family bHLH Transcription Factor 1 (Twist1) is a transcription factor involved in embryonic development, mesodermal differentiation, and has been implicated in tumor progression. It has been shown to regulate macrophage plasticity and promote renal fibrosis through mechanisms involving galectin-3. It affects macrophage migration, phagocytosis, and polarization, highlighting its potential role in inflammatory responses and cancer (91-95).
Twist2	Twist Family bHLH Transcription Factor 2 (Twist2), as part of the twist family proteins, is also known for its roles in embryonic development, cell lineage differentiation, and cancer progression, often influencing the tumor microenvironment and immune cell behavior. Twist2 is less researched than Twist1 (94-96).

2 Materials und Methods

2.1 Materials

2.1.1 Consumables

Item	Supplier
12 well Cell Culture Plates	Greiner Bio-One, Frickenhausen, Germany
96 well Fast Thermal Cycling Plate	Life technologies GmbH, Darmstadt, Germany
Cell Culture Dish 94x16mm	Greiner Bio-One, Frickenhausen, Germany
Cell strainer (70µm)	Greiner Bio-One, Frickenhausen, Germany
CellStar tubes (15ml and 50ml)	Greiner Bio-One, Frickenhausen, Germany
Counting slide dual chamber	Bio-Rad, München, Germany
Cryotubes	Greiner Bio-One, Frickenhausen, Germany
Serological Pipettes (5/10/25 ml)	Greiner Bio-One, Frickenhausen, Germany
Needle (21G, 26G)	BD Biosciences, Heidelberg, Germany
Optical Adhesive Covers	Life technologies GmbH, Darmstadt, Germany
Safe-lock tubes (0.5/1.5/2 ml)	Eppendorf, Hamburg, Germany
Sapphire Pipette Tips (10/200/1000 µl)	Greiner Bio-One, Frickenhausen, Germany
Syringes (5 ml)	BD Biosciences, Heidelberg, Germany

2.1.2 Reagents

Item	Supplier
100 bp DNA ladder	Bio & Sell GmbH, Feucht, Germany
6X DNA Loading Dye	Thermo Fisher Scientific, Schwerte, Germany
Agarose	AppliChem GmbH, Darmstadt, Germany
Ammonium Chloride	Carl Roth GmbH, Karlsruhe, Germany
DEPC treated nuclease-free Water	Carl Roth GmbH, Karlsruhe, Germany
Dimethyl sulfoxide (DMSO)	Sigma Aldrich, Steinheim, Germany
Dulbecco's PBS	Sigma Aldrich, Steinheim, Germany
0.5M EDTA	Thermo Fisher Scientific, Schwerte, Germany
Ethanol Absolute	Carl Roth GmbH, Karlsruhe, Germany
Ethidium Bromide 0.025 % (15 ml)	Carl Roth GmbH, Karlsruhe, Germany
Fetal Calf Serum (FCS)	Sigma Aldrich, Steinheim, Germany
HEPES (1 M)	Sigma Aldrich, Steinheim, Germany
Hydrochloric acid (HCl)	Carl Roth GmbH, Karlsruhe, Germany
LPS	Sigma Aldrich, Steinheim, Germany
Trypan Blue Solution	Sigma Aldrich, Steinheim, Germany
Opti-MEM Reduced Serum Medium	Thermo Fisher Scientific, Schwerte, Germany
Penicillin-Streptomycin (Pen/Strep)	Thermo Fisher Scientific, Schwerte, Germany
Potassium hydrogen carbonate	Carl Roth GmbH, Karlsruhe, Germany

Item	Supplier
Recombinant mouse IL-13	Immunotool GmbH, Friesoythe, Germany
Recombinant mouse IL-4	Immunotool GmbH, Friesoythe, Germany
Recombinant mouse Interferon-γ	Immunotool GmbH, Friesoythe, Germany
Recombinant mouse Macrophage Colony-Stimulating Factor (M-CSF)	Immunotool GmbH, Friesoythe, Germany
Resiquimod Hydrochloride (R848)	InvivoGen, San Diego, USA
Sodium EDTA	Carl Roth GmbH, Karlsruhe, Germany
TRIS	Merck Chemicals GmbH, Darmstadt, Germany

2.1.3 Kits and Transfection Reagents

Kit	Manufacturer
Luna® Universal One-Step RT-qPCR Kit	New England Biolabs, Frankfurt/Main, Germany
Monarch® Total RNA Miniprep Kit	New England Biolabs, Frankfurt/Main, Germany
TransIT-TKO® Transfection Reagent	Mirus Bio, Darmstadt, Germany
TransIT-X2® Transfection Reagent	Mirus Bio, Darmstadt, Germany
INTERFERin® Transfection Reagent	Polyplus-transfection SA, Illkirch, France

2.1.4 Cell culture media, supplements, and solutions

Medium/Buffer	Recipe/Supplements
BMDM growth medium	Gibco™ DMEM, high glucose, GlutaMAX™, Supplement, pyruvate (Thermo Fischer Scientific) +10% heat-inactivated FCS +1% Pen/Strep +50 ng/µl M-CSF
Red Blood Cell (RBC) lysis buffer	174 mM NH4Cl 10 mM KHCO3 (1 g) 0.1 mM Sodium-EDTA (0.2 ml) Dissolved into distilled H_2O (1 L) Adjusted to pH 7.3 with HCl
TAE buffer	40 mM TRIS-acetate 1 mM EDTA pH 8
Wash medium	Gibco™ DMEM, high glucose, GlutaMAX™, Supplement, pyruvate (Thermo Fischer Scientific) +10% heat-inactivated FCS +1% Pen/Strep
EDTA-HEPES buffer	1 ml of 1 M HEPES 0.6 ml of 0.5 M EDTA PBS ad 50 ml

2.2 Instruments and Software

Item	Manufacturer
A&B applied biosystems step one plus real-time PCR system	Real-time PCR system, Life technologies GmbH, Darmstadt, Germany
Bio-Rad Gel Doc XR+	Bio-Rad, München, Germany
Bio-Rad TC10 automated cell counter	Bio-Rad, München, Germany

Item	Manufacturer
Centrifuge 5804R Eppendorf	Hamburg, Germany
Centrifuge Heraeus Fresco 21	Thermo Fisher Scientific, Schwerte, Germany
Centrifuge VWR mini star	VWR International, Darmstadt, Germany
NanoDrop™ Lite Spectrophotometer	Thermo Fisher Scientific, Schwerte, Germany

2.3 Software, Tools and Databases

Item	Provider
GraphPad Prism 7	GraphPad Software Inc., San Diego, USA
BioRender.com	Science Suite Inc., Toronto, Canada
Image Lab Software	Bio-Rad, München, Germany
StepOnePlus™ System	Thermo Fisher Scientific, Schwerte, Germany
Ensembl.com	European Bioinformatics Institute, Cambridge, UK
Primer-BLAST	NCBI-NLM, Bethesda, USA
UNAFold	Washington University, St. Louis, USA
UCSC Genome Browser	UC Santa Cruz, California, USA

2.4 Methods

2.4.1 Cell Culture

Cell culture is a cornerstone technique in biomedical research, enabling detailed study of cellular behavior in a controlled environment. For this project, instead of utilizing established cell lines, primary cells were use and harvested from 8 to 20 weeks old MDR2 knockout (Mdr2KO) mice. This approach was chosen to enhance the biological relevance of the *in vitro* studies.

2.4.1.1 Extraction of Bone Marrow Cells

Bone marrow cells were aseptically harvested from the femurs and tibias of Mdr2KO mice. Employing a 21 G needle and a 5 ml syringe prefilled with wash medium, the open ends of the bones were flushed to collect the bone marrow into a cell culture dish containing 10 ml of the same medium. To eliminate cell aggregates, bone fragments, hair, and tissue, the cell suspension was passed through a 70 µm cell strainer into a 50 ml tube and centrifuged at 350 g for 8 minutes at 4°C. Red blood cells were lysed by adding 3-5ml of RBC lysis buffer, followed by incubation at room temperature for 5 minutes. The lysing process was stopped by adding DMEM washing medium up to 10ml. Subsequently, the cells were centrifuged again under the same conditions, and the supernatant was carefully removed. The cell count was determined using an automated cell counter and trypan blue, and the cells were resuspended in 90% FCS with 10% DMSO before being aliquoted into cryotubes (1ml cell suspension per tube, containing 4 million cells each). The tubes were initially placed in a -80°C freezer. Following a negative result for mycoplasma contamination, confirmed via PCR, the samples were then permanently stored in a liquid nitrogen tank. *(Figure 7, Steps 1-2)*

2.4.1.2 Cultivation of BMDMs

At the start of a new experiment (Day 0), the necessary number of bone marrow cell vials was thawed, based on the size of the experiment. The cell suspension was quickly thawed using a water bath and each vial was resuspended in 9 ml of pre-warmed DMEM wash medium and subsequently centrifuged at 350 g for 8 minutes to remove the DMSO. The pellet was then resuspended in 10 ml of DMEM growth medium and transferred to a 10 cm cell culture dish, which was then placed in an incubator. After 48 hours, an additional 10 ml of fresh complete

medium was added to each dish. On Day 5, the media in each dish was completely replaced. By Day 7, the development of mature BMDMs was assessed microscopically. The cells transitioned from small and round to larger, adherent, and with a spiculated morphology, indicating successful maturation. Typically, a confluence of 70-80% was achieved by Day 7 *(Figure 7, Steps 3-4)*

2.4.1.3 Macrophage Harvest and Polarization

On Day 7, macrophages were harvested from the cell culture dish following the removal of the medium and the addition of 3ml of EDTA-HEPES buffer to facilitate cell detachment. The collected cells were washed with PBS and centrifuged at 350 g for 8 minutes at 4°C. Subsequently, cells were resuspended in supplemented DMEM (excluding M-CSF) to achieve a density of 2.5×10^5 cells/ml. To induce polarization, naïve macrophages (MØ) were treated with either 20ng/ml IL-4 and IL-13 for the M2 phenotype or 20 ng/ml IFNγ and 1µg/ml of LPS for the M1 phenotype. 1 ml of the cell suspension was seeded into each well of a 12 well plate, corresponding to 250,000 cells per well, to attain an over 80% confluence prior to transfection. *(Figure 7, Steps 5-6)*

2.4.2 siRNA Transfection

siRNA transfections were conducted using the protocols provided from the manufacturers of the transfection reagents used *(specifics described below)*. Transfection complexes were prepared immediately before use, combining transfection reagent with a pooled mixture of four siRNA sequences for each target in Opti-MEM Reduced Serum Medium to achieve a final siRNA concentration of 25 nM per well. Complexes were incubated at room temperature for 15–30 minutes to allow for complex formation. The complexes were then added dropwise to the M2 polarized macrophages, ensuring even distribution by gently rocking the plate. Each siRNA was transfected in duplicate wells. Cells were incubated with the siRNA complexes for 24–48 hours, without changing the growth medium post-transfection. *(Figure 7, Step 7)*

2.4.2.1 siRNA Sequences

Control and targeting siRNA sequences for mouse were acquired from Dharmacon™, a Horizon Discovery Group Company (Cambridge, UK), which guarantees sufficient target

knockdown for their siRNA products, while also minimizing off-target effects and immunogenicity. For each targeted gene four individual siRNA sequences were ordered (ON-TARGETplus™ *Set of 4*). The individual siRNAs were resuspended in RNase-free siRNA Buffer according to the product information and later pooled together to a 10 µM for the experiments. Control siRNAs were also acquired from Dharmacon™: Non-targeting Control siRNA #2, and Anti-Luc siRNA 1. All sequences are provided in the following tables.

Table I: Targeting siRNA sequences

Target	**siRNA Sequences**
ICOS-L	Sequence 1: GUCUAUUGGCAAAUCGAAA Sequence 2: GAGUUCACAUGCCGGGUAU Sequence 3: GGACAAUAGCCUAAUAGAC Sequence 4: ACAACGAGCUGUCUGCUUA
LAG3	Sequence 1: UCCCAAAUCCUUCGGGUUA Sequence 2: GAUCCUAACUUUCUACGAA Sequence 3: UAGAGGAGCUGGAGCGAGA Sequence 4: GAGGCUUCUUGGAGCGACA
LGALS9	Sequence 1: CUCUAGAAGUGGCGGGUGA Sequence 2: AGAAUGCUGUUGUCCGAAA Sequence 3: GGCCAGAGCUUCUCGGUGU Sequence 4: ACACGAAGCAGAACGGACA
Havcr2	Sequence 1: CCAUCGAGGAGAACGUAUA Sequence 2: GCAUAUGCUUAACACGAUA Sequence 3: GGACUGAGUAUCUGGCGAA Sequence 4: CUUAAAUGGUAUUCCUGUA
LRRC32	Sequence 1: GUGCUAGAUCUGCGGAACA Sequence 2: GGACCUAAUCUGCCGCUUU Sequence 3: GCAAUCUGGUGGAGCGACU Sequence 4: CGUCCAGAGGAUUGCGAGA
TIGIT	Sequence 1: ACUUUAAUGUCCUGAGCUA Sequence 2: CCACAGCAGGCACGAUAGA Sequence 3: AUUUACAAGGGGAGAAUAU Sequence 4: GCUUCAGUCUUCAGUGAUC
STAT6	Sequence 1: AGGCUUCACCAUCGAGUAA Sequence 2: CCAAGACAACAACGCCAAA Sequence 3: UGGAUGAAGUCCUGCGAAC Sequence 4: UGGUCAUCGUGCAUGGUAA
PIK3CG	Sequence 1: ACACAAACCUGUUGAUCAU Sequence 2: CCCGAGAGCUUUAGAGUUC Sequence 3: CAACGAAACCAUUGGAAUC Sequence 4: GCACUCCGCUUGAUAUGUG
CCR2	Sequence 1: UCGGUUGGGUUGUAAAGUA Sequence 2: GCAGAUCGAGUGAGCUCUA Sequence 3: CCGAAGGUAUCUCUCCAUA Sequence 4: AACAAGAUGAUCACCAUUA

Target	siRNA Sequences
SIRPA	Sequence 1: GAACACUUUCCUCGAGUUA Sequence 2: UGGAAACGUAUCACGGAAU Sequence 3: CGGAUGGGACCUAUAAUUA Sequence 4: CCGUGAACCCUAGUGGAAA
AIRE	Sequence 1: ACUACAAUCUGGAGGGGUA Sequence 2: CCUAAACCAGUCCOGGAAA Sequence 3: CGGAGUGGUAGCAGCCUAA Sequence 4: GCUCCCACCUGAAGACUAA
AHR	Sequence 1: CGACAUAACGGACGAAAUC Sequence 2: GUGCAGAGUUGAGGUGUUU Sequence 3: UCAGAGCUCUUUCCGGAUA Sequence 4: CAAGGGAGGUUAAAGUAUC
Twist1	Sequence 1: CCGGAGACCUAGAUGUCAU Sequence 2: CCCAGCGGGUCAUGGCUAA Sequence 3: AAUCAUAGUCAGUGAAUUC Sequence 4: AUUGAUGACCCAUGGUAAA
GPR65	Sequence 1: CGAGAAGAUUCGCGUUUAU Sequence 2: AAACGAGUGUUGAAUAUUG Sequence 3: CAGCCAACAUCGGAUCUUU Sequence 4: UGGCAGACGUUUACGGUGU
PVR	Sequence 1: GGAUAUAACUGGAGCACGA Sequence 2: CUUAAGUGUAGAAGACGAA Sequence 3: CAAGAUUACACCUAGGCUA Sequence 4: GUUAAGCGCCAGGGCAAUA
TMEM173	Sequence 1: UCAAUCAGCUACAUAACAA Sequence 2: GCAUCAAGAAUCGGGUUUA Sequence 3: AACAUUCGAUUCCGAGAUA Sequence 4: CCAACAGCGUCUACGAGAU
Nectin2	Sequence 1: GACUAUGACUGGAGCACGA Sequence 2: GCGUCAAGGUCACGUGUAG Sequence 3: GUCCUUUGUCAGAGCGAGA Sequence 4: GACUGAGGGUAGAGGACGA
Olfr2	Sequence 1: UCAUUGGUUCCGAGGAGAA Sequence 2: GGUGCUGACUGAAAACAUA Sequence 3: AAUCAGCAGAGAUGGUUA Sequence 4: GCGCAAUCAAGAAGUCAAA
Fra2	Sequence 1: GCACAUGGCUCUCCCCAGA Sequence 2: GCUCACCCAGAAGCAGUA Sequence 3: GGAGUGAAAUUUGCUAUUA Sequence 4: GAACUUGUUUCUAGUGCUA
CXCL2	Sequence 1: GAACAAAGGCAAGGCUAAC Sequence 2: AAAGAUAUCGAUUCGCUAA Sequence 3: GCCCAGAUGUUGUUAUGUU Sequence 4: UCGGAUGGCUUUCAUGGAA
PPARG	Sequence 1: CGAAGAACCAUCCGAUUGA Sequence 2: ACCCAAUGGUUGCUGAUUA Sequence 3: UCACAAUGCCAUCAGGUUU Sequence 4: CGACAUGAAUUCCUUAAUG

Target	siRNA Sequences
Twist2	Sequence 1: UGGAAUUCUUGCCCGCAUA Sequence 2: CAAGAAAUCGAGCGAAGAU Sequence 3: CCGUGACUGUUUCGAGGAA Sequence 4: GCCACGCGGUUGUGUAUAA

Table II Control siRNA Sequences

Control siRNA	Sequence
Anti-Luc siRNA 1	GAUUAUGUCCGGUUAUGUA
Non-targeting Control siRNA #2	UGGUUUACAUGUUGUGUGA

2.4.2.2 Transfection Reagents

Three different commercially available transfection reagents were used in this project: TransIT-X2®, TransIT-TKO®, and INTERFERin®. The used amounts for transfection are described in the following table:

Table III: siRNA transfection protocols

Kit	siRNA (pooled stock of 10 μM)	Transfection Reagent (recommended in protocol)	OptiMEM serum free medium
TransIT-X2®	2.8 μl	3 μl	100 μl
TransIT-TKO®	2.8 μl	5 μl	100 μl
INTERFERin®	4.6 μl	4 μl	200 μl

2.4.3 RNA extraction

At the end of the experiment, 24 after transfection, RNA was extracted from the cells. The total RNA was isolated and purified from cultured cells in multiwell plates utilizing a protocol based on the Monarch® Total RNA Isolation Kit. The process commenced with sample disruption, where media was removed from the wells, followed by rinsing with PBS. Monarch RNA lysis buffer was applied directly to the cells to ensure thorough lysing. The lysate was then

transferred to a gDNA Removal Column to eliminate genomic DNA, with the flow-through containing the RNA collected for further processing. An equal volume of ethanol (≥ 95%) was added to the flow-through, mixed thoroughly by pipetting, and then transferred to an RNA Purification Column for binding. The RNA was washed and DNase I treatment was applied directly to the column to remove any residual genomic DNA. This was followed by additional wash steps to thoroughly clean the RNA, which was then eluted in nuclease-free water. RNA quality and quantity were assessed using spectrophotometric measurements (NanoDrop), with an absorbance ratio A260/280 of about 2.0 being excepted as pure. Samples were stored at -80°C for long-term preservation or immediately used for downstream applications. *(Figure 7, Step 8)*

2.4.4 RT-q-PCR

The RT-qPCR assays were performed using a one-step protocol adapted from the Luna® Universal One-Step RT-qPCR Kit. For each assay, reactions were set up initially in triplicate, and after validation in duplicate. The reaction set up is provided in *Table IV.*

Reaction components were thawed, mixed by inversion pipetting or gentle vortexing, and briefly centrifuged to collect the liquid at the tube's bottom. Assay mixes, excluding the RNA template, were prepared with a 10% volume overage and aliquoted into qPCR plates. RNA templates were then added, and plates were sealed with optically transparent film.

Table IV: RT-qPCR Reaction Set Up

Component and Stock Concentration	20 µl Reaction	Final Concentration
Luna Universal One-Step Reaction Mix (2X)	10 µl	1X
PrimerPair 3.2 µM (1.6 µM each forward and reverse)	5 µl	0.8 µM (0.4 µM each forward and reverse)
Luna RT Enzyme Mix (20X)	1 µl	1X
Template RNA 0.125ng/µl *(for siRNA experiments)* 2.5ng/µl *(for annealing temperature optimization)* 2.5-0.0024 ng/µl *(for primer efficiency testing)*	 4 µl 1 µl 4 µl	 0.5ng per well 2.5ng per well 10ng-0.0006ng per well
Nuclease-free Water	to 20 µl	

Plates were spun briefly to remove bubbles and ensure liquid collection at the bottom. The RT-qPCR thermocycling conditions, summarized in *Table V,* included an initial reverse transcription step at 55°C for 10 minutes, followed by an initial denaturation at 95°C for 1 minute. This was followed by 40 cycles of denaturation at 95°C for 15 seconds and extension at 60°C for 1 minute, with plate reads included at the end of each extension step to monitor amplification in real-time. A final melt curve analysis was performed to verify product specificity. This approach allowed for the quantitative analysis of gene expression levels across various samples, providing a robust framework for the evaluation of gene regulation under different experimental conditions.

Table V: RT-qPCR thermocycling conditions

Step	Temperature	Duration	Cycles
Reverse Transcription	55°C	10 minutes	1
Initial Denaturation	95°C	1 minute	1
Denaturation Extension	95°C 60°C	15 seconds 1 minute	40
Melt Curve	60°C-95°C	various	1

2.4.4.1 Primers

All primers underwent thorough validation steps and were optimized at an annealing temperature of 60°C. qPCR efficiency of these primers was also tested using a RNA dilution series, to ensure robust results. Further details on primer design and validation are provided in *Chapter 3.1.*

Table VI: RT-qPCR primer sequences and pair efficiency

Target	**Forward Primer** *(5'→3')*	**Reverse Primer** *(5'→3')*	**Efficiency**
PPIA	GCC GAT GAC GAG CCC TTG G	CCC TGG CAC ATG AAT CCT GGA A	98%
Tbp	TGG AAT TGT ACC GCA GCT TCA AAA T	GCA GTT GTC CGT GGC TCT CT	103%

Target	**Forward Primer** *(5'→3')*	**Reverse Primer** *(5'→3')*	**Efficiency**
CD206	TTG GAG GCT GAT TAC GAG CAG TG	GGA CAT GCC AGG GTC ACC TTT	95%
iNOS	TTG GTG AAG GGA CTG AGC TGT T	AAG AGA AAC TTC CAG GGG CAA GC	98%
Arg1	AGA GAT TAT CGG AGC GCC TT	GGT CTC TCA CGT CAT ACT CTG TTT C	107%
CCL2	TAA AAA CCT GGA TCG GAA CCA AA	GCA TTA GCT TCA GAT TTA CGG GT	103%
YM1	AGA AGG GAG TTT CAA ACC TGG T	GTC TTG CTC ATG TGT GTA AGT GA	95%
Timp	TCA TCA CGG GCC GCC TAA	TCC GTC CAC AAA CAG TGA GT	105%
IL-10	AGC CTT ATC GGA AAT GAT CCA GT	GGC CTT GTA GAC ACC TTG GT	110%
IL-12	TTA GCC AGT CCC GAA ACC TG	AGG CAA CTC TCG TTC TTG TGT A	100%
Fra2	CAC TCC CGG CAC TTC AAA C	GAG TCT GAT GAC TGG TCC CC	110%
SIRPA	ACC CAG ATC CAG GAC ACA AAT GAC	TGG TTG TTA GGC TCA GGG GC	102%
Nectin2	TGT AGA GTG GAA CAC GAG AG	GGA TAC TTC TGG AGG GTA GC	100%
GPR65	CAA GAG AAG CAT CCC TCC AGA	ATT GGA GAT TGG TCG GTG CAA	100%
PPARγ	CGG GCT GAG AAG TCA CGT T	TGT GTC AAC CAT GGT AAT TTC AGT	95%
STAT6	TCA GCA CCT TGG AGA GCA TCT A	GTT CTT CCT GCT TCC GAT GG	102%
AHR	TCA GAG ACT GGC AGG ATT TGC	ATG GAT GAC ATC AGA CTG CTG AA	110%
Tmem173	TCA GAG CTT GAC TCC AGC GG	TAC AGT CTT CGG CTC CCT GC	110%
LGALS9	TGT TCT CTA CTC CTG GAA TCC	AAA GCC CAT TTG GAA TGG G	105%
ICOS-L	ACG CCA TTT CAA CTT GAG TGG	TCC CTG GAG ACT TGT AAG GCA	103%

Target	Forward Primer *(5'→3')*	Reverse Primer *(5'→3')*	Efficiency
Havcr2	GAC ATC AAA GCA GCC AAG G	CGT GGT TAG GGT TCT TGG A	108%
PIK3CG	ACA AAT GAT CCT CCT CCG CAT C	CTG GGC AGT ACG AAC TCA ATG G	110%
Pvr2	TCG TCT TTG TCC TCG CTG TAG T	TGA ATA CTG GAC GTT CTC CCT CT	106%
LRRC32	ACC TGA CTC ACC TCA ATC TCT C	GCT GTT GCA GCT CAA GTC TAG T	92%
CCR2	AGG AGC CAT ACC TGT AAA TGC	GCC GTG GAT GAA CTG AGG TAA	90%

2.4.4.2 RT-q-PCR plate set-up

For primer validation within RT-qPCR assays, each well received 4µl of macrophage RNA at 0.625ng/µl, totaling 2.5ng RNA per well, to facilitate the determination of optimal annealing temperatures via a plate-wide temperature gradient (56°C -66°C in 2°C steps). For the assessment of primer efficacy in qPCR, an 8-step dilution series (1:4 ratio), starting at a concentration of 10 ng/well, was utilized. Further details are elaborated in *Chapter 3.1.*

For siRNA investigations, 2.5ng RNA per well were used. For each sample, two reference genes (REF), PPIA and TBP, were tested alongside the Gene of Interest (GOI). Duplication of wells for each REF and GOI marker was executed to ensure qPCR technical replicates. An internal control was included as a No Reverse Transcriptase Control (NTC) for every marker and sample, pipetted in single wells.

2.4.4.3 Relative Gene Expression Analysis

The relative expression of target genes was normalized for each sample, following the best practices (97, 98). In brief, this normalization was achieved by dividing the relative quantity of a target gene by the geometric mean of the relative quantities of two reference genes, Peptidylprolyl Isomerase A (PPIA) and TATA-Box Binding Protein (TBP). These reference genes were chosen for their stable expression across the experimental conditions, thereby providing a reliable baseline for comparison. Following normalization, the average expression level for each gene within biological groups was calculated. Statistical analyses were then performed on these normalized values to assess differences in gene expression across experimental conditions. The statistical approach considered the log-transformed nature of

qPCR data. The final expression levels were reported following a linear transformation of these results, allowing for a more intuitive interpretation of gene expression differences. A practical example is provided in the *Appendix.*

2.4.5 Agarose Gel Electrophoresis

A 2% agarose gel was prepared by dissolving 2 g of agarose in 100 ml of TAE buffer (by heating in a microwave for 1-2 minutes until the agarose was completely dissolved. The solution was slightly cooled before adding 2-drops of ethidium bromide solution. The mixture was poured into a gel casting tray with a well comb in place and allowed to solidify at room temperature for 30 minutes. DNA samples from RT-qPCR products were mixed with 6X loading dye in a ratio of 1:1 and briefly mixed by pipetting. 10 µL were loaded into each well

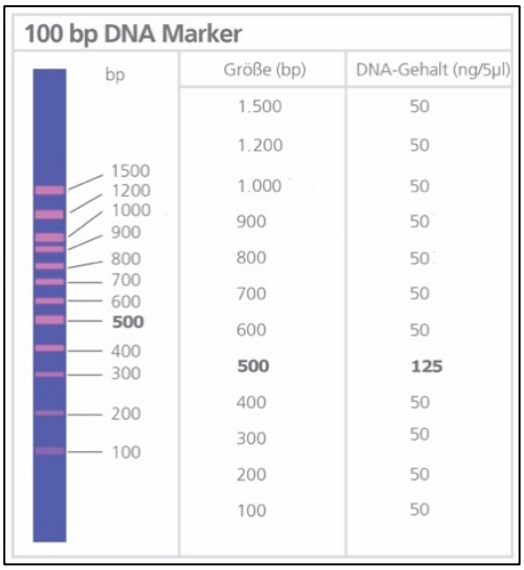

Figure 6: DNA ladder for gel electrophoresis

Graphical Illustration of the 100bp DNA ladder from Bio & Sell GmbH including size and amount approximations.

of the agarose gel. The gel was placed in an electrophoresis tank and submerged with 1X TAE buffer, ensuring the gel was completely covered by buffer. A 100 bp DNA ladder was loaded into the first well (occasionally in the last well also), followed by the DNA samples in subsequent wells. Electrophoresis was run at 120 V for 45-60 minutes, or until the dye front reached approximately 80% of the gel length. After electrophoresis, the gel was visualized

and documented under UV light and analyzed using *Bio-Rad Gel Doc XR+* and the Image Lab Software to estimate the size of the DNA fragments by comparing them to the DNA ladder *(Figure 6)*.

2.5 Statistical Analysis

Statistical analyses were conducted using GraphPad Prism 7. All data are presented as means ± SD. Differences between groups were assessed using a two-tailed Student's t-test. Significance levels were represented by calculated p-values, with notations as follows: $p < 0.05$ (*) for significant, $p < 0.01$ (**) for highly significant, and $p < 0.001$ (***) for very highly significant. The sample size (n) was set to two, unless otherwise specified.

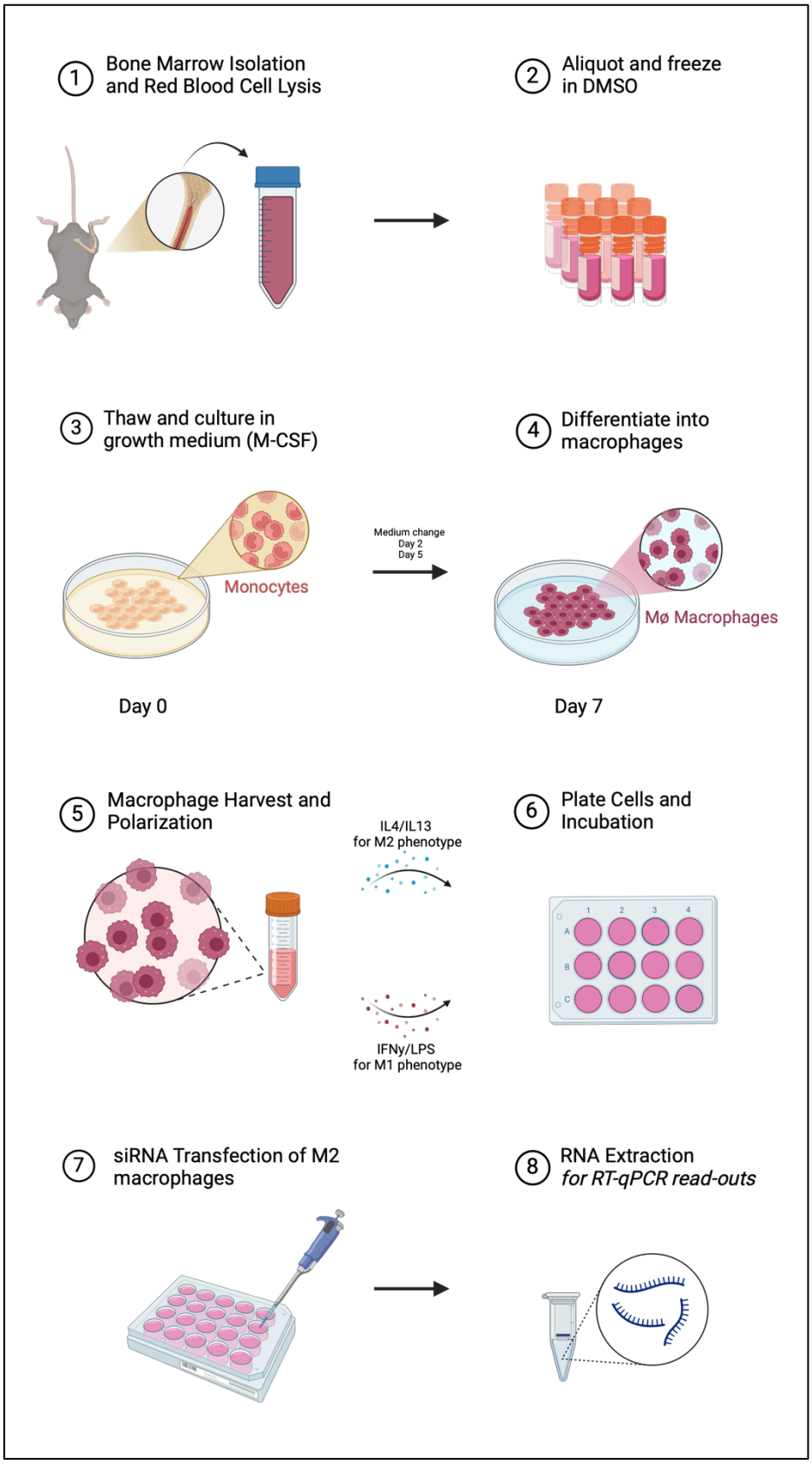

Figure 7: Experimental design

Graphical illustration of the experiment workflow. Figure created in BioRender.

3 Results

Before screening the siRNA candidates, it was essential to first optimize and validate the polarization model and the experimental design, including the primers used for RT-qPCR. This validation was crucial to establish proof of concept. The results of this preliminary work are detailed in *Chapters 3.1 to 3.3*. The outcomes of the screening assay, along with some additional data, are presented in *Chapters 3.4 and 3.5.*

3.1 Primer Design and Validation for RT-q-PCR SYBR-Green Assay

RT-qPCR primer design and validation was performed following strict steps to ensure robust and reproducible experiment data (99). In the following subsection, the design and validation process are explained, also using the real example of the primer validation for SIRPA, but this process was used for all primers used in the experiments, be it primers for reference gene, marker genes, or siRNA target genes.

3.1.1 Primer Sequence Design and *In Silico* Validation

The initial step in designing valid RT-qPCR primers involves a comprehensive understanding of the target gene and its transcripts. To accomplish this, widely recognized databases such as Ensembl[1] was utilized. These resources provided detailed information on gene transcript variants and their functional structures. Special attention was given to exon-exon junctions and introns within the genomic DNA. *(Figure 8)*

Following the initial research, the Primer-BLAST[2] tool from the NCBI library was employed to identify suitable primer pairs for the target gene transcripts. The PrimerBlast search settings and filters were carefully chosen to ensure the primers' specificity and efficiency:

1. Exon-Exon Junction Spanning: Primers must span at least one exon-exon junction. This criterion helps in distinguishing between genomic DNA and cDNA, enhancing the specificity of the assay.
2. PCR Product Size: Set between 70-150 base pairs to optimize amplification efficiency and specificity.

[1] www.ensembl.org
[2] www.ncbi.nlm.nih.gov/tools/primer-blast/

3. Intronic Separation: Primers are designed to be separated by at least one intron on the genomic DNA, further ensuring that the amplified product is from cDNA rather than genomic DNA.
4. Transcript Variant Recognition: Primers should recognize different transcript variants, allowing for a comprehensive analysis of gene expression.

The sequences generated from PrimerBlast were assessed using the IDT OligoAnalyzer™ Tool[3] to analyze the thermodynamic characteristics of primer pairs and their amplicons, including:

1. Melting Temperature (Tm): The temperature at which half of the DNA duplex dissociates to become single-stranded, indicating the primer's binding strength.
2. Hairpin Formation (ΔG): The change in Gibbs free energy (ΔG) associated with potential hairpin structures, which can affect primer specificity and efficiency.
3. Dimer Formation (Homo & Hetero Dimer ΔG): The change in Gibbs free energy (ΔG) related to the formation of primer dimers, either between identical primers (homodimers) or between different primers (heterodimers), which can compete with target amplification.

Finally, UNAFold's mFold[4] (for secondary structure prediction) and UCSC Genome Browser's BLAT Search[5] (for sequence similarity) were utilized to ensure that primer pairs do not form unintended secondary structures or bind to non-target sequences, thereby maximizing the specificity of the PCR reaction. Primer pairs that demonstrated optimal *in silico* results were selected for ordering and subsequent wet lab validation.

3.1.2 Wet Lab Primer Validation

Primer pair stocks were prepared at a concentration of 3.2µM, with each primer (forward and reverse) contributing 1.6µM to the mixture.

To determine the optimal annealing temperature for the primer pair, a qPCR experiment was conducted across different temperature zones ranging from 56°C to 66°C, in increments of 2°C. A technical control was also included once at 60°C.

The one-step RT-qPCR reaction, with a total volume of 20µL, included 1µL of M1-Macrophage-RNA (2.5ng) as the template, 10µL of Luna Universal One-Step Reaction mix, 5µL of Primer-Pair Stock, and 1µL RT Enzyme Mix, omitting the RT Enzyme Mix for no-RT

[3] https://eu.idtdna.com/pages/tools/oligoanalyzer
[4] http://www.unafold.org/mfold/applications/dna-folding-form.php
[5] https://genome.ucsc.edu/cgi-bin/hgBlat

control samples. Nuclease-free water was added to bring the volume to 20µL. Subsequently, melt curve and agarose gel electrophoresis analyses of the qPCR products were performed.

Based on the melt curve analysis and gel results presented in *Figure 9*, Sirpa1, Sirpa2, and Sirpa4.1 primers were determined to be unspecific.

Conversely, Sirpa3 and Sirpa4.2 demonstrated high specificity, indicated by single peaks in the melt curve and single bands on the gel corresponding to their expected amplicon lengths. The No-RT-Controls for these primers showed significantly higher Ct values and multiple gel bands, confirming the absence of genomic DNA replication. The optimal annealing temperature was established at 60°C for future experiments, as no significant Ct value changes were observed across the temperature gradient.

Consequently, the primer pairs Sirpa3 and Sirpa4.2 were selected for further validation.

To evaluate the qPCR efficiency of the primer pairs, a 1:4 serial dilution of RNA from M1-Macrophage-RNA was conducted. The dilution ranged from a starting concentration of 2.5ng/µl to an end concentration of 0.0024ng/µl. Technical no reverse transcriptase (NRT) controls were inserted at the first, fourth, and eighth dilutions, as shown in *Figure 10 (A)*.

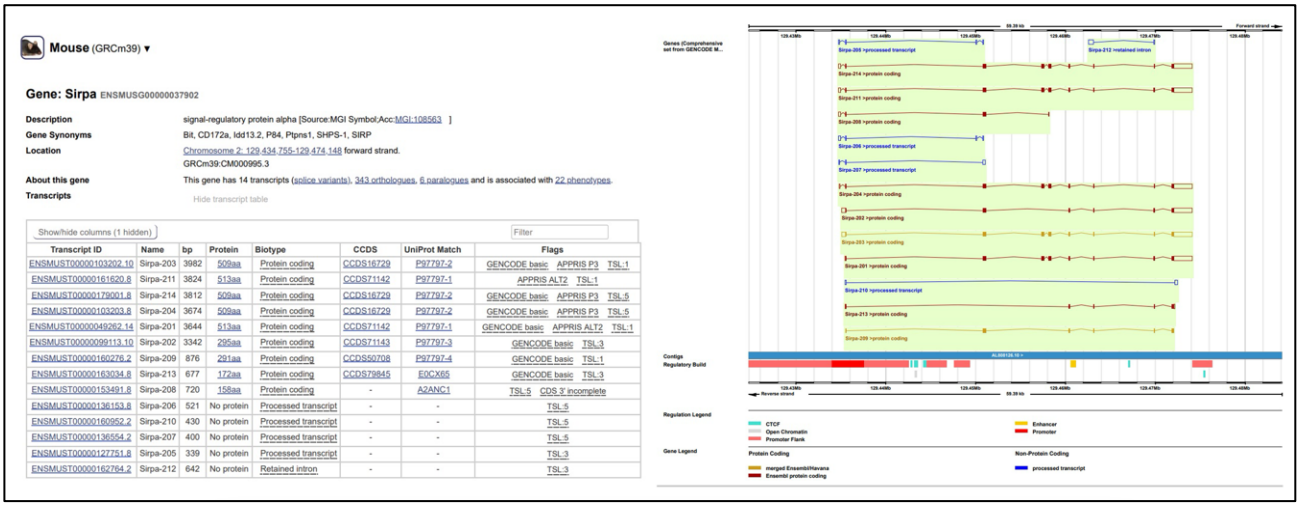

Figure 8: Target gene and its transcripts

Ensembl Data Base Information for the murine gene SIRPA and its known transcripts.

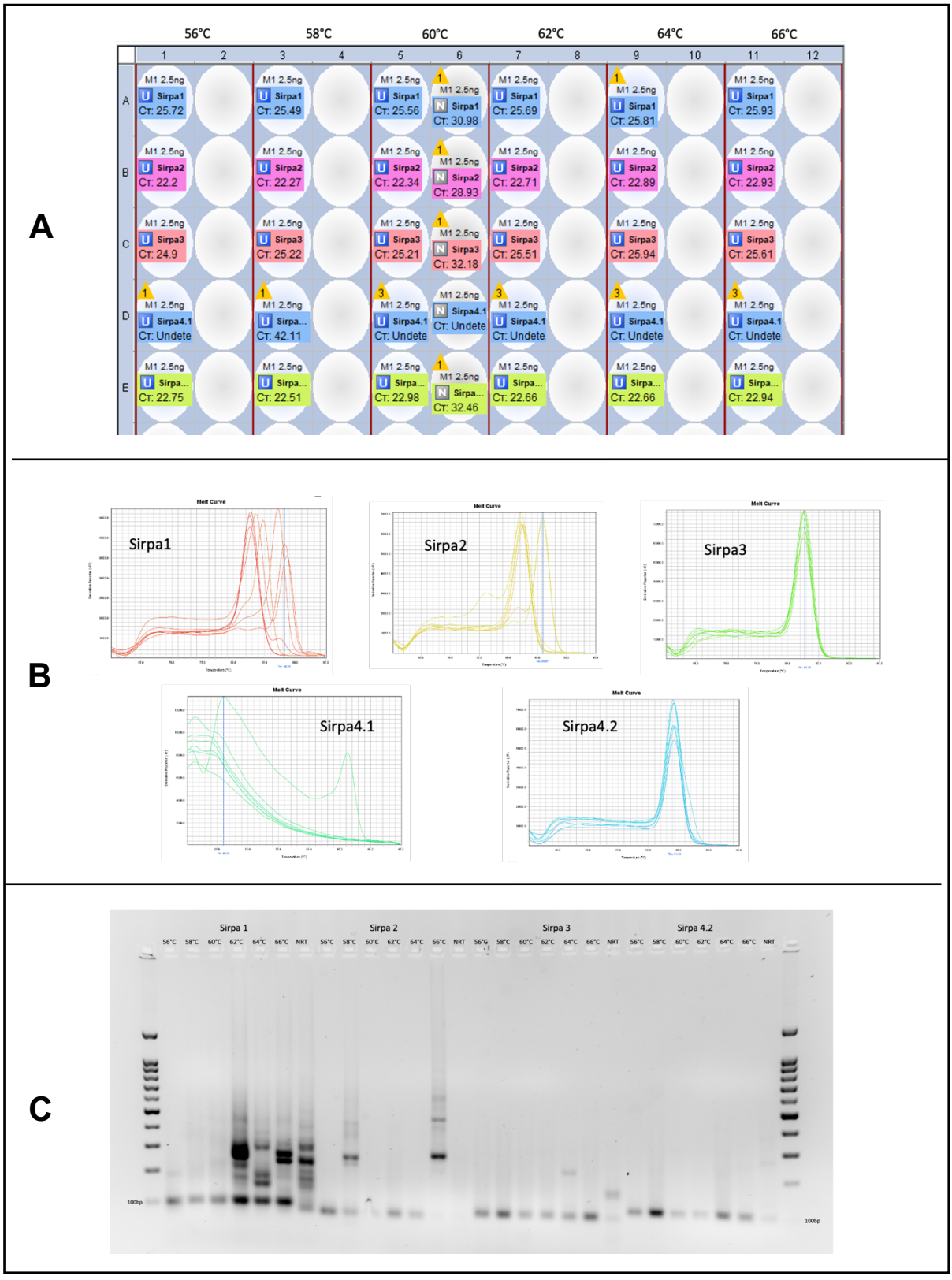

Figure 9: Testing the annealing temperature of primer pairs

Threshold Values (Ct) of different SIRPA primer pairs throughout a temperature gradient. Wells marked with the grey N label represent the no-RT-controls (A). Melt Curve analysis of the amplification products of the primers (B). Agarose Gel Electrophoresis of the qPCR products (C).

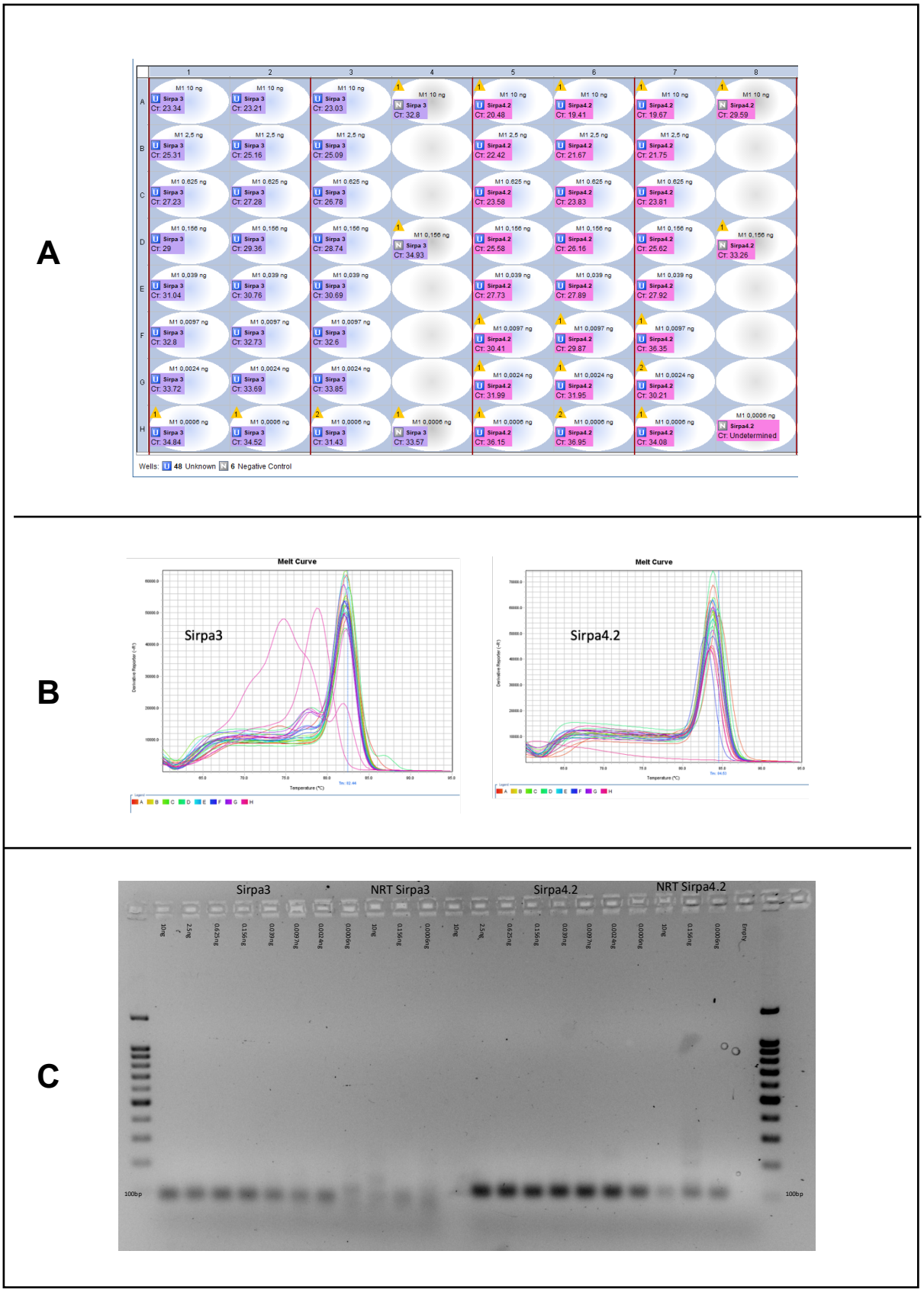

Figure 10: Testing the qPCR efficiency of primer pairs

Threshold Values (Ct) of primer pairs SIRPA3 and SIRPA 4.2 using a serial dilution of RNA. Wells marked with the grey N label represent the no-RT-controls (A). Melt Curve analysis of the amplification products (B). Agarose Gel Electrophoresis of the qPCR products.

The one-step RT-qPCR setup included 4µl of template RNA varying from 10ng to 0.0006ng, alongside 10µl of Luna Universal One-Step Reaction mix, 5µl of the selected Primer-Pair Stock (either Sirpa3 or Sirpa4.2), and 1µl of RT Enzyme Mix, which was omitted for no-RT samples, with nuclease-free water added to reach a total volume of 20µl. Primer specificity was confirmed through melt curve analysis and gel electrophoresis, ensuring the correct target amplification. *(Figure 10, B and C)*

qPCR efficiency, illustrated in **Figure *11***, was determined by plotting the mean Ct values against the log of RNA concentration, calculating the efficiency as [$10^{(-1/slope)}$ – 1], with the ideal range being 90-110%.

Considering all data, Sirpa4.2, with an efficiency of 102,34%, emerged as the most suitable primer pair for future experiments, demonstrating its validity and robustness for qPCR analysis. This design and validation steps were taken for all other primers used.

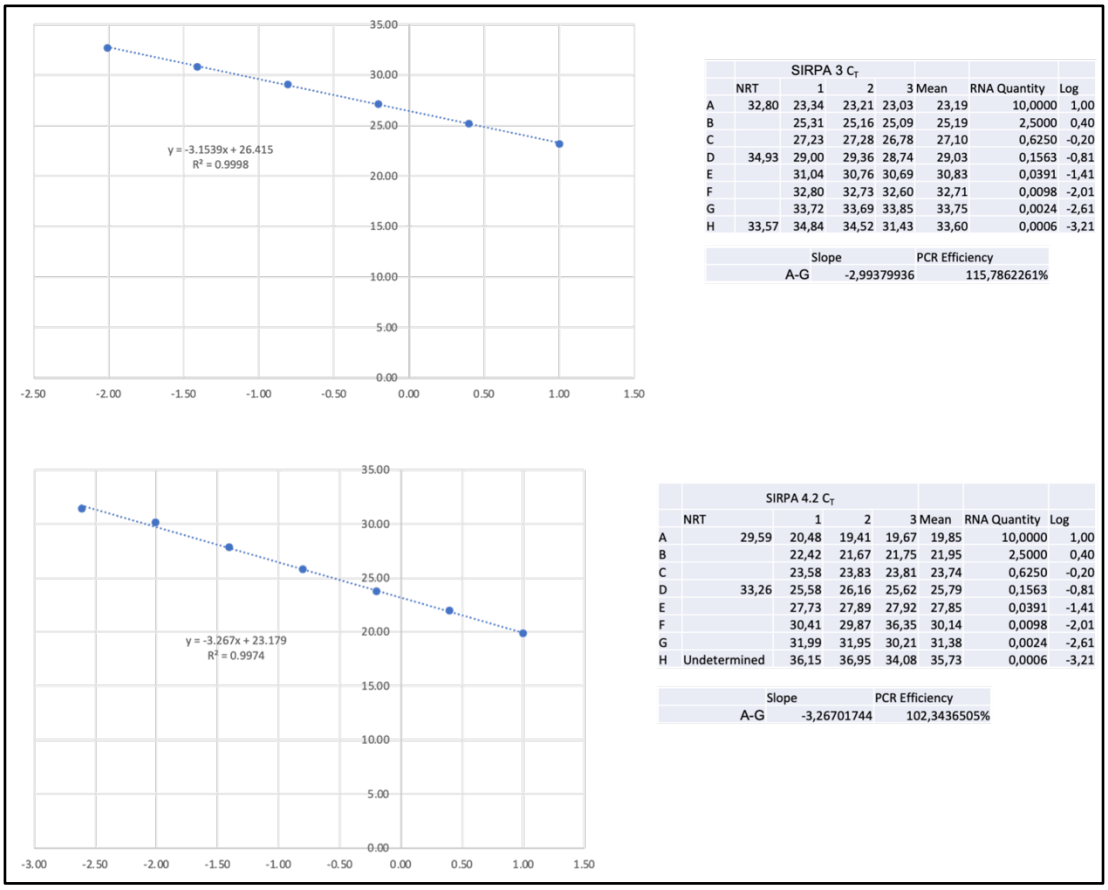

SIRPA 3 C_T

	NRT	1	2	3	Mean	RNA Quantity	Log
A	32,80	23,34	23,21	23,03	23,19	10,0000	1,00
B		25,31	25,16	25,09	25,19	2,5000	0,40
C		27,23	27,28	26,78	27,10	0,6250	-0,20
D	34,93	29,00	29,36	28,74	29,03	0,1563	-0,81
E		31,04	30,76	30,69	30,83	0,0391	-1,41
F		32,80	32,73	32,60	32,71	0,0098	-2,01
G		33,72	33,69	33,85	33,75	0,0024	-2,61
H	33,57	34,84	34,52	31,43	33,60	0,0006	-3,21

	Slope	PCR Efficiency
A-G	-2,99379936	115,7862261%

SIRPA 4.2 C_T

	NRT	1	2	3	Mean	RNA Quantity	Log
A	29,59	20,48	19,41	19,67	19,85	10,0000	1,00
B		22,42	21,67	21,75	21,95	2,5000	0,40
C		23,58	23,83	23,81	23,74	0,6250	-0,20
D	33,26	25,58	26,16	25,62	25,79	0,1563	-0,81
E		27,73	27,89	27,92	27,85	0,0391	-1,41
F		30,41	29,87	36,35	30,14	0,0098	-2,01
G		31,99	31,95	30,21	31,38	0,0024	-2,61
H	Undetermined	36,15	36,95	34,08	35,73	0,0006	-3,21

	Slope	PCR Efficiency
A-G	-3,26701744	102,3436505%

Figure 11: Calculation of primer pair efficiency

Calculations and linear graphical illustration of qPCR efficiency of primer pair SIRPA 3 (above) SIRPA 4.2 (below).

3.2 Characterization of Macrophage Polarization

To characterize the two opposite macrophage phenotypes, gene expression analysis was performed utilizing RT-qPCR. Primers for a collection of marker genes, recognized in existing literature for differentiating the transcriptomic landscapes of the macrophage states, were validated for the *in vitro* polarization model. The target genes selected for analysis included CD206, Arg1, Timp1, YM1, CCL2, iNOS, IL-12, and IL-10. The outcomes of these analyses are shown in *Figure 12* and *Figure 13*.

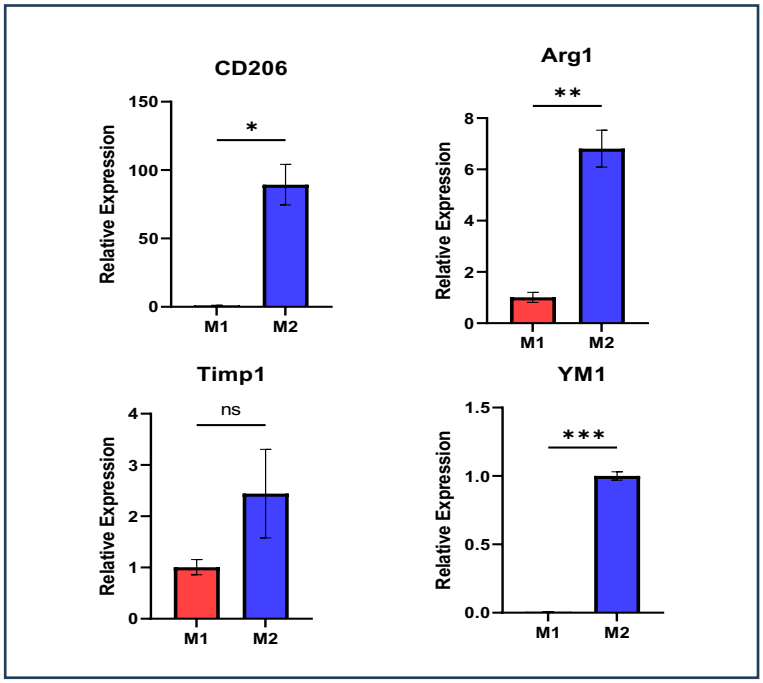

Figure 12: M2 markers

2.5x10^5 differentiated BMDMs were seeded in a 12 well plate, polarized for 48 hours using either IFNγ and LPS or IL-4 and IL-13 to induce the M1 or M2 phenotype and RNA samples were extracted. Gene Expression Analysis of M1 versus M2 Macrophages Target Genes: Arg1, CD206, Timp1, and YM1. Reference genes: TBP and PPIA. Expression levels relative to the M1 group.

Macrophages polarized with IL4 and IL13, designated as M2 macrophages, exhibited elevated expression levels of CD206, Arg1, Timp1, and YM1. Conversely, macrophages treated with IFNγ and LPS, referred to as M1 macrophages, demonstrated heightened expression of CCL2, iNOS, and IL12.

Notably, M1 macrophages also presented increased levels of IL10. Given that IL10 is predominantly associated with M2 macrophages in the literature, it was excluded as a marker from further analysis.

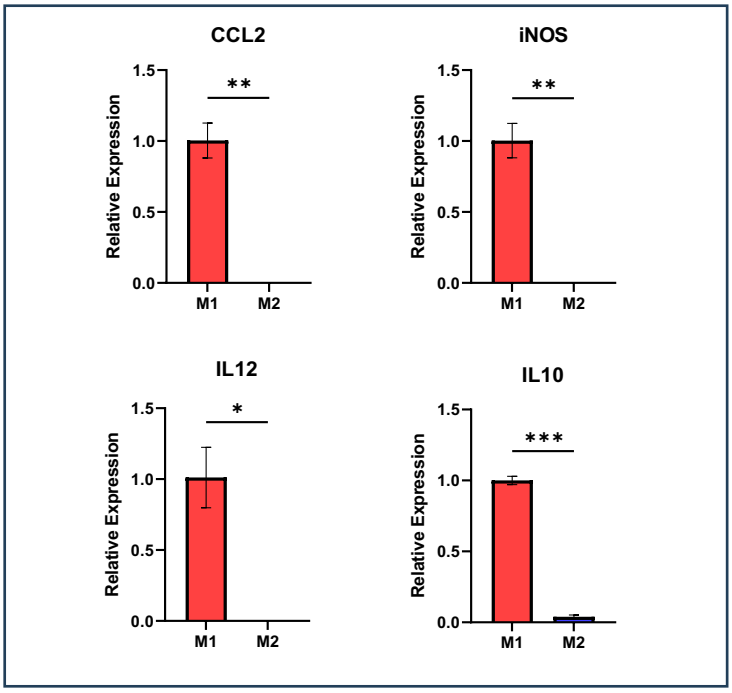

Figure 13: M1 markers

2.5x10^5 differentiated BMDMs were seeded in a 12 well plate, polarized for 48 hours using either IFNγ and LPS or IL-4 and IL-13 to induce the M1 or M2 phenotype and RNA samples were extracted. Gene Expression Analysis of M1 versus M2 Macrophages Target Genes: CCL2, iNOS, IL-12, IL-10. Reference genes: TBP and PPIA. Expression levels relative to the M1 group.

The selection of RT-qPCR markers was based on delineating the distinct states of macrophages. Establishing baseline profiles enabled the detection of phenotypic alterations during the experiments. By characterizing M1 and M2 phenotypes through qPCR-based gene expression profiles, phenotype transitions could also be identified. A decrease in M2 marker expression coupled with an increase in M1 markers would indicate a shift toward the M1 phenotype, and vice versa.

3.3 Optimization of Experimental Parameters

The initial phase of this research project was dedicated to refining the experimental parameters. Given the straightforward nature of the experimental design, precise optimization was essential to ensure the validity of results for the large-scale screening of novel siRNAs. This involved establishing optimal incubation periods for each step of the process, from polarization and treatment (specifically, transfection) to the extraction of RNA samples. Moreover, selecting an appropriate control siRNA and transfection reagent constituted a critical component of the optimization phase. Most importantly, it was crucial to demonstrate the feasibility of the methodological approach to explore the phenotypic transition in macrophages.

3.3.1 Determination of Optimal Incubation Intervals

In the absence of definitive benchmarks for incubation durations within the experimental framework, three distinct temporal sequences bridging cell polarization and siRNA transfection to RNA isolation were evaluated.

Scenario A involved a 24-hour incubation following cell polarization before the application of treatment, with RNA isolation conducted 24 hours subsequently. In Scenario B, treatment was administered 24 hours post-polarization, with RNA isolation occurring 48 hours after treatment. Scenario C extended the incubation period to 48 hours post-polarization before treatment, with RNA samples extracted 24 hours later.

A pilot experiment using resiquimod (R948)—a TLR7/8 agonist recognized for its capacity to activate, i.e., enhance the innate immune response (100, 101)—was conducted not only to determine the optimal incubation intervals but also to validate the hypothesis that a macrophage phenotypic transition from M2 to M1 is feasible.

The effects of resiquimod across the three different scenarios were explored, administering 100nM of the agent (initially dissolved in water and subsequently diluted with PBS), and the gene expression of the extracted RNA was analyzed, focusing on CD206, iNOS, and Arg1 as indicative markers.

The gene expression analyses, depicted in *Figure 14,* show a consistent shift from the M2 to the M1 phenotype among macrophages treated with resiquimod. Across all incubation intervals, there was a notable reduction in the expression levels of M2-associated markers CD206 and Arg1, alongside an elevation in the M1 marker iNOS, when compared to the baseline of untreated, M2-polarized macrophages.

Despite the uniform significance of the results across each interval, the fold changes, although marginal, were most pronounced during scenario C. Here, the application of resiquimod resulted in a substantial reduction in the expression of CD206 and Arg1 by 29- and 43-fold, respectively, and amplified iNOS expression by up to 100-fold, as calculated from mean values of both groups. Therefore, for all subsequent experiments, macrophages would undergo transfection 48 hours following polarization, with RNA samples extracted 24 hours post-treatment (according to Scenario C).

These outcomes not only underscore the plausibility of inducing a phenotypic switch but also underscore the robustness of the experimental framework and detection methods.

Furthermore, these findings align with existing literature, reinforcing resiquimod's role as a powerful agent in promoting the pro-inflammatory capabilities of macrophages, including the transition of M2 polarized macrophages to an M1 state.

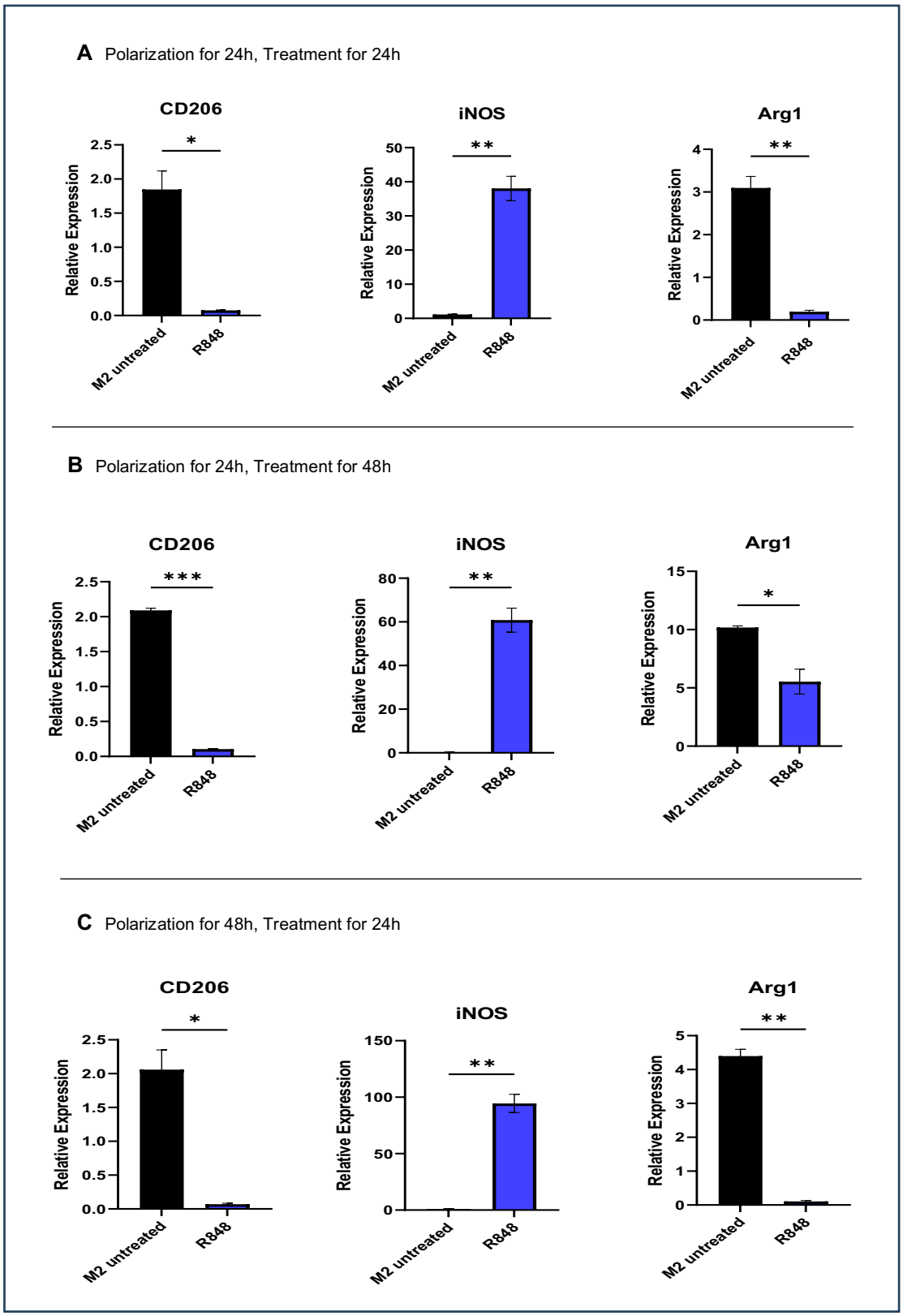

Figure 14: Incubation interval testing with resiquimod (R848)

Effects of R848 treatment compared to untreated M2 macrophages in three different scenarios (A, B, C). Target Genes: CD206, iNOS and Arg1. Reference genes: TBP and PPIA. Expression levels relative to a third sample not shown in the graphs for better visualization.

3.3.2 Transfection Control Group Assessment

To ensure that the transfection control would have no influence on the macrophage phenotype, an assessment of the control group was necessary. Addressing this issue required a dual approach, examining both the control siRNA and the transfection reagents employed.

Two alternative control siRNA sequences were tested: a non-targeting scrambled sequence siRNA (siNTC) and an siRNA targeting Luciferase (siLUC), commonly employed as a control in various assays. M2 macrophages were transfected with these siRNAs using three different commercial transfection reagents: TransIT-X2® (R1), TransIT-TKO® (R2), and INTERFERin® (R3).

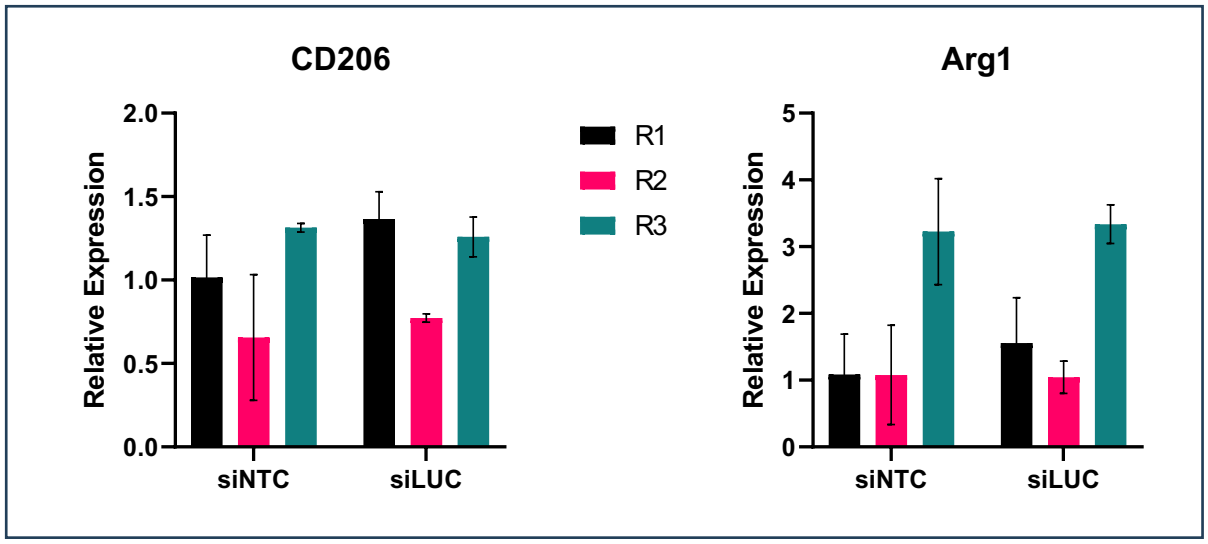

Figure 15: Effects of different control siRNA and transfection reagents on M2 polarized macrophages

Comparison of M2 macrophages transfected with either siNTC or siLUC, using one of the transfection reagents TransIT-X2® (R1), TransIT-TKO® (R2), or INTERFERin® (R3). Target Genes: CD206 and Arg1. Reference genes: TBP and PPIA. Expression levels relative to siNTC-R1 group.

Gene expression analysis, focusing on M2 macrophage markers CD206 and Arg1, facilitated comparisons across groups and the results are presented in *Figure 15.* The premise was that groups exhibiting higher expression levels of these markers were more aligned with the M2 phenotype, mirroring the expression profile of untreated M2 macrophages.

The comparison between control siRNA sequences revealed no apparent differences between siNTC and siLUC, leading to the selection of Luciferase siRNA as our control based on its cost-efficiency and similar performance to the scrambled sequence.

However, significant variability was observed among the transfection reagents, particularly when comparing TransIT-TKO® (R2) against the alternatives TransIT-X2® (R1) and INTERFERin® (R3). This highlighted the crucial role of reagent choice in minimizing unintended phenotype reprogramming effects in our control group.

Further investigation of the effects of R1 and R3 was decided upon, which exhibited fewer off-target effects compared to R2 when using siLUC. Differentiating between the nonspecific impacts of control siRNA and the potential modulatory actions of the transfection reagents involved comparing gene expression levels of various M1 and M2 markers among untreated M2 macrophages, M2 macrophages transfected with siLUC using R1 or R3, and the transfection reagents alone.

The results, which are shown in *Figure 16,* further supported prior findings, spotlighting the modulatory capabilities of the transfection reagents as siRNA vehicles. The comprehensive marker panel revealed significant effects, particularly on Arg1 and CCL2.

Observations indicated that transfection reagents alone mirrored the gene expression alterations seen with siLUC control, without notable differences between TransIT-X2® (R1) and INTERFERin® (R3). Therefore, the ongoing analysis of control group optimization continued to search for the most suitable transfection reagent.

3.3.3 Transfection Reagents Assessment

The search to identify a transfection reagent with minimal to no influence on the gene expression profiles of untreated M2 macrophages firstly required an assessment of transfection efficiency. The efficacy of an siRNA targeting Fra2 (siFra2) in knocking down its target's expression in M2 macrophages was evaluated using both TransIT-X2® (R1) and INTERFERin® (R3).

Also, considering findings from *Chapter 3.3.2*, which implicated the transfection reagent as a significant factor in unintended phenotypic alterations, reduced dosages of these reagents were tested alongside their standard recommended amounts.

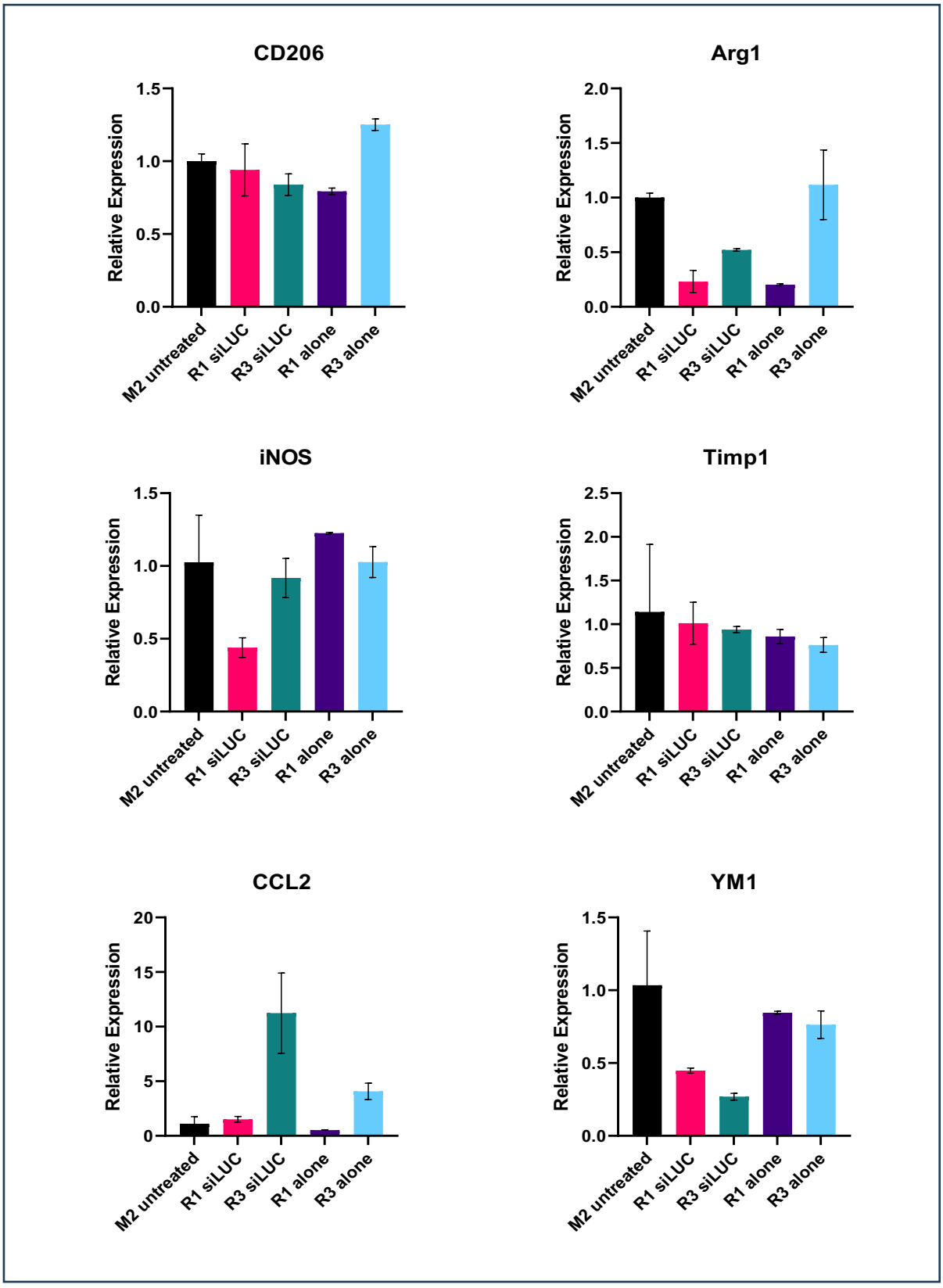

Figure 16: Effects of transfection reagents on M2 phenotype gene expression

Effects of TransIT-X2® (R1) or INTERFERin® (R3) alone and siLUC transfection using either R1 or R3, compared to untreated M2 macrophages. Target Genes: CD206, Arg1, iNOS, Timp1, CCL2, YM1. Reference genes: TBP and PPIA. Expression levels relative to untreated M2 macrophages.

The results, illustrated in *Figure 17* , demonstrated that TransIT-X2® (R1) achieved superior transfection efficiency, manifesting an 80% target knockdown for both standard and reduced dosages, compared to the 50% knockdown by INTERFERin® (R3) and a 25% knockdown by a reduced dosage of R3. Consequently, TransIT-X2® emerged as the most effective transfection reagent among those tested.

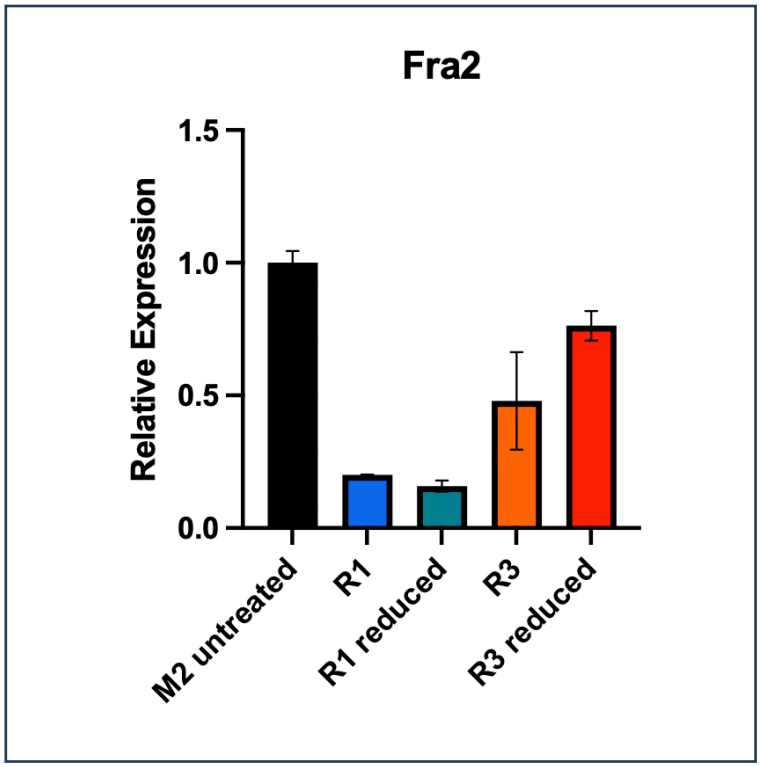

Figure 17: Effects of the amount of transfection reagent on knockdown efficiency

siFra2 Knockdown Efficiency of TransIT-X2® (R1) and INTERFERin® (R3) using the recommended amount, or half the recommended amount (R1 and R3 reduced), compared to non-transfected (untreated) M2 macrophages.Target Genes: Fra2. Reference genes: TBP and PPIA. Expression levels relative to untreated M2 macrophages.

Notably, halving the quantity of the transfection reagent did not compromise gene knockdown efficiency, suggesting a strategy to lessen off-target effects without forfeiting transfection effectiveness.

With these insights, the final phase of the evaluation involved re-testing the non-targeting control siRNA (siLUC) using the selected TransIT-X2® vehicle at both the standard and reduced dosages, as depicted in **Figure *18***. The aim was to align the gene expression profile

of the transfection control group as closely as possible with that of untreated M2 macrophages, thereby minimizing any transfection-induced phenotypic modulations.

As anticipated, reducing the transfection reagent dosage mitigated the undesired effects on macrophage phenotype, with nearly indistinguishable expression levels of CD206 and Arg1 between untreated M2 macrophages and the siLUC group at the reduced dosage. However, some deviations in iNOS and CCL2 expression persisted.

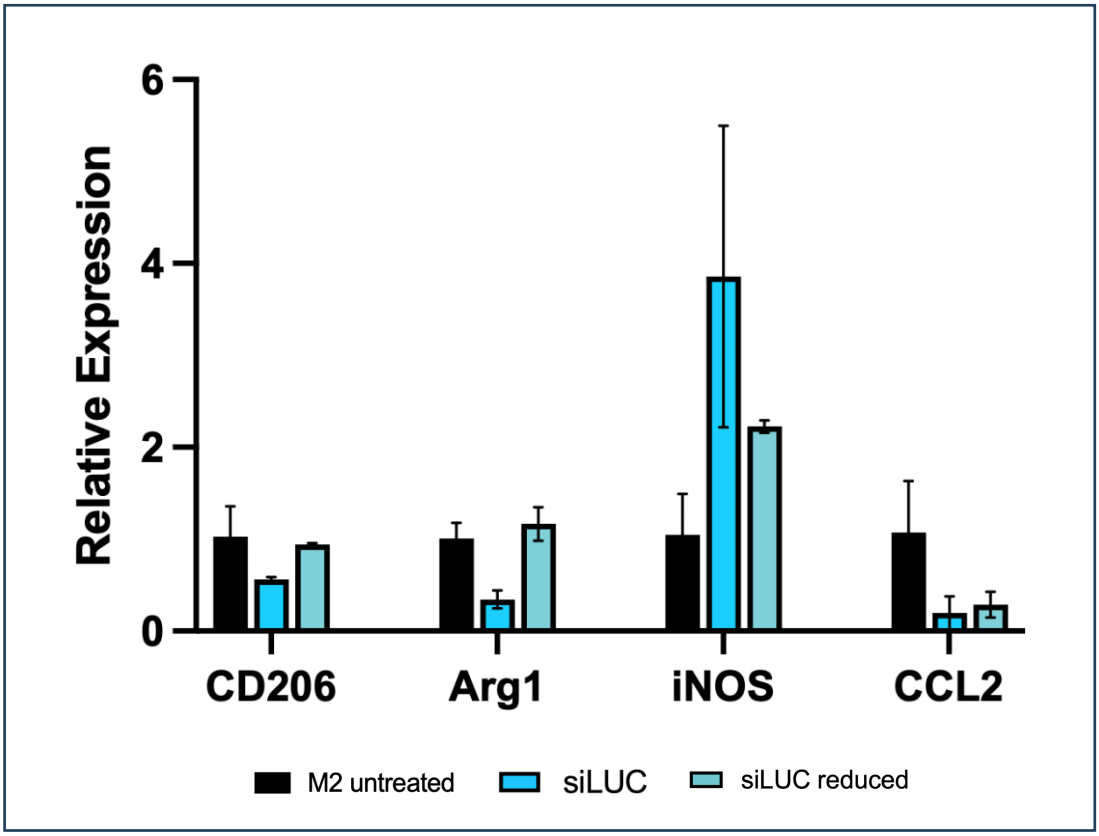

Figure 18: Gene expression levels of the optimized control group

M2 macrophages were transfected with the control siLUC using either the recommended amount of transfection reagent (siLUC) or half the amount (siLUC reduced). Gene expression analysis comparison of the two different control groups and untreated M2 macrophages was conducted. Target Genes: CD206, Arg1, iNOS, CCL2. Reference genes: TBP and PPIA. Expression levels relative to untreated M2 macrophages.

While ideally the transfection control should mirror the native phenotype entirely, it was determined that certain discrepancies induced by the transfection process itself are inevitable. Thus, further optimization efforts to completely eliminate these differences were deemed impractical, marking the end to the optimization of the experimental parameters.

3.3.4 Optimized Assay for Screening siRNA

To recapitulate the results from the past sections, a brief description of the optimized assay is provided in this subsection to give clear overview of the target screening process that follows in the next chapter.

After generating macrophages from BMDMs as described in the Methods part of this thesis, the cells were polarized towards the M2 phenotype using 25ng/µl IL-4 and IL-13 and incubated for 48 hours. Subsequently the cells were transfected with a pooled sequence mixture of targeting siRNA or control Luciferase siRNA, using 3,75µl/well TransIT-X2® transfection reagent. 24 hours after transfection RNA samples were extracted for downstream RT-qPCR read outs. Relative Gene Expression Analyses were performed relative to the transfection control group, as to minimize potential modulating effects from the transfection process.

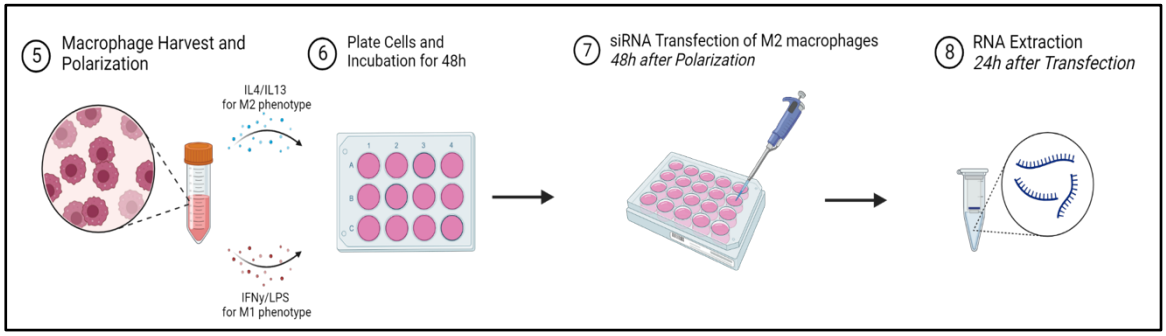

Figure 19: Final optimized assay

Graphical illustration of the optimized steps of assay. M2 macrophages were transfected with targeting siRNAs or control siLUC using halved amounts of TransIT-X2® 48 hours after polarization and subsequently incubated for 24 hours before RNA extraction. Figure created in BioRender.

3.4 Screening for Phenotypic Reprogramming via Novel siRNA Targets

Following the establishment of an optimized assay protocol, a screening process was started to evaluate the phenotypic reprogramming potential of novel siRNA candidates on M2 polarized macrophages.

The evaluation process entailed RT-qPCR analyses, focusing initially on two hallmark M2 markers, CD206 and Arg1. These markers served as primary indicators for phenotypic shifts. A reduction in their expression levels, relative to the control siLUC sample, was interpreted as a transition towards the M1 phenotype, whereas an increase suggested a reinforcement of

the M2 phenotype. For siRNA targets demonstrating significant effects, an expanded spectrum of markers was subsequently analyzed.

It is important to note that prior to the screening assay, target gene suppression was tested, despite the assurances of our siRNA provider, Horizon Discovery. However, due to the challenges associated with designing reliable RT-qPCR primers—especially for genes with small transcripts or those lacking exon-intron junctions—this testing was only possible for approximately 65% of the targets.

3.4.1 Assessing the Efficiency of Target siRNA Knockdown

To demonstrate that the screening results were not influenced by inadequate siRNA transfection efficiency, the target gene knockdown *(achieved by the mix of four siRNAs)* across the samples was first examined. This step necessitated the careful design and validation of robust RT-qPCR primers, a prerequisite for ensuring the reliability of the data. This comprehensive primer design was achievable for 13 of the 20 targets under investigation.

In instances where valid primers were available, a comparative analysis of relative gene expression post-siRNA transfection against the control sample (siLUC) was conducted, with findings illustrated in *Figure 20.*

The data clearly demonstrated effective target knockdown by the siRNA transfection across all evaluated samples. Most siRNAs achieved knockdown efficiencies exceeding 80%, with certain targets like siLGALS9, siTmem173, and siAhr showing knockdown levels of 95% or more.

These results are congruent with the performance assurances provided by Horizon Discovery, which guarantees a minimum of 75% target knockdown for their siRNA products.

However, siICOSL and siCCR2 exhibited a 50% target knockdown. The outcome in both these cases is most likely attributed to suboptimal qPCR primers and genomic DNA contamination of the samples.

Based on these findings, it appears rational to consider omitting detailed knockdown efficiency testing in future investigations, given the high efficacy rates observed.

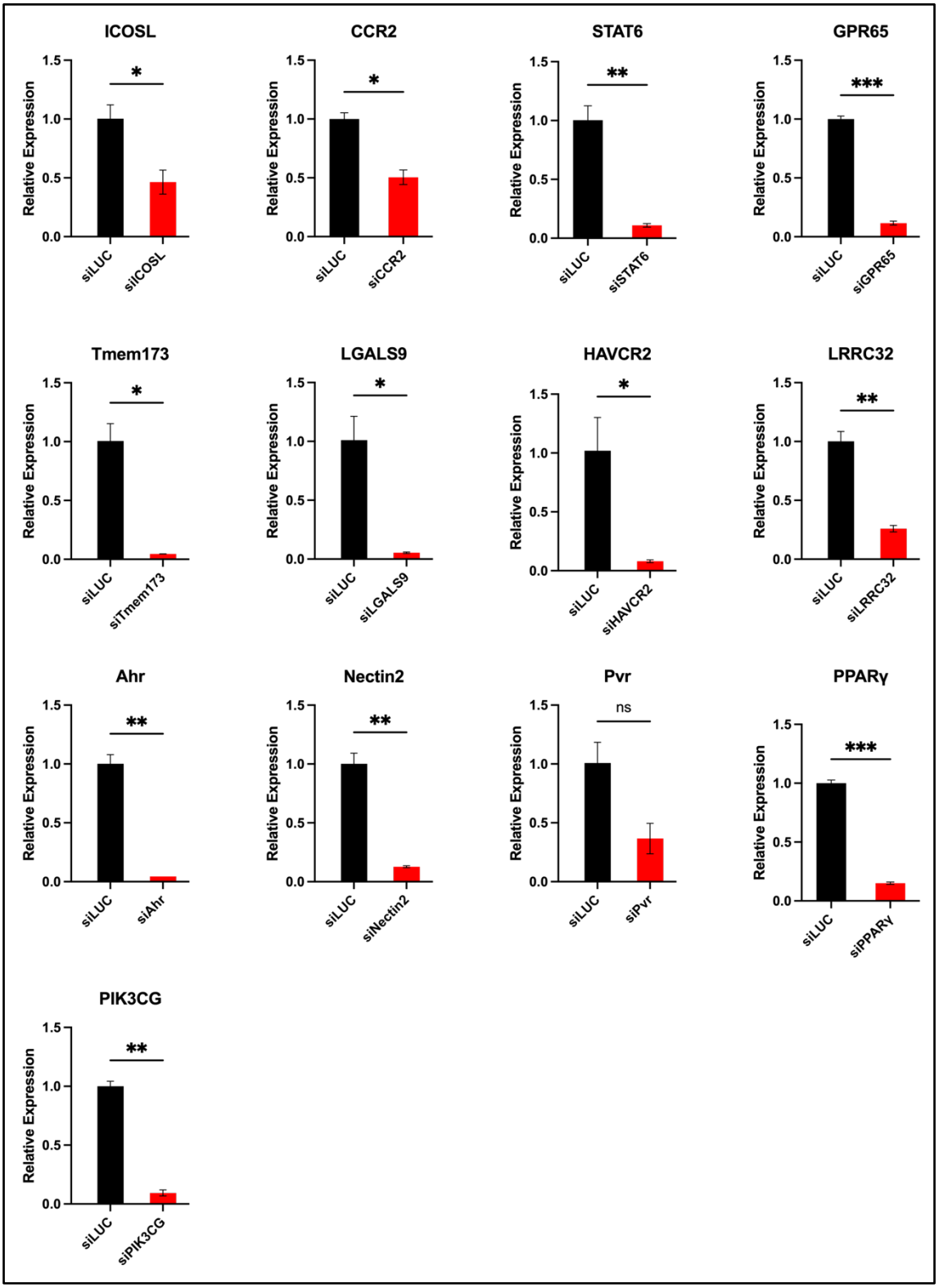

Figure 20: Target siRNA knockdown efficiency

Comparison of target gene expression levels between targeting siRNA group and transfection control group (siLUC). Reference genes: TBP and PPIA. Expression levels relative to transfection control group.

3.4.2 Initial Screening using CD206 and Arg1

This initial phase aimed to detect potential siRNA candidates for further analysis based on their influence on CD206 and Arg1 expression levels. Despite the varied significance levels of the results and the limitations imposed by small sample sizes, this screening process was intended for identifying trends in transcriptomic alterations.

The preliminary findings, shown in *Figure 21* and *Figure 22*, revealed that siRNAs targeting Twist1 and STAT6 led to a pronounced decrease in CD206 expression compared to the siLUC control group, suggesting a potential shift towards the M1 phenotype. Conversely, siRNA treatments aimed at Pvr and Tigit were associated with a notable increase in CD206 expression, suggesting an enhancement of M2 characteristics. This pattern was similarly observed, though not reaching statistical significance, in samples treated with siRNAs directed against Tmem173, Nectin2, CCR2, GPR65, Olfr2, and PPARγ, indicating potential M2 phenotype-enhancing effects.

In parallel, the expression of Arg1 was diminished following transfection with siTwist1 and siSTAT6, further supporting the notion of a reprogramming towards the M1 phenotype, in line with the observations related to CD206. Conversely, statistically significant elevated Arg1 levels were recorded for siTmem173 and siCXCL2, and trends indicating increased expression for siRNAs targeting Nectin2, Olfr2, Ahr, ICOS-L, and PPARγ.

3.4.3 Expanded Marker Analysis for siSTAT6 and siTwist1

After their identification as promising candidates for reprogramming M2 macrophages towards an M1 phenotype, siSTAT6 and siTwist1 were subjected to further study. This next stage of analysis focused on additional phenotype-defining markers: iNOS, CCL2, and YM1, with findings detailed in Figure 23.

In line with prior observations, siSTAT6 demonstrated a significant reduction in YM1 levels, coupled with an elevation in CCL2 levels. This pattern underscores siSTAT6's potential to facilitate a phenotypic shift towards the M1 state. Although expression of the M1 marker iNOS appeared marginally reduced in comparison to the control group, this variance did not reach statistical significance.

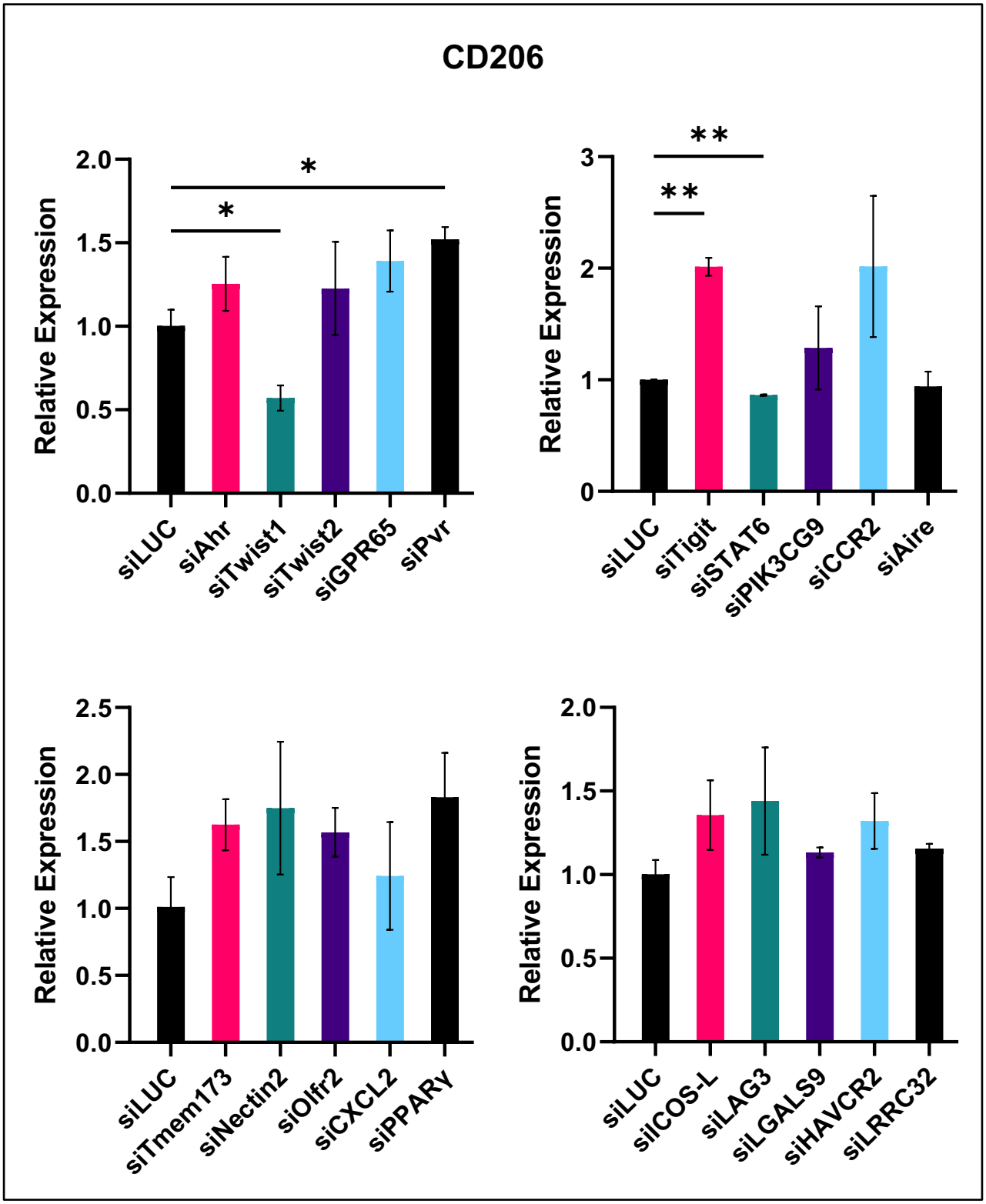

Figure 21: Initial siRNA screening using CD206 expression

48 hours after polarization, M2 macrophages were transfected with targeting siRNA (a pool of 4 sequences) or with the non-targeting siLUC. RNA samples were collected after 24 hours of treatment incubation. RT-qPCR analyses of the targeting siRNAs were conducted in batches of 5 and compared to siLUC . Target Gene: CD206. Reference genes: TBP and PPIA. Expression levels relative to transfection control group.

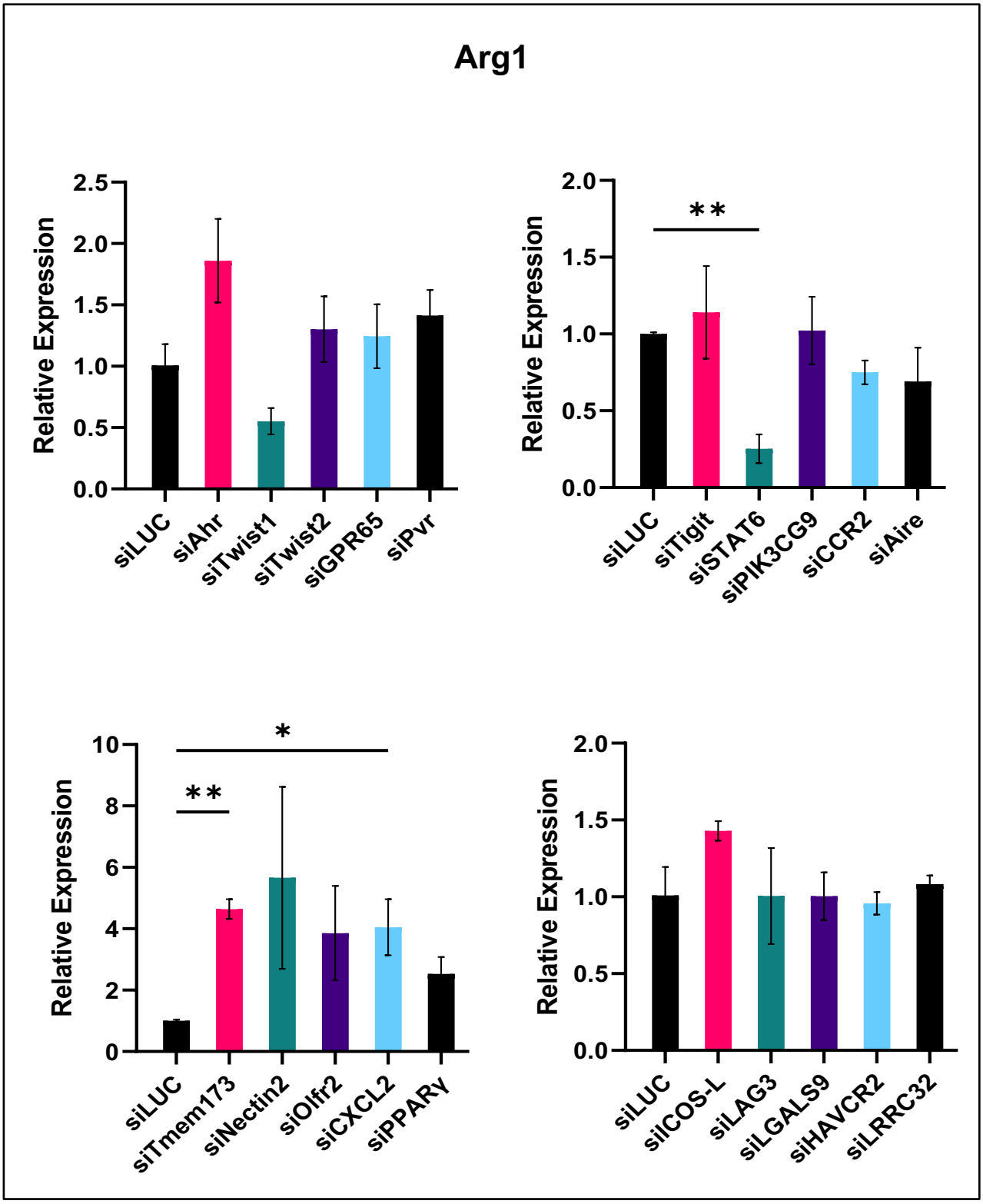

Figure 22: Initial siRNA screening using Arg1 expression

48 hours after polarization, M2 macrophages were transfected with targeting siRNA (a pool of 4 sequences) or with the non-targeting siLUC. RNA samples were collected after 24 hours of treatment incubation. RT-qPCR analyses of the targeting siRNAs were conducted in batches of 5 and compared to siLUC. Target Gene: Arg1. Reference genes: TBP and PPIA. Expression levels relative to transfection control group.

Conversely, siTwist1 exhibited trends indicative of an M1 phenotype transition, with an increase in iNOS levels and a decrease in YM1 levels, neither of which were statistically significant. Notably, CCL2 levels remained unchanged relative to the siLUC control group, suggesting a nuanced effect on macrophage reprogramming.

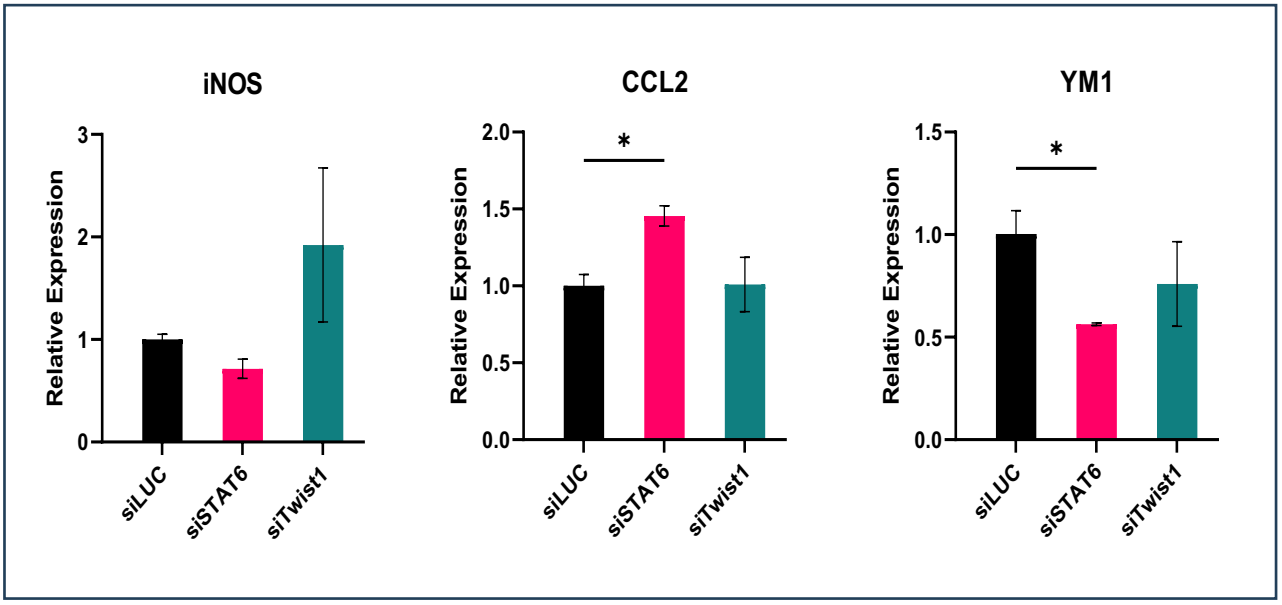

Figure 23: Extended panel of markers for siSTAT6 and siTwist1

for siSTAT6 and siTwist1, the two promising candidates emerging from the initial screening as promising candidates, the expression levels of further markers were compared to the control group. Target Genes: iNOS, CCL2, YM1. Reference genes: TBP and PPIA. Expression levels relative to transfection control group.

These data suggest that both siSTAT6 and siTwist1, while reducing CD206 and Arg1 expression, simultaneously downregulate other M2 markers while upregulating M1 markers, reinforcing their significance as potential candidates for M2 macrophage reprogramming.

The collected evidence positions siSTAT6 and siTwist1 as important subjects for further exploration, particularly regarding their application as novel therapeutic agents within macrophage-focused immunotherapy strategies.

3.5 Additional Data

3.5.1 Target Gene Expression Across Macrophage Phenotypes

To further delve into the biological functions of the targeted genes in macrophage polarization, the expression levels of a selection of targeted genes was investigated in M1 and M2 polarized macrophages and the fold changes were compared, as shown in *Figure 24*.

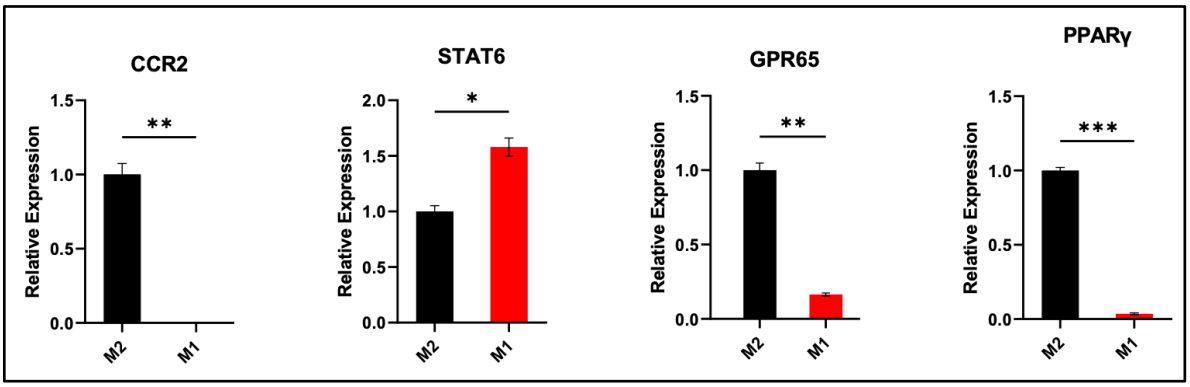

Figure 24: Target Gene Expression in M1- and M2-type macrophages

BMDMs were polarized for 48 hours using either IFNγ and LPS or IL-4 and IL-13 to induce the M1 or M2 phenotype before extracting RNA samples. Comparative gene expression analysis was conducted between M1 and M2 macrophages. Target Genes: CCR2, STAT6, Gpr65, and PPARγ. Reference genes: TBP and PPIA. Expression levels relative to the M2 group.

Expression levels of CCR2, STAT6, GPR65 and PPARγ showed differences between the two macrophage phenotypes. Interestingly, M2 macrophages showed strikingly higher expression levels of CCR2 (1000-fold change), GPR65 (10-fold change), and PPARγ (30-fold change), when compared to M1 macrophages. Yet siRNA inhibition of these genes, resulted in an enhanced M2 phenotype rather than a reprogramming towards the M1 phenotype, as previously seen in *Chapter 3.4.2*.

STAT6 on the other hand, had 1,5-fold higher expression levels in M1 macrophages compared to M2 macrophages, but siRNA targeted STAT6 inhibition showed a phenotype switch from the M2 towards the M1 phenotype.

The results underscore the complexity of macrophage phenotype regulation and suggest that certain siRNAs may influence macrophage polarization regardless of their target expression level differences between the two phenotypes.

3.5.2 Effects of siSIRPA and siFra2 on M2 Macrophages

siFra2 and siSIRPA were investigated using the optimized screening assay to examine their effects on M2 macrophages.

The transfection with both siRNAs yielded significant target gene knockdown, aligning with outcomes observed for previously tested targets—achieving a 90% knockdown for siSIRPA and 75% for siFra2, as shown in *Figure 25*.

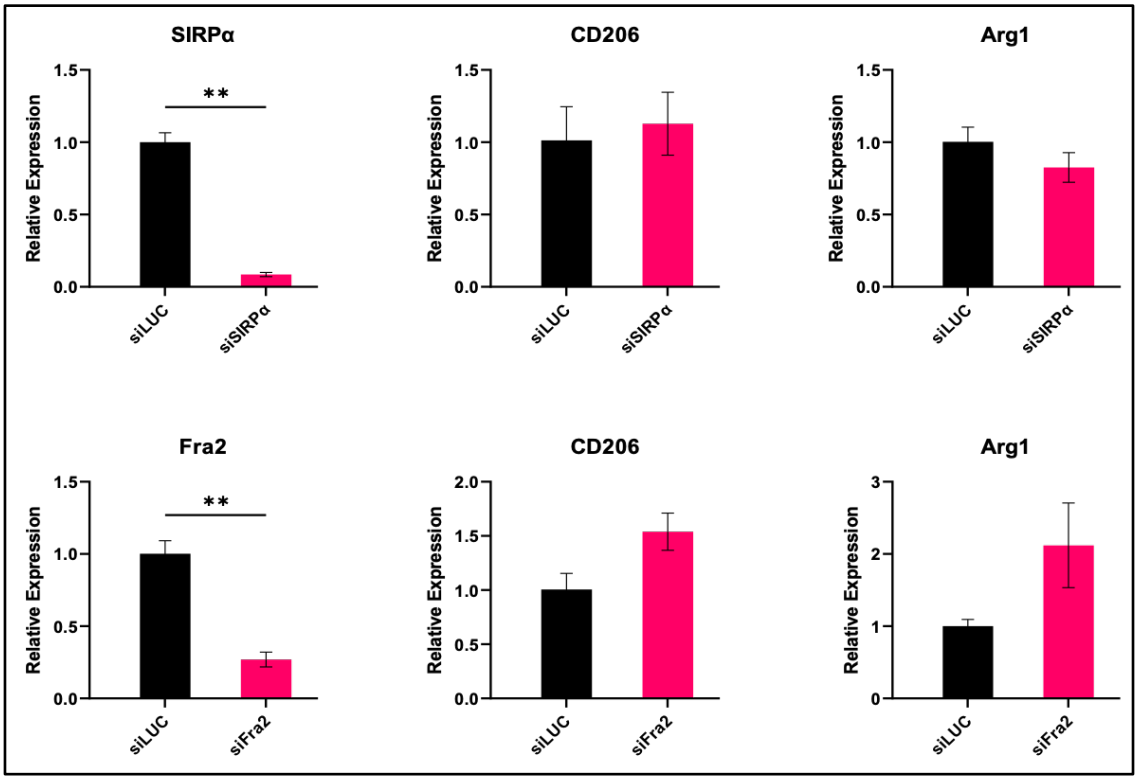

Figure 25: siSIRPA and siFra2 effects on M2 macrophages

Similarly to the initial screening of the other targeting siRNAs, M2 macrophages were transfected with siSIRPA or siFra2 and compared to siLUC. Target knockdown efficiency and CD206 and Arg1 marker expression levels were investigated. Target Genes: SIRPA, Fra2, CD206, and Arg1. Reference genes: TBP and PPIA. Expression levels relative to transfection control group (siLUC).

The results of the siSIRPA transfection revealed no detectable changes in the expression levels of the phenotypic markers when compared to the control group. In contrast, siFra2 transfection was associated with an increase in the expression levels of both CD206 and Arg1. These trends, even though statistically not significant, indicate an enhanced M2 phenotype.

4 Discussion

Immunotherapies have become an important research focus in the past decades, with much of the work concentrating on cells of the adaptive immune system, such as T lymphocytes. However, more recently there has been a growing interest in therapies based on the innate immune system and especially on macrophages.

As bridges between the innate and the adaptive system, macrophages also represent attractive targets for novel therapies, since they are one of the most abundant immune cells present in most tissue and play central roles in the pathophysiology of inflammation, fibrosis and malignancies.

Therefore, the foundation of macrophage-based therapeutic strategies lies in the numerous functions of macrophages and particularly in their phenotypic plasticity. In diseases, macrophages lose their homeostatic low-level physiological functions and change their phenotype into subtypes that functionally contribute to inflammation and either the progression or regression of these pathologies. Hence, switching their phenotype is a practical approach for developing new therapies.

Additionally, several other strategies are being explored, such as inhibiting macrophage interactions with other cells in the microenvironment, blocking monocyte migration and differentiation into macrophages, and enhancing phagocytic activity, or by targeting immune checkpoints, including the use of employing bi-specific antibodies. Other approaches include depleting TAMs, employing cell-based strategies like CAR-macrophages (CAR-M) or *ex vivo* polarization followed by adaptive transfer *in vivo*, and targeting macrophage immune resistance mechanisms other than classical checkpoints to sensitize cancers to further immunotherapies (102-105).

Some of these innovative macrophage-based strategies are currently being tested in early-phase clinical trials for various solid tumors. These trials have shown that such treatments are generally well-tolerated, can provoke a substantial immune response against tumors, and, in some cases, result in significant tumor reduction and prolonged survival, especially when combined with other treatments such as checkpoint inhibitors or chemotherapy (106, 107). Examples include a Phase IIb trial assessing the effect of *motixafortide* (a CXCR4 inhibitor) combined with pembrolizumab in patients with metastatic pancreatic cancer (Trial No. NCT02826486) and A Phase I/II trial confirming the safety and efficacy of intratumoral *tilsotolimod* (a TLR9 agonist) in combination with ipilimumab or pembrolizumab in patients with anti-PD-1 refractory metastatic melanoma (Trial No. NCT03445533).

Combining macrophage-based therapies with other treatments, such as chemotherapy, radiotherapy, or classical immune checkpoint inhibitors, bears potential to enhance the overall therapeutic efficacy by leveraging the complementary mechanisms of different treatments, hereby reducing the development of therapy resistance in cancer.

4.1 siRNA Targeted Macrophage Reprogramming

In this research project, my aim was to shift macrophages from an immunosuppressive M2 phenotype to a pro-inflammatory M1 phenotype using siRNA. We selected various target genes for gene silencing through RNA interference and designed a screening assay to observe the effects on macrophage phenotypes.

I isolated murine bone marrow cells in large quantities, pooled them, and froze them for later use without compromising their subsequent differentiation into macrophages or their *in vitro* polarized M1 and M2 subsets, in line with other studies (108), and by doing so improved workflow efficiency.

My studies also highlighted that different transfection reagents influenced not only transfection efficiency but also had intrinsic modest reprogramming effects on macrophages, as detailed in *Chapter 3.3.3*. While these effects are not entirely unavoidable, I was able to mitigate them, ensuring that side effects were minimized and that the combined efficacy of the siRNA treatment and vehicle exceeded that of the vehicle alone. Additionally, I successfully optimized the transfection control group by using specific siRNA sequences targeting Luciferase and by reproducibly obtaining reliable readouts by employing only half the protocol-recommended amount of transfection reagent. This optimization not only ensured reliable data but also conserved resources, contributing to more sustainable research practices.

A notable drawback in optimizing and conceptually validating our assays was the absence of a positive siRNA control; that is, a siRNA that would clearly yield the desired—yet, in many aspects, still elusive—macrophage repolarization. However, we used resiquimod for validation, a strong *in vitro* M2 to M1 macrophage polarizing agent. Notably, treatment with resiquimod resulted in a simultaneous shift of all markers used in the gene expression analysis, lowering M2 markers and increasing M1 markers.

Resiquimod has been tested as an immunomodulator in combination therapies for cancer and has shown positive outcomes. Our results confirm and complement other studies, demonstrating that resiquimod is a potent M1-polarizing agent *in vitro*, suggesting that its

potential as an immune modulator *in vivo* is likely due to its phenotype-shifting effects on macrophages. However, its efficacy *in vivo* still requires further investigation (109-113).

For our siRNAs, the effects were not as pronounced as with resiquimod treatment. Initial screening revealed that not all siRNA targets affecting CD206 expression also impacted Arg1 expression equally, suggesting independent regulation of these markers. This indicates that classic RT-qPCR markers used for characterizing macrophages are surrogate markers and do not necessarily correlate functionally with the phenotype, especially in *in vivo* settings. Therefore, a broader panel of markers, rather than a single marker, should be utilized for accurate macrophage polarization assessment that would allow for the prediction of *in vivo* efficacy in fibrosis or cancer. The screening results for siSTAT6 and siTwist1, which demonstrated reprogramming towards the M1 phenotype, led to further testing with an expanded set of RT-qPCR markers.

Additionally, partly functional assays such as flow cytometry or ELISA cytokine measurement could be employed to better determine the effects of siRNA-mediated gene knockdown on macrophage phenotypes, thus enhancing our understanding of the roles these genes may play in macrophage polarization potential *in vivo*.

However, the positive trends still provide favorable grounds for further evaluations of these siRNAs. The effects might even be more pronounced *in vivo*, as unlike resiquimod, which activates several pathways, siRNA inhibits specific targets that may not be stimulated in the current assay to the same extent as they would be within the complex *in vivo* microenvironment.

This highlights another critical factor of the established polarization assay, which is the experimental design. The complexity of target interactions *in vivo*, which our screening assay cannot replicate, means that knocking down such targets might reprogram macrophages only in the presence of yet ill-defined stimuli from the surrounding microenvironment.

In the case of siSTAT6, the experimental design might be suitable to best test for its effects, particularly when using IL-4 in the cell culture medium to polarize naïve macrophages towards the M2 phenotype. Since the IL-4 signaling pathway includes STAT6 as a key downstream transcription factor, inhibiting its transcription could interrupt this pathway, thereby enhancing the modulatory effects of siRNA this setting, but not necessarily in other, in vivo settings.

Another interesting variation to consider is testing the effects of the siRNAs on unpolarized naïve macrophages before introducing polarizing agents in the culture medium. *In vivo*, the effects of STAT6 inhibition could play a threefold role. While we show that *in vitro* generated M2 macrophages can switch their phenotype towards the M1 end of the spectrum, we can

assume that the M1 phenotype can also be induced in naïve macrophages. Moreover, in M1-polarized macrophages, siSTAT6 could prevent the transition towards the M2 end of the spectrum, rather than inducing a switch from M2 to M1, as illustrated in *Figure 26*.

In contrast, some of the other targeted genes encode structures that are not necessarily activated or stimulated in a steady state within our assay, like for example CCR2. Knocking down the expression of CCR2 transcripts and thereby inhibiting the CCR2 receptors may not play a direct role in macrophage polarization. However, the inhibited CCR2 signaling, could potentially shift macrophages towards an M1 phenotype (114, 115). Therefore, if our design included the ligand to stimulate the receptor before transfecting with siRNA targeting CCR2, we could potentially achieve a phenotype switch.

Another interesting result was the transfection of siPPARγ. PPARγ activation promotes the expression of genes that support tissue repair and anti-inflammatory functions, and its expression levels were higher even in our model of M2 macrophages. Contrary to results from other researchers (75), our siRNA-mediated knockdown resulted in a slight increase of M2 markers. While these contradictory results require further investigation, they possibly suggest some form of crosstalk between PPARγ and different transcription pathways and other regulatory mechanisms that occur in the multicellular *in vivo* environment.

siRNA targets that did not alter macrophage phenotypes in our assay may still provide feasible tools for macrophage immunotherapies and possess therapeutic potential *in vivo*. Targets like LAG3, TIGIT, SIRPA etc., offer promising avenues for therapeutic interventions, with various studies exploring antibody-based approaches to inhibit them (116-118). Their potential *in vivo* effects could be linked to mechanisms involving other immune cells or cells of the tumor microenvironment, such as T-lymphocytes or other myeloid cells, fibroblasts, thrombocytes, or even changes in the cancer cells themselves. This highlights the complexity of the regulatory pathways and the differences between various therapeutic approaches in inhibiting a certain target, and the final need for *in vivo* validation.

Lastly, when using established cell-based assay to screen siRNAs for modulating effects, it is also important to consider the target's half-life and the target's function. Receptors or transmembrane proteins like CCR2, GPR65, LRRC32, LAG3, and PVR have half-lives ranging from several hours to days, unlike transcription factors such as Twist1, Twist2, AIRE, AHR, STAT6, and PPARγ, which typically last from minutes to several hours (119-121). This variation of half-lives could potentially influence the modulatory effects of siRNA-mediated knockdown on macrophage phenotypes, with longer incubation times post-transfection possibly revealing additional positive effects for targets with longer half-lives.

Despite all these and other limitations, the established assay is a useful tool for initial screening purposes to enhance workflow and reduce costs and time, while providing preliminary data as foundation for *in vivo* studies.

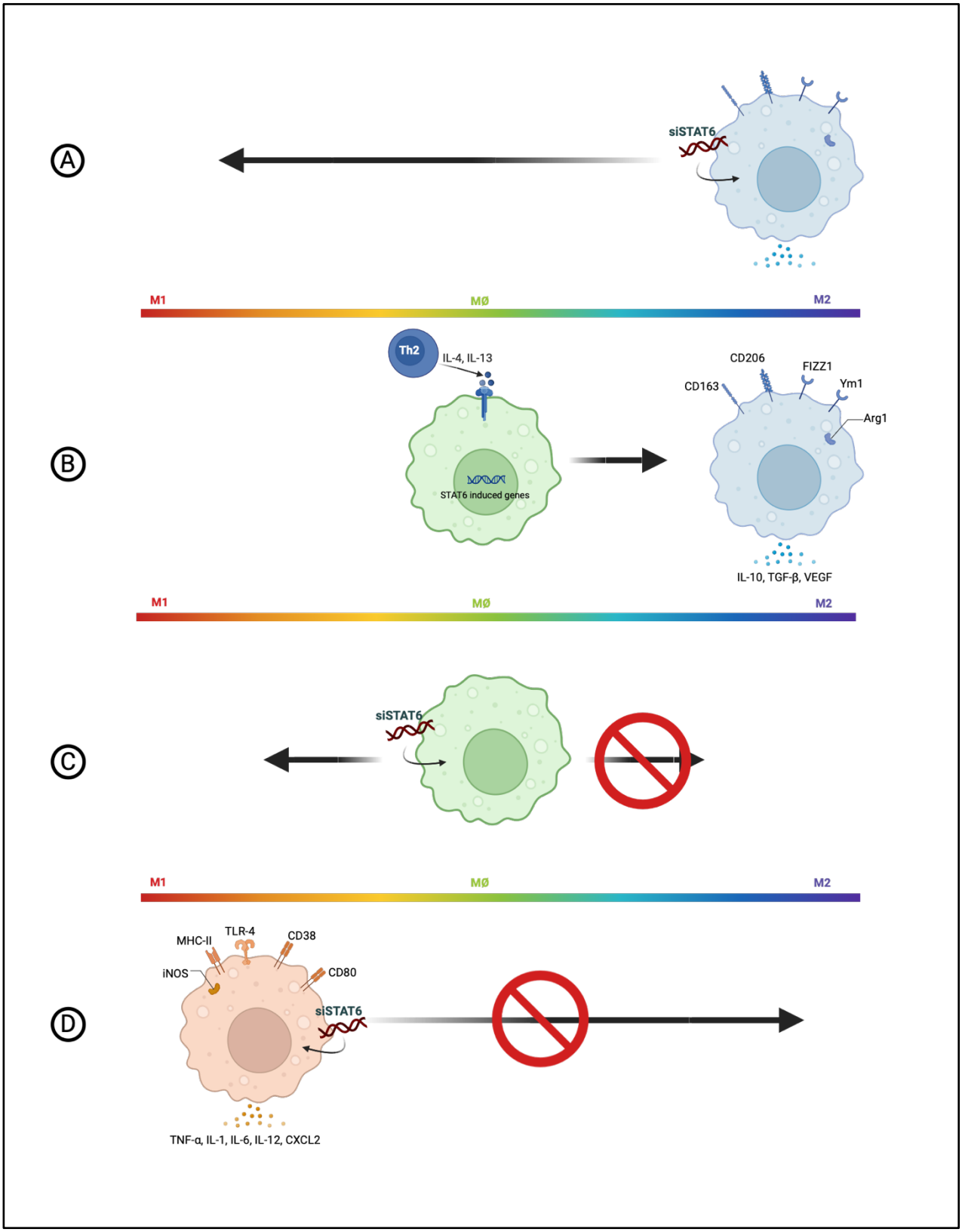

Figure 26: Inhibition of STAT6 expression in differently polarized macrophages by siRNA treatment

Our previous experiments demonstrate that treatment with siSTAT6 shifts the phenotype of M2 polarized macrophages towards away from the M2 spectrum (A). Given that STAT6 is a crucial component of the Th2-induced IL-4 signaling pathway (B), we argue that siSTAT6 treatment could promote the M1 phenotype across various macrophage polarization states. Besides M2 to M1 transition, this treatment may facilitate the polarization of naïve macrophages (MØ) towards the M1 end of the spectrum (C) and prevent the transition from M1 to M2 (D). Created in BioRender. Begaj, K. (2024) BioRender.com/n22n022

4.1.1 The Emerging Role of siRNA-based Therapies

Synthetically engineered siRNAs have emerged as a powerful tool in modern therapeutic strategies, particularly due to their specific inhibition of certain cellular targets by knocking down gene transcription. Notably, several siRNA-based therapeutics that target hepatocytes have already been approved for the highly effective treatment of rare diseases characterized by the overexpression of a misfolded protein or excessive expression of a metabolic enzyme. These diseases include alpha-1-antitrypsin deficiency or transthyretin misfolding (TTR neuro- and cardiomyopathy), LDL receptor deficiency (familial homozygous hyperlipidemia), and overproduction of lipoprotein(a) or aminolevulinate synthase (acute hepatic porphyria) (122-128).

While monoclonal antibodies also offer high specificity for target inhibition, their inability to penetrate the cell membrane limits their use against intracellular targets, such as metabolic transcripts, enzymes or transcription factors. Conversely, siRNAs do not face this limitation, enhancing their therapeutic scope. siRNAs are also relatively easy to design and produce, with computational models providing fast and reliable preliminary *in silico* evaluations of knockdown efficacy and target specificity. The efficacy of these siRNAs is underscored by the findings presented in this thesis, where all tested siRNAs demonstrated high levels of target knockdown, as detailed in *Figure 20.*

The *in vitro* reprogramming effects of siRNAs were less pronounced in our studies compared to those achieved by the small molecule resiquimod. However, resiquimod, a structural analog of imiquimod (which is approved for topical treatment of squamous and basal cell carcinomas), has shown limited clinical applicability due to its poor bioavailability and potential toxicity, which remain significant challenges for systemic use (110).

Conversely, the chemical structure of siRNA and its immunogenic potential are possible concerns for siRNA therapies. For instance, control siRNAs may activate TLR, which could explain some macrophage reprogramming effects seen in *Chapter 3.3.2,* which underline the importance of evaluating unintended immunogenic responses. Therefore, modifications have been introduced into our siRNA molecules, such as limited length and reduced GC content, to reduce nonspecific immunogenicity (129).

Nevertheless, with the approval of siRNA-based drugs, including *Inclisiran* as the first approved siRNA therapeutic for hyperlipidemia in 2020, followed by the other drugs mentioned above, we have gained valuable insights into the safety and effectiveness of siRNA therapies. This provides a strong foundation for rapidly translating such therapies into the clinic using novel siRNA candidates aimed at more common diseases. However, these targets are

typically expressed in non-parenchymal, i.e., non-epithelial cells of the liver and other organs, which currently requires the use of lipoplexes as carriers. These lipoplexes are prominently taken up by macrophages, fibroblasts, and endothelial cells (130-133), unlike the currently approved hepatocyte-targeting siRNAs that are directly conjugated to N-acetyl-galactosamine (NGal) moieties, which are internalized by the hepatocyte-specific asialoglycoprotein receptor.

The transition from bench to bedside for novel siRNA candidates is facilitated by basket clinical trials and expedited FDA approval processes, now more feasible than ever (134, 135). Ongoing clinical trials underscore this progress, heralding a new era of personalized medicine where siRNA treatments can be precisely tailored to an individual's genetic profile and specific disease state, optimizing efficacy while minimizing side effects.

4.2 Understanding Macrophage Plasticity

The ability of macrophages to polarize into different phenotypes while also remaining their plasticity to transit between the different states, certainly makes them an intriguing part of the immune system. The traditional binary classification in M1 and M2 is considered to be a reductionist approach since it does not capture the complexity and plasticity of macrophages states observed *in vivo* through single-cell RNA sequencing (scRNA-seq) (136, 137). In this line, the spectrum model of macrophage activation considers the cell phenotypes to be dynamic and proposes that macrophages exist along a continuum of activation states rather than discrete categories (138, 139).

In our studies, our RNA interference strategy mainly targeted genes with higher expression levels in extremely polarized M2-type macrophages, aiming to shift their transcription profile towards that of M1 macrophages. This approach often yielded results that were not as anticipated. For instance, targeting genes such as GPR65 or PPARγ produced results that were opposite to what we anticipated. These findings suggest that the regulatory mechanisms controlling macrophage polarization are more complex than previously understood, potentially involving feedback loops or interactions not accounted for by our model.

The often-unexpected outcomes of our RNA interference experiments highlight the intricate regulatory networks governing macrophage polarization. Our findings align with recent studies suggesting that macrophage activation is not simply a linear process but is influenced by a multitude of factors and interactions. For example, our *in vitro* polarization model revealed that M1 macrophages exhibited significantly higher levels of the anti-inflammatory cytokine IL-10 or of the M2-related transcription factor STAT6, compared to M2 macrophages. This

contradicts the traditional paradigm of M1 being strictly pro-inflammatory and M2 being anti-inflammatory. Similar results were reported by Gerrick et al. (140), who observed that macrophages polarized with IL-4 and IL-13 were deficient in IL-10 expression, yet their subsequent exposure to LPS induced high IL-10 levels while maintaining other M2 markers.

These findings support the concept introduced by Katkar and Ghosh *(Figure 27)*, who proposed the existence of "brake and accelerator" macrophage populations, which spatially and temporally co-exist and are able to regulate their own and each other's behaviors. According to this concept, pro-inflammatory macrophages have the capability to modulate excessive inflammatory responses by switching on or promoting anti-inflammatory mechanisms (141).

This could explain the higher IL-10 expression levels observed in our M1 polarized macrophages, suggesting the presence of an internal regulatory mechanism aimed at maintaining homeostasis. This idea is further supported by the higher STAT6 levels detected in our M1 macrophages, which may play a role in this regulatory process.

Likewise, Pizzurro and Miller-Jensen's systems biology approach (142) proposes that macrophage activation states should be defined as a combination of functional modules that are regulated by underlying network motifs such as switch-like activation, mutual-inhibition, and positive and negative feedback. Similarly to the studies reviewed by the authors, in our

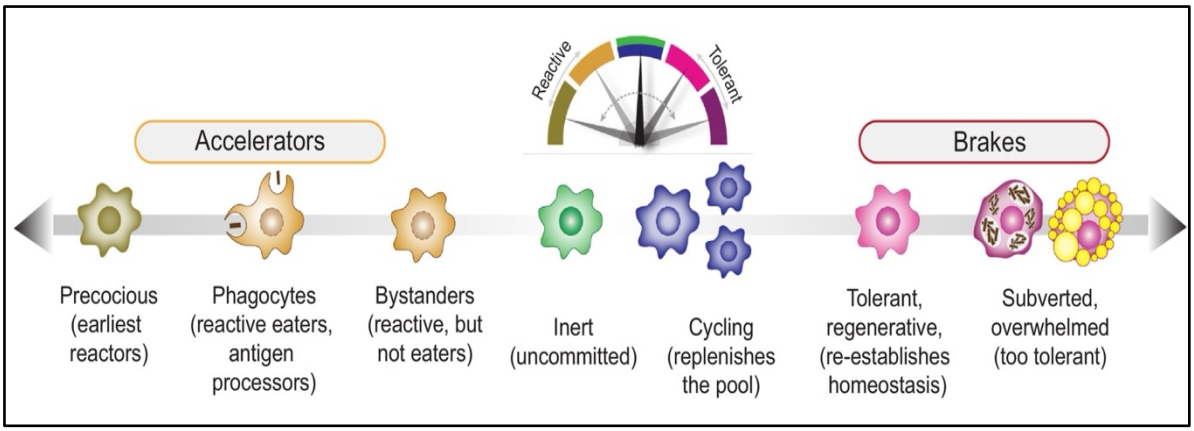

Figure 27: Accelerators and Brakes; a new model of macrophage phenotypes by Katkar and Ghosh

The different macrophage subpopulations multitask along a reactivity-tolerance spectrum. For a physiological immune response and achieve homeostasis it is crucial to maintain a population-level equilibrium between inflammatory (accelerators) and noninflammatory (brake) macrophages. However, in disease this equilibrium is shifted and certain subpopulations are more present than others. The authors also argue that these subpopulations can change their spatial distribution upon perturbations and can cooperate with each-other to achieve the most optimal outcome. Figure from Katkar and Ghosh, Trends in Immunology (2023).

experiments we observed a switch-like activation of the pro-inflammatory phenotype on previously M2 polarized macrophages treated with resiquimod *(***Figure *14)***, suggesting an ultra-sensitivity towards the TLR pathway. On the other hand, mutual inhibition—a network motif for generating responses to two opposing inputs—could be used to explain lack of clear effects of potentially M1 inducing target siRNAs in our assay, with minor residual amounts of IL-4 and IL-13 in the medium, serving as opposing co-stimulators.

While the presented research offers interesting insights into the biology of macrophages, significant gaps in our understanding still persist. Particularly, the *in vivo* complexity of macrophage phenotypes remains inadequately represented by the extreme polarization states commonly used in *in vitro* models. Although more mechanistic research on macrophages extends beyond the scope of this dissertation, it is essential to refine these models and enhance our understanding of the regulatory mechanisms influencing macrophage polarization, especially towards the phenotype of the elusive regenerative macrophage in fibrosis (low inflammatory and antifibrotic) or the potent anti-cancer macrophage. This understanding will advance translational research and drive the development of innovative treatments.

4.3 Interpreting Results for Liver Disease

Chronic liver diseases, namely liver fibrosis and liver cancer, pose a significant global health challenge due to their high incidence and prevalence, and the burden they place on healthcare systems. The urgent need for developing new therapeutic options is underscored by the prevalence of liver diseases and the limited efficacy of current therapies, which insufficiently address the frequently advanced disease states resulting from a typically long-term indolent disease course prior to liver decompensation and death (143). Therefore, exploring innovative treatment modalities to stop the progression of or reverse advanced fibrosis, or to effectively treat all stages of liver cancer, is imperative to provide hope and improved outcomes for patients suffering from these conditions.

In liver fibrosis treatment, the effectiveness of targeting macrophages is highly dependent on the timing of the intervention (31, 144, 145).

Other unpublished results from our lab show that siRNA targeting Fra2 can effectively inhibit fibrosis progression in an *in vivo* mouse model of CCL4-induced liver fibrosis, as well as in advanced biliary fibrosis (patent application number EP22202390.5, Oct 19, 2022). The results from *Chapter 3.5.2* indicating that Fra2 knockdown promotes an M2 phenotype, might

suggest that targeting Fra2 generates an M2-type macrophage that may resemble the elusive resolution/regenerative macrophage, which exhibits both modest anti-inflammatory and potent antifibrotic activities. The extent to which the two novel siRNA candidates that emerged from our screening assay—siTwist1 and siSTAT6—can potentially address fibrosis in both early and later stages of the disease needs to be demonstrated. Thus, certain siRNA targets may ultimately prove to be differentially effective in various stages of fibrogenesis.

In the case of hepatocellular carcinoma, mitigating its immunosuppressive and inaccessible tumor microenvironment requires a likely better definable switch of TAMs towards the pro-inflammatory, anti-tumoral M1 phenotype (146, 147).

Our siRNA targeting Twist1 and STAT6 have shown potential *in vitro* to drive this reprogramming. Additionally, these transcription factors also engage directly in hallmark processes of hepatocarcinogenesis, including promoting cell cycle progression, inhibiting apoptosis, triggering epithelial-mesenchymal transition (EMT) and facilitating metastasis (148-151).

This suggests that *in vivo* applications of *siTwist1* and *siSTAT6* could target both the tumor-promoting pathways of the cancer cells and the exhausted immune response from tumor associated macrophages, thereby providing a synergistic effect.

These findings support the promising hypothesis that targeting macrophages could lead to effective new treatments for liver diseases in clinical settings. However, the complex nature of macrophage polarization and the pathogenesis of liver diseases demand further research. Detailed studies are needed to elucidate the specific roles and mechanisms through which macrophage polarization influences these conditions.

4.3.1 Broader Implication of Macrophage Reprogramming

The potential of siRNA-mediated macrophage reprogramming extends far beyond the treatment of hepatocellular carcinoma and liver fibrosis, touching upon many diseases where inflammation and immune dysregulation play a pivotal role.

It's important to acknowledge that while our screening tool aims to identify siRNAs that push macrophages towards an antitumor, pro-inflammatory M1 phenotype, findings showing a switch to the anti-inflammatory M2 phenotype are also of significant interest, especially for autoinflammatory and autoimmune diseases. For instance, chronic inflammatory diseases such as rheumatoid arthritis (RA) and inflammatory bowel disease (IBD) represent areas where macrophage-targeted therapies could transform patient outcomes (152-154).

In this context, siRNAs like siTmem173 emerge as potential therapeutic agents due to the enhancement of the anti-inflammatory, pro-resolution M2 phenotype shown in our testing in *Chapter 3.4.2.*

4.4 Conclusion and Future Directions

Our screening assay offers a rapid and efficient method to identify promising siRNA targets for therapeutic purposes, while also providing hints for future basic research on macrophage biology. This "rapid discovery" approach has already highlighted potential candidates such as siSTAT6 and siTwist1, which are undergoing further validation as outlined in the *Project Overview (Figure 5).*

The next steps involve further *in vitro* analyses to better characterize the effects of siRNA treatment on a functional level and toxicity while referring to general safety of the siRNA and its delivery system to provide efficiency of treatment and minimize *off target* or *off organ* side effects. Enhanced delivery methods, such as modified nanoparticles or lipoplexes, add a layer of security, enhancing the effectiveness of siRNA therapies and reducing off-target effects. Notably, these carriers tend to accumulate in the liver, making liver diseases an ideal application for such therapies. Research continues to target siRNA delivery to other organs, increasing the specificity of therapies like macrophage reprogramming (130, 155, 156). For example, nanoparticles modified with a mannose structure can specifically bind to the mannose receptor CD206, overexpressed on M2 macrophages, directing siRNA-loaded nanoparticles precisely to these cells (131, 157).

Following *in vitro* studies, the siRNA candidates will be tested *in vivo* using mouse models for liver fibrosis (CCL4-induced fibrosis and Mdr2-KO mice) and syngeneic models of hepatocellular carcinoma.

While animal models provide a vital ethical foundation for our experimental studies, it is crucial to address the translational validity of these models. The significant biological differences between human and murine macrophages, including gene expression profiles and polarization patterns, warrant thorough investigation to ensure the relevance of our findings to human conditions (158, 159).

In the quest to harness the therapeutic potential that macrophages provide, it is imperative to characterize macrophages and develop new models or methods to delineate macrophage phenotypes. Concurrently, the urgency to devise novel therapies cannot be overstated.

With the principle of “primum non nocere” (first, do no harm) guiding us, our commitment as medical professionals is to expedite the development of therapeutic options to address chronic inflammation and its associated conditions such as cancer and fibrosis in order to meet the pressing needs of the present.

5 References

1. Locati M, Curtale G, Mantovani A. Diversity, Mechanisms, and Significance of Macrophage Plasticity. Annu Rev Pathol. 2020;15:123-47.
2. Park MD, Silvin A, Ginhoux F, Merad M. Macrophages in health and disease. Cell. 2022;185(23):4259-79.
3. Murray PJ, Wynn TA. Protective and pathogenic functions of macrophage subsets. Nat Rev Immunol. 2011;11(11):723-37.
4. Hirayama D, Iida T, Nakase H. The Phagocytic Function of Macrophage-Enforcing Innate Immunity and Tissue Homeostasis. Int J Mol Sci. 2017;19(1).
5. Arango Duque G, Descoteaux A. Macrophage cytokines: involvement in immunity and infectious diseases. Front Immunol. 2014;5:491.
6. Schupp J, Krebs FK, Zimmer N, Trzeciak E, Schuppan D, Tuettenberg A. Targeting myeloid cells in the tumor sustaining microenvironment. Cell Immunol. 2019;343:103713.
7. Franklin RA. Fibroblasts and macrophages: Collaborators in tissue homeostasis. Immunol Rev. 2021;302(1):86-103.
8. Hassanshahi A, Moradzad M, Ghalamkari S, Fadaei M, Cowin AJ, Hassanshahi M. Macrophage-Mediated Inflammation in Skin Wound Healing. Cells. 2022;11(19).
9. Amici SA, Dong J, Guerau-de-Arellano M. Molecular Mechanisms Modulating the Phenotype of Macrophages and Microglia. Front Immunol. 2017;8:1520.
10. Ley K, Pramod AB, Croft M, Ravichandran KS, Ting JP. How Mouse Macrophages Sense What Is Going On. Front Immunol. 2016;7:204.
11. Glass CK, Natoli G. Molecular control of activation and priming in macrophages. Nat Immunol. 2016;17(1):26-33.
12. Funes SC, Rios M, Escobar-Vera J, Kalergis AM. Implications of macrophage polarization in autoimmunity. Immunology. 2018;154(2):186-95.
13. Mills CD, Kincaid K, Alt JM, Heilman MJ, Hill AM. M-1/M-2 macrophages and the Th1/Th2 paradigm. J Immunol. 2000;164(12):6166-73.
14. Murray PJ, Allen JE, Biswas SK, Fisher EA, Gilroy DW, Goerdt S, et al. Macrophage activation and polarization: nomenclature and experimental guidelines. Immunity. 2014;41(1):14-20.
15. Orecchioni M, Ghosheh Y, Pramod AB, Ley K. Macrophage Polarization: Different Gene Signatures in M1(LPS+) vs. Classically and M2(LPS-) vs. Alternatively Activated Macrophages. Front Immunol. 2019;10:1084.
16. Ying W, Cheruku PS, Bazer FW, Safe SH, Zhou B. Investigation of macrophage polarization using bone marrow derived macrophages. J Vis Exp. 2013(76).
17. Sica A, Mantovani A. Macrophage plasticity and polarization: in vivo veritas. J Clin Invest. 2012;122(3):787-95.
18. Martinez FO, Gordon S, Locati M, Mantovani A. Transcriptional profiling of the human monocyte-to-macrophage differentiation and polarization: new molecules and patterns of gene expression. J Immunol. 2006;177(10):7303-11.
19. Rodríguez-Morales P, Franklin RA. Macrophage phenotypes and functions: resolving inflammation and restoring homeostasis. Trends in Immunology. 2023;44(12):986-98.
20. Casari M, Siegl D, Deppermann C, Schuppan D. Macrophages and platelets in liver fibrosis and hepatocellular carcinoma. Front Immunol. 2023;14:1277808.
21. Austermann J, Roth J, Barczyk-Kahlert K. The Good and the Bad: Monocytes' and Macrophages' Diverse Functions in Inflammation. Cells. 2022;11(12).
22. Hourani T, Holden JA, Li W, Lenzo JC, Hadjigol S, O'Brien-Simpson NM. Tumor Associated Macrophages: Origin, Recruitment, Phenotypic Diversity, and Targeting. Front Oncol. 2021;11:788365.
23. Rőszer T. Understanding the Mysterious M2 Macrophage through Activation Markers and Effector Mechanisms. Mediators Inflamm. 2015;2015:816460.

24. Mantovani A, Marchesi F, Malesci A, Laghi L, Allavena P. Tumour-associated macrophages as treatment targets in oncology. Nat Rev Clin Oncol. 2017;14(7):399-416.
25. Messex JK, Byrd CJ, Liou GY. Signaling of Macrophages that Contours the Tumor Microenvironment for Promoting Cancer Development. Cells. 2020;9(4).
26. Tian Z, Hou X, Liu W, Han Z, Wei L. Macrophages and hepatocellular carcinoma. Cell Biosci. 2019;9:79.
27. Capece D, Fischietti M, Verzella D, Gaggiano A, Cicciarelli G, Tessitore A, et al. The inflammatory microenvironment in hepatocellular carcinoma: a pivotal role for tumor-associated macrophages. Biomed Res Int. 2013;2013:187204.
28. Wynn TA, Vannella KM. Macrophages in Tissue Repair, Regeneration, and Fibrosis. Immunity. 2016;44(3):450-62.
29. Hammerich L, Tacke F. Hepatic inflammatory responses in liver fibrosis. Nat Rev Gastroenterol Hepatol. 2023;20(10):633-46.
30. Weng SY, Wang X, Vijayan S, Tang Y, Kim YO, Padberg K, et al. IL-4 Receptor Alpha Signaling through Macrophages Differentially Regulates Liver Fibrosis Progression and Reversal. EBioMedicine. 2018;29:92-103.
31. Schuppan D, Ashfaq-Khan M, Yang AT, Kim YO. Liver fibrosis: Direct antifibrotic agents and targeted therapies. Matrix Biol. 2018;68-69:435-51.
32. Ramachandran P, Dobie R, Wilson-Kanamori JR, Dora EF, Henderson BEP, Luu NT, et al. Resolving the fibrotic niche of human liver cirrhosis at single-cell level. Nature. 2019;575(7783):512-8.
33. Fallowfield J. Macrophage-derived vascular endothelial growth factor and angiogenesis within the hepatic scar-new pathways unmasked in the resolution of fibrosis. Hepatology. 2015;61(6):1790-2.
34. Kazankov K, Jorgensen SMD, Thomsen KL, Moller HJ, Vilstrup H, George J, et al. The role of macrophages in nonalcoholic fatty liver disease and nonalcoholic steatohepatitis. Nat Rev Gastroenterol Hepatol. 2019;16(3):145-59.
35. Fire A, Xu S, Montgomery MK, Kostas SA, Driver SE, Mello CC. Potent and specific genetic interference by double-stranded RNA in Caenorhabditis elegans. Nature. 1998;391(6669):806-11.
36. Kara G, Calin GA, Ozpolat B. RNAi-based therapeutics and tumor targeted delivery in cancer. Adv Drug Deliv Rev. 2022;182:114113.
37. Saw PE, Song EW. siRNA therapeutics: a clinical reality. Sci China Life Sci. 2020;63(4):485-500.
38. Gavrilov K, Saltzman WM. Therapeutic siRNA: principles, challenges, and strategies. Yale J Biol Med. 2012;85(2):187-200.
39. Wittrup A, Lieberman J. Knocking down disease: a progress report on siRNA therapeutics. Nat Rev Genet. 2015;16(9):543-52.
40. Guo P, Coban O, Snead NM, Trebley J, Hoeprich S, Guo S, Shu Y. Engineering RNA for targeted siRNA delivery and medical application. Adv Drug Deliv Rev. 2010;62(6):650-66.
41. Storz P. Roles of differently polarized macrophages in the initiation and progressionof pancreatic cancer. Front Immunol. 2023;14:1237711.
42. Laskin DL, Malaviya R, Laskin JD. Role of Macrophages in Acute Lung Injury and Chronic Fibrosis Induced by Pulmonary Toxicants. Toxicol Sci. 2019;168(2):287-301.
43. Aras S, Zaidi MR. TAMeless traitors: macrophages in cancer progression and metastasis. Br J Cancer. 2017;117(11):1583-91.
44. Braga TT, Agudelo JS, Camara NO. Macrophages During the Fibrotic Process: M2 as Friend and Foe. Front Immunol. 2015;6:602.
45. Bock KW. Aryl hydrocarbon receptor (AHR) functions: Balancing opposing processes including inflammatory reactions. Biochem Pharmacol. 2020;178:114093.
46. Cui Z, Feng Y, Li D, Li T, Gao P, Xu T. Activation of aryl hydrocarbon receptor (AhR) in mesenchymal stem cells modulates macrophage polarization in asthma. J Immunotoxicol. 2020;17(1):21-30.

47. Yang X, Liu H, Ye T, Duan C, Lv P, Wu X, et al. AhR activation attenuates calcium oxalate nephrocalcinosis by diminishing M1 macrophage polarization and promoting M2 macrophage polarization. Theranostics. 2020;10(26):12011-25.
48. de Albuquerque JAT, Banerjee PP, Castoldi A, Ma R, Zurro NB, Ynoue LH, et al. The Role of AIRE in the Immunity Against Candida Albicans in a Model of Human Macrophages. Front Immunol. 2018;9:567.
49. Källberg E, Mehmeti-Ajradini M, Gunnarsdottir FB, Göransson M, Bergenfelz C, Fredriksson RA, et al. AIRE is expressed in breast cancer TANs and TAMs to regulate the extrinsic apoptotic pathway and inflammation. J Leukoc Biol. 2023.
50. Kalra R, Bhagyaraj E, Tiwari D, Nanduri R, Chacko AP, Jain M, et al. AIRE promotes androgen-independent prostate cancer by directly regulating IL-6 and modulating tumor microenvironment. Oncogenesis. 2018;7(5):43.
51. Bartneck M, Koppe C, Fech V, Warzecha KT, Kohlhepp M, Huss S, et al. Roles of CCR2 and CCR5 for Hepatic Macrophage Polarization in Mice With Liver Parenchymal Cell-Specific NEMO Deletion. Cell Mol Gastroenterol Hepatol. 2021;11(2):327-47.
52. Wang W, Ai J, Liao B, Xiao K, Lin L, Chen H, Zhou L. The roles of MCP-1/CCR2 mediated macrophage recruitment and polarization in bladder outlet obstruction (BOO) induced bladder remodeling. Int Immunopharmacol. 2021;99:107947.
53. Cai H, Chen Y, Chen X, Sun W, Li Y. Tumor-associated macrophages mediate gastrointestinal stromal tumor cell metastasis through CXCL2/CXCR2. Cell Immunol. 2023;384:104642.
54. Xu-Vanpala S, Deerhake ME, Wheaton JD, Parker ME, Juvvadi PR, MacIver N, et al. Functional heterogeneity of alveolar macrophage population based on expression of CXCL2. Science Immunology. 2020;5(50):eaba7350.
55. Zhang Q, Wang J, Yao X, Wu S, Tian W, Gan C, et al. Programmed Cell Death 10 Mediated CXCL2-CXCR2 Signaling in Regulating Tumor-Associated Microglia/Macrophages Recruitment in Glioblastoma. Front Immunol. 2021;12:637053.
56. Huang S, Wang J, Liu F, Dong L. Alternatively activated macrophages promote airway inflammation through JAK3-STAT5-Fra2 in asthma. Inflamm Res. 2022;71(7-8):873-85.
57. Zhang K, Zhang MX, Meng XX, Zhu J, Wang JJ, He YF, et al. Targeting GPR65 alleviates hepatic inflammation and fibrosis by suppressing the JNK and NF-κB pathways. Mil Med Res. 2023;10(1):56.
58. Campbell AP, Smrcka AV. Targeting G protein-coupled receptor signalling by blocking G proteins. Nat Rev Drug Discov. 2018;17(11):789-803.
59. Katagata M, Okayama H, Nakajima S, Saito K, Sato T, Sakuma M, et al. TIM-3 Expression and M2 Polarization of Macrophages in the TGFβ-Activated Tumor Microenvironment in Colorectal Cancer. Cancers (Basel). 2023;15(20).
60. Liu Y, Liu Y, Zhang X, Chen M, Hu Y. [Hepatitis A virus cell membrane protein receptor 2 promotes endotoxin tolerance in mouse macrophages]. Zhonghua Wei Zhong Bing Ji Jiu Yi Xue. 2021;33(4):472-7.
61. Amatore F, Gorvel L, Olive D. Role of Inducible Co-Stimulator (ICOS) in cancer immunotherapy. Expert Opin Biol Ther. 2020;20(2):141-50.
62. Liu L, Wang P, Xie S-Q, Pu W-J, Xu J, Xia C-M. IL-33 Involved in the Progression of Liver Fibrosis Through Innate Immunity Cells (Mφ) Regulated by ICOS/ICOSL Signaling in Early Stage of Mice Schistosomiasis. bioRxiv. 2022:2022.09.05.506595.
63. Kim YJ, Won CH, Lee MW, Choi JH, Chang SE, Lee WJ. Correlation Between Tumor-Associated Macrophage and Immune Checkpoint Molecule Expression and Its Prognostic Significance in Cutaneous Melanoma. J Clin Med. 2020;9(8).
64. Brauneck F, Oliveira-Ferrer L, Muschhammer J, Sturmheit T, Ackermann C, Haag F, et al. Immunosuppressive M2 TAMs represent a promising target population to enhance phagocytosis of ovarian cancer cells in vitro. Front Immunol. 2023;14:1250258.
65. Ni X, Wu W, Sun X, Ma J, Yu Z, He X, et al. Interrogating glioma-M2 macrophage interactions identifies Gal-9/Tim-3 as a viable target against PTEN-null glioblastoma. Sci Adv. 2022;8(27):eabl5165.

66. Li Y, Sang Y, Chang Y, Xu C, Lin Y, Zhang Y, et al. A Galectin-9-Driven CD11c(high) Decidual Macrophage Subset Suppresses Uterine Vascular Remodeling in Preeclampsia. Circulation. 2024.
67. Wei S, Lu J, Lou J, Shi C, Mo S, Shao Y, et al. Gastric Cancer Tumor Microenvironment Characterization Reveals Stromal-Related Gene Signatures Associated With Macrophage Infiltration. Front Genet. 2020;11:663.
68. Jiang A, Qin Y, Springer TA. Loss of LRRC33-Dependent TGFβ1 Activation Enhances Antitumor Immunity and Checkpoint Blockade Therapy. Cancer Immunol Res. 2022;10(4):453-67.
69. Hahn SA, Neuhoff A, Landsberg J, Schupp J, Eberts D, Leukel P, et al. A key role of GARP in the immune suppressive tumor microenvironment. Oncotarget. 2016;7(28):42996-3009.
70. Gorvel L, Olive D. Targeting the "PVR-TIGIT axis" with immune checkpoint therapies. F1000Res. 2020;9.
71. Orecchioni M, Matsunami H, Ley K. Olfactory receptors in macrophages and inflammation. Front Immunol. 2022;13:1029244.
72. Orecchioni M, Kobiyama K, Winkels H, Ghosheh Y, McArdle S, Mikulski Z, et al. Olfactory receptor 2 in vascular macrophages drives atherosclerosis by NLRP3-dependent IL-1 production. Science. 2022;375(6577):214-21.
73. Wu Y, Zhan S, Chen L, Sun M, Li M, Mou X, et al. TNFSF14/LIGHT promotes cardiac fibrosis and atrial fibrillation vulnerability via PI3Kγ/SGK1 pathway-dependent M2 macrophage polarisation. J Transl Med. 2023;21(1):544.
74. Zhu M, Dong D, Dai Z, Zhao Y. Egln1 Deficiency Controls Macrophage Polarization Mediating Obliterative Pulmonary Vascular Remodeling and Severe PAH. A107 BYSTANDERS NO MORE: INFLAMMATION, IMMUNITY AND THROMBOSIS IN PULMONARY VASCULAR AND LUNG DISEASE. p. A2674-A.
75. Hörhold F, Eisel D, Oswald M, Kolte A, Röll D, Osen W, et al. Reprogramming of macrophages employing gene regulatory and metabolic network models. PLoS Comput Biol. 2020;16(2):e1007657.
76. Liu S, Zhang H, Li Y, Zhang Y, Bian Y, Zeng Y, et al. S100A4 enhances protumor macrophage polarization by control of PPAR-γ-dependent induction of fatty acid oxidation. J Immunother Cancer. 2021;9(6).
77. Li A, Ji B, Yang Y, Ye B, Zhu Q, Hu X, et al. Single-cell RNA sequencing highlights the role of PVR/PVRL2 in the immunosuppressive tumour microenvironment in hepatocellular carcinoma. Front Immunol. 2023;14:1164448.
78. Zhang D, Liu Y, Ma J, Xu Z, Duan C, Wang Y, et al. Competitive binding of CD226/TIGIT with poliovirus receptor regulates macrophage polarization and is involved in vascularized skin graft rejection. Am J Transplant. 2023;23(7):920-34.
79. Sugimura-Nagata A, Koshino A, Inoue S, Matsuo-Nagano A, Komura M, Riku M, et al. Expression and Prognostic Significance of CD47-SIRPA Macrophage Checkpoint Molecules in Colorectal Cancer. Int J Mol Sci. 2021;22(5).
80. Matlung HL, Szilagyi K, Barclay NA, van den Berg TK. The CD47-SIRPalpha signaling axis as an innate immune checkpoint in cancer. Immunol Rev. 2017;276(1):145-64.
81. Singla B, Lin HP, Ahn W, Xu J, Ma Q, Sghayyer M, et al. Loss of myeloid cell-specific SIRPα, but not CD47, attenuates inflammation and suppresses atherosclerosis. Cardiovasc Res. 2022;118(15):3097-111.
82. Tao K, Wei Z, Xia Y, Zhao R, Xu H. High SIRPA Expression Predicts Poor Prognosis and Correlates with Immune Infiltrates in Patients with Esophageal Carcinoma. J Healthc Eng. 2022;2022:3565676.
83. Jiao B, An C, Tran M, Du H, Wang P, Zhou D, Wang Y. Pharmacological Inhibition of STAT6 Ameliorates Myeloid Fibroblast Activation and Alternative Macrophage Polarization in Renal Fibrosis. Front Immunol. 2021;12:735014.
84. Shi JH, Liu LN, Song DD, Liu WW, Ling C, Wu FX, et al. TRAF3/STAT6 axis regulates macrophage polarization and tumor progression. Cell Death Differ. 2023;30(8):2005-16.

85. Brauneck F, Fischer B, Witt M, Muschhammer J, Oelrich J, da Costa Avelar PH, et al. TIGIT blockade repolarizes AML-associated TIGIT(+) M2 macrophages to an M1 phenotype and increases CD47-mediated phagocytosis. J Immunother Cancer. 2022;10(12).
86. Annese T, Tamma R, Ribatti D. Update in TIGIT Immune-Checkpoint Role in Cancer. Front Oncol. 2022;12:871085.
87. Dai E, Han L, Liu J, Xie Y, Zeh HJ, Kang R, et al. Ferroptotic damage promotes pancreatic tumorigenesis through a TMEM173/STING-dependent DNA sensor pathway. Nat Commun. 2020;11(1):6339.
88. Zhou L, Xu Q, Huang L, Zhan P, Jin J, Ye M, et al. Host stimulator of interferon genes is essential for the efficacy of anti-programmed cell death protein 1 inhibitors in non-small cell lung cancer. Immunology. 2022;167(4):495-507.
89. Zou B, Liu J, Klionsky DJ, Tang D, Kang R. Extracellular SQSTM1 as an inflammatory mediator. Autophagy. 2020;16(12):2313-5.
90. Luo X, Li H, Ma L, Zhou J, Guo X, Woo SL, et al. Expression of STING Is Increased in Liver Tissues From Patients With NAFLD and Promotes Macrophage-Mediated Hepatic Inflammation and Fibrosis in Mice. Gastroenterology. 2018;155(6):1971-84.e4.
91. Ning X, Zhang K, Wu Q, Liu M, Sun S. Emerging role of Twist1 in fibrotic diseases. J Cell Mol Med. 2018;22(3):1383-91.
92. Wang Y, Lin Y, Cheng C, Chen P, Zhang P, Wu H, et al. NF-κB/TWIST1 Mediates Migration and Phagocytosis of Macrophages in the Mice Model of Implant-Associated Staphylococcus aureus Osteomyelitis. Front Microbiol. 2020;11:1301.
93. Wu Q, Sun S, Wei L, Liu M, Liu H, Liu T, et al. Twist1 regulates macrophage plasticity to promote renal fibrosis through galectin-3. Cell Mol Life Sci. 2022;79(3):137.
94. Zheng S, Hedl M, Abraham C. Twist1 and Twist2 Contribute to Cytokine Downregulation following Chronic NOD2 Stimulation of Human Macrophages through the Coordinated Regulation of Transcriptional Repressors and Activators. J Immunol. 2015;195(1):217-26.
95. Ren J, Crowley SD. Twist1: A Double-Edged Sword in Kidney Diseases. Kidney Dis (Basel). 2020;6(4):247-57.
96. Ding N, Liu D, Duan X, Zhang J, Ma S, Chen Y. Twist2 Reduced NLRP3-Induced Inflammation of Infantile Pneumonia via Regulation of Mitochondrial Permeability Transition by FOXO1. Int Arch Allergy Immunol. 2022;183(10):1098-113.
97. Taylor SC, Nadeau K, Abbasi M, Lachance C, Nguyen M, Fenrich J. The Ultimate qPCR Experiment: Producing Publication Quality, Reproducible Data the First Time. Trends Biotechnol. 2019;37(7):761-74.
98. Bustin SA, Benes V, Garson JA, Hellemans J, Huggett J, Kubista M, et al. The MIQE guidelines: minimum information for publication of quantitative real-time PCR experiments. Clin Chem. 2009;55(4):611-22.
99. Bustin S, Huggett J. qPCR primer design revisited. Biomolecular Detection and Quantification. 2017;14:19-28.
100. Amlie-Lefond C, Paz DA, Connelly MP, Huffnagle GB, Whelan NT, Whelan HT. Innate immunity for biodefense: a strategy whose time has come. J Allergy Clin Immunol. 2005;116(6):1334-42.
101. Vasilakos JP, Tomai MA. The use of Toll-like receptor 7/8 agonists as vaccine adjuvants. Expert Rev Vaccines. 2013;12(7):809-19.
102. Na YR, Kim SW, Seok SH. A new era of macrophage-based cell therapy. Experimental & Molecular Medicine. 2023;55(9):1945-54.
103. Kumari N, Choi SH. Tumor-associated macrophages in cancer: recent advancements in cancer nanoimmunotherapies. J Exp Clin Cancer Res. 2022;41(1):68.
104. Anderson NR, Minutolo NG, Gill S, Klichinsky M. Macrophage-Based Approaches for Cancer Immunotherapy. Cancer Res. 2021;81(5):1201-8.
105. Mantovani A, Longo DL. Macrophage Checkpoint Blockade in Cancer — Back to the Future. New England Journal of Medicine. 2018;379(18):1777-9.

106. Nasir I, McGuinness C, Poh AR, Ernst M, Darcy PK, Britt KL. Tumor macrophage functional heterogeneity can inform the development of novel cancer therapies. Trends in Immunology. 2023;44(12):971-85.
107. Wang S, Yang Y, Ma P, Huang H, Tang Q, Miao H, et al. Landscape and perspectives of macrophage -targeted cancer therapy in clinical trials. Mol Ther Oncolytics. 2022;24:799-813.
108. Marim FM, Silveira TN, Lima DS, Jr., Zamboni DS. A Method for Generation of Bone Marrow-Derived Macrophages from Cryopreserved Mouse Bone Marrow Cells. PLOS ONE. 2010;5(12):e15263.
109. Anfray C, Varela CF, Ummarino A, Maeda A, Sironi M, Gandoy S, et al. Polymeric nanocapsules loaded with poly(I:C) and resiquimod to reprogram tumor-associated macrophages for the treatment of solid tumors. Front Immunol. 2023;14:1334800.
110. Frega G, Wu Q, Le Naour J, Vacchelli E, Galluzzi L, Kroemer G, Kepp O. Trial Watch: experimental TLR7/TLR8 agonists for oncological indications. Oncoimmunology. 2020;9(1):1796002.
111. Li H, Somiya M, Kuroda S. Enhancing antibody-dependent cellular phagocytosis by Re-education of tumor-associated macrophages with resiquimod-encapsulated liposomes. Biomaterials. 2021;268:120601.
112. Figueiredo P, Lepland A, Scodeller P, Fontana F, Torrieri G, Tiboni M, et al. Peptide-guided resiquimod-loaded lignin nanoparticles convert tumor-associated macrophages from M2 to M1 phenotype for enhanced chemotherapy. Acta Biomater. 2021;133:231-43.
113. Anfray C, Mainini F, Digifico E, Maeda A, Sironi M, Erreni M, et al. Intratumoral combination therapy with poly(I:C) and resiquimod synergistically triggers tumor-associated macrophages for effective systemic antitumoral immunity. J Immunother Cancer. 2021;9(9).
114. Li X, Yao W, Yuan Y, Chen P, Li B, Li J, et al. Targeting of tumour-infiltrating macrophages via CCL2/CCR2 signalling as a therapeutic strategy against hepatocellular carcinoma. Gut. 2017;66(1):157-67.
115. Fei L, Ren X, Yu H, Zhan Y. Targeting the CCL2/CCR2 Axis in Cancer Immunotherapy: One Stone, Three Birds? Front Immunol. 2021;12:771210.
116. Bouwstra R, van Meerten T, Bremer E. CD47-SIRPα blocking-based immunotherapy: Current and prospective therapeutic strategies. Clin Transl Med. 2022;12(8):e943.
117. Chiang EY, Mellman I. TIGIT-CD226-PVR axis: advancing immune checkpoint blockade for cancer immunotherapy. J Immunother Cancer. 2022;10(4).
118. Nguyen LT, Ohashi PS. Clinical blockade of PD1 and LAG3--potential mechanisms of action. Nat Rev Immunol. 2015;15(1):45-56.
119. Schwanhäusser B, Busse D, Li N, Dittmar G, Schuchhardt J, Wolf J, et al. Global quantification of mammalian gene expression control. Nature. 2011;473(7347):337-42.
120. Toyama BH, Hetzer MW. Protein homeostasis: live long, won't prosper. Nat Rev Mol Cell Biol. 2013;14(1):55-61.
121. Azpeitia E, Wagner A. Short Residence Times of DNA-Bound Transcription Factors Can Reduce Gene Expression Noise and Increase the Transmission of Information in a Gene Regulation System. Front Mol Biosci. 2020;7:67.
122. Bergmark BA, Marston NA, Prohaska TA, Alexander VJ, Zimerman A, Moura FA, et al. Olezarsen for Hypertriglyceridemia in Patients at High Cardiovascular Risk. N Engl J Med. 2024;390(19):1770-80.
123. Maurer MS, Kale P, Fontana M, Berk JL, Grogan M, Gustafsson F, et al. Patisiran Treatment in Patients with Transthyretin Cardiac Amyloidosis. N Engl J Med. 2023;389(17):1553-65.
124. Strnad P, Mandorfer M, Choudhury G, Griffiths W, Trautwein C, Loomba R, et al. Fazirsiran for Liver Disease Associated with Alpha(1)-Antitrypsin Deficiency. N Engl J Med. 2022;387(6):514-24.
125. O'Donoghue ML, Rosenson RS, Gencer B, López JAG, Lepor NE, Baum SJ, et al. Small Interfering RNA to Reduce Lipoprotein(a) in Cardiovascular Disease. N Engl J Med. 2022;387(20):1855-64.

126. Balwani M, Sardh E, Ventura P, Peiró PA, Rees DC, Stölzel U, et al. Phase 3 Trial of RNAi Therapeutic Givosiran for Acute Intermittent Porphyria. N Engl J Med. 2020;382(24):2289-301.
127. Tsimikas S, Karwatowska-Prokopczuk E, Gouni-Berthold I, Tardif JC, Baum SJ, Steinhagen-Thiessen E, et al. Lipoprotein(a) Reduction in Persons with Cardiovascular Disease. N Engl J Med. 2020;382(3):244-55.
128. Benson MD, Waddington-Cruz M, Berk JL, Polydefkis M, Dyck PJ, Wang AK, et al. Inotersen Treatment for Patients with Hereditary Transthyretin Amyloidosis. N Engl J Med. 2018;379(1):22-31.
129. Dong Y, Siegwart DJ, Anderson DG. Strategies, design, and chemistry in siRNA delivery systems. Adv Drug Deliv Rev. 2019;144:133-47.
130. Jimenez Calvente C, Sehgal A, Popov Y, Kim YO, Zevallos V, Sahin U, et al. Specific hepatic delivery of procollagen alpha1(I) small interfering RNA in lipid-like nanoparticles resolves liver fibrosis. Hepatology. 2015;62(4):1285-97.
131. Leber N, Kaps L, Yang A, Aslam M, Giardino M, Klefenz A, et al. alpha-Mannosyl-Functionalized Cationic Nanohydrogel Particles for Targeted Gene Knockdown in Immunosuppressive Macrophages. Macromol Biosci. 2019;19(7):e1900162.
132. Leber N, Kaps L, Aslam M, Schupp J, Brose A, Schäffel D, et al. SiRNA-mediated in vivo gene knockdown by acid-degradable cationic nanohydrogel particles. J Control Release. 2017;248:10-23.
133. Kaps L, Huppertsberg A, Choteschovsky N, Klefenz A, Durak F, Schrors B, et al. pH-degradable, bisphosphonate-loaded nanogels attenuate liver fibrosis by repolarization of M2-type macrophages. Proc Natl Acad Sci U S A. 2022;119(12):e2122310119.
134. Guo F, Li Y, Yu W, Fu Y, Zhang J, Cao H. Recent Progress of Small Interfering RNA Delivery on the Market and Clinical Stage. Mol Pharm. 2024.
135. Chen Y, Li Y, Li C, Zhang D, Liu Y, Zhang J, et al. The current perspective and opportunities of small nucleic acid-based therapeutics. Drug Dev Res. 2024;85(2):e22164.
136. Wang J, Zhu N, Su X, Gao Y, Yang R. Novel tumor-associated macrophage populations and subpopulations by single cell RNA sequencing. Front Immunol. 2023;14:1264774.
137. Ma R-Y, Black A, Qian B-Z. Macrophage diversity in cancer revisited in the era of single-cell omics. Trends in Immunology. 2022;43(7):546-63.
138. Murray PJ. Macrophage Polarization. Annu Rev Physiol. 2017;79:541-66.
139. Mantovani A, Sica A, Sozzani S, Allavena P, Vecchi A, Locati M. The chemokine system in diverse forms of macrophage activation and polarization. Trends in Immunology. 2004;25(12):677-86.
140. Gerrick KY, Gerrick ER, Gupta A, Wheelan SJ, Yegnasubramanian S, Jaffee EM. Transcriptional profiling identifies novel regulators of macrophage polarization. PLoS One. 2018;13(12):e0208602.
141. Katkar G, Ghosh P. Macrophage states: there's a method in the madness. Trends in Immunology. 2023;44(12):954-64.
142. Pizzurro GA, Miller-Jensen K. Reframing macrophage diversity with network motifs. Trends Immunol. 2023;44(12):965-70.
143. Devarbhavi H, Asrani SK, Arab JP, Nartey YA, Pose E, Kamath PS. Global burden of liver disease: 2023 update. J Hepatol. 2023;79(2):516-37.
144. Schuppan D, Surabattula R, Wang XY. Determinants of fibrosis progression and regression in NASH. J Hepatol. 2018;68(2):238-50.
145. Wang C, Ma C, Gong L, Guo Y, Fu K, Zhang Y, et al. Macrophage Polarization and Its Role in Liver Disease. Front Immunol. 2021;12:803037.
146. Zheng H, Peng X, Yang S, Li X, Huang M, Wei S, et al. Targeting tumor-associated macrophages in hepatocellular carcinoma: biology, strategy, and immunotherapy. Cell Death Discov. 2023;9(1):65.
147. Foerster F, Gairing SJ, Ilyas SI, Galle PR. Emerging immunotherapy for HCC: A guide for hepatologists. Hepatology. 2022.

148. Giannelli G, Koudelkova P, Dituri F, Mikulits W. Role of epithelial to mesenchymal transition in hepatocellular carcinoma. J Hepatol. 2016;65(4):798-808.
149. Park H, Lee S, Lee J, Moon H, Ro SW. Exploring the JAK/STAT Signaling Pathway in Hepatocellular Carcinoma: Unraveling Signaling Complexity and Therapeutic Implications. Int J Mol Sci. 2023;24(18).
150. Dhanasekaran R, Baylot V, Kim M, Kuruvilla S, Bellovin DI, Adeniji N, et al. MYC and Twist1 cooperate to drive metastasis by eliciting crosstalk between cancer and innate immunity. Elife. 2020;9.
151. Zou H, Feng X, Cao JG. Twist in hepatocellular carcinoma: pathophysiology and therapeutics. Hepatol Int. 2015;9(3):399-405.
152. Zhang K, Guo J, Yan W, Xu L. Macrophage polarization in inflammatory bowel disease. Cell Commun Signal. 2023;21(1):367.
153. Hegarty LM, Jones GR, Bain CC. Macrophages in intestinal homeostasis and inflammatory bowel disease. Nat Rev Gastroenterol Hepatol. 2023;20(8):538-53.
154. Tardito S, Martinelli G, Soldano S, Paolino S, Pacini G, Patane M, et al. Macrophage M1/M2 polarization and rheumatoid arthritis: A systematic review. Autoimmun Rev. 2019;18(11):102397.
155. Ahn I, Kang CS, Han J. Where should siRNAs go: applicable organs for siRNA drugs. Exp Mol Med. 2023;55(7):1283-92.
156. Bockamp E, Rosigkeit S, Siegl D, Schuppan D. Nano-Enhanced Cancer Immunotherapy: Immunology Encounters Nanotechnology. Cells. 2020;9(9).
157. Kaps L, Leber N, Klefenz A, Choteschovsky N, Zentel R, Nuhn L, Schuppan D. In Vivo siRNA Delivery to Immunosuppressive Liver Macrophages by alpha-Mannosyl-Functionalized Cationic Nanohydrogel Particles. Cells. 2020;9(8).
158. Groisberg R, Maitra A, Subbiah V. Of mice and men: lost in translation. Ann Oncol. 2019;30(4):499-500.
159. Spiller KL, Wrona EA, Romero-Torres S, Pallotta I, Graney PL, Witherel CE, et al. Differential gene expression in human, murine, and cell line-derived macrophages upon polarization. Exp Cell Res. 2016;347(1):1-13.

6 Appendix

6.1 RT-qPCR Relative Gene Expression Analysis

The normalization and analysis of RT-qPCR data were carried out in accordance with established best practices (97).

This section outlines the methodology applied across all experiments within this thesis, utilizing the siSIRPA transfection experiment as a representative example.

The aim was to assess the efficacy of siSIRPA in knocking down the expression of its target gene, SIRPA, by comparing the expression levels in siSIRPA-transfected samples against those in control samples transfected with siLUC.

Initially, the average cycle threshold (Ct) values from the qPCR technical replicates were recorded in an Excel spreadsheet for each reference gene (REF) and gene of interest (GOI), as illustrated in *(Figure 28, rows 4-7; columns C, F, and I)*

Subsequently, the software automatically calculated the mean Ct values for the biological replicates of the control group, i.e. those transfected with siLUC (*Figure 28, row 10; columns C, F, and I)*.

Following this, for each sample, the difference in Ct values (delta Ct) relative to the control group's average was computed for each REF and GOI *(Figure 28, columns D, G, and J)*

The calculation of relative quantities (RQ) was then performed by raising the sum of 1 plus the primer qPCR efficiency to the power of the delta Ct.

Next, the geometric mean of the RQs for the reference genes was determined for each sample *(***Figure *28**, *column L)*

The relative expression level of the gene of interest (*Figure 28, column M),* in this case SIRPA, was obtained by dividing the GOI RQ (*Figure 28, column K*) by the geometric mean of the reference genes for each sample.

Finally, the mean expression level and standard deviation for each biological group were calculated and presented (*Figure 28, columns N and O*).

The results were subsequently exported to GraphPad Prism, where graphs were generated, and statistical analyses were performed. This step facilitated the visualization of gene expression differences and the assessment of statistical significance.

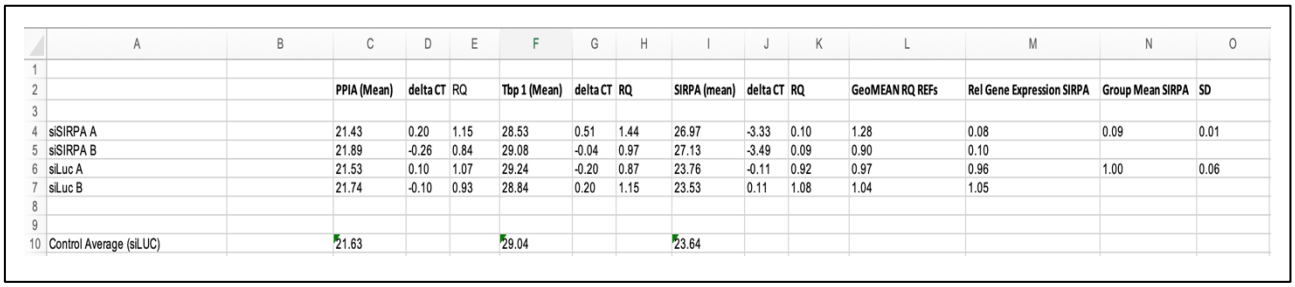

	A	B	C	D	E	F	G	H	I	J	K	L	M	N	O
1															
2			PPIA (Mean)	delta CT	RQ	Tbp 1 (Mean)	delta CT	RQ	SIRPA (mean)	delta CT	RQ	GeoMEAN RQ REFs	Rel Gene Expression SIRPA	Group Mean SIRPA	SD
3															
4	siSIRPA A		21.43	0.20	1.15	28.53	0.51	1.44	26.97	-3.33	0.10	1.28	0.08	0.09	0.01
5	siSIRPA B		21.89	-0.26	0.84	29.08	-0.04	0.97	27.13	-3.49	0.09	0.90	0.10		
6	siLuc A		21.53	0.10	1.07	29.24	-0.20	0.87	23.76	-0.11	0.92	0.97	0.96	1.00	0.06
7	siLuc B		21.74	-0.10	0.93	28.84	0.20	1.15	23.53	0.11	1.08	1.04	1.05		
8															
9															
10	Control Average (siLUC)		21.63			29.04			23.64						

Figure 28: Data normalization and relative gene expression analysis

Excel Spread Sheet of RT-qPCR Data Normalization and Relative Gene Expression Analysis using SIRPA knockdown as an example. The data were exported to GraphPad and for statistical analysis and graphical illustration.

7 Acknowledgements

[redacted]

8 Curriculum Vitae